**Rutherford Laboratory**
CHILTON, DIDCOT, OXON. OX11 0QX

RL-77-027/A

# MEASUREMENT OF THE POLARIZATION PARAMETER FOR ANTIPROTON-PROTON ANNIHILATION INTO CHARGED PION AND KAON PAIRS BETWEEN 1.0 AND 2.2 GeV/c

A.A. Carter, M. Coupland, E. Eisenhandler, C. Franklyn*, W.R. Gibson,

C. Hojvatt, D.R. Jeremiah**, P.I.P. Kalmus and T.W. Pritchard

Queen Mary College, London E1 4NS, England

M. Atkinson, P.J. Duke, D.T. Williams and J.N. Woulds

Daresbury Laboratory, Daresbury, Warrington, Cheshire, England

G.T.J. Arnison, A. Astbury, D. Hill and D.P. Jones††

Rutherford Laboratory, Chilton, Didcot, Oxfordshire, England

* Now at Atomic Energy Board, Pelindaba, Pretoria, R.S.A.

† Now at Fermi National Accelerator Laboratory, Batavia, Illinois, U.S.A.

** Now at the Home Office, London, England.

†† Now at Science Research Council, London, England.

March 1977

# MEASUREMENT OF THE POLARIZATION PARAMETER FOR ANTIPROTON-PROTON ANNIHILATION INTO CHARGED PION AND KAON PAIRS BETWEEN 1.0 AND 2.2 GeV/c

A.A. Carter, M. Coupland, E. Eisenhandler, C. Franklyn*, W.R. Gibson, C. Hojvat†, D.R. Jeremiah**, P.I.P. Kalmus and T.W. Pritchard

Queen Mary College, London E1 4NS, England

M. Atkinson, P.J. Duke, D.T. Williams and J.N. Woulds

Daresbury Laboratory, Daresbury, Warrington, Cheshire, England

G.T.J. Arnison, A. Astbury, D. Hill and D.P. Jones††

Rutherford Laboratory, Chilton, Didcot, Oxfordshire, England

Abstract

The polarization parameter P for the reactions $\bar{p}p \to \pi^-\pi^+$ and $\bar{p}p \to K^-K^+$ has been measured over essentially the full angular range at 11 laboratory momenta between 1.0 and 2.2 GeV/c, using a proton target polarized perpendicular to the scattering plane. The angles and momenta of both final state particles were determined from wire spark chambers, using the deflection caused by the polarized target magnet. Between 1000 and 5300 $\pi^-\pi^+$ events, and 140 and 1300 $K^-K^+$ events, were measured at each momentum. Differential cross-sections for $\bar{p}p \to \pi^-\pi^+$ were obtained. These are in excellent agreement with previous results. The polarization parameter for both channels is very close to +1 over much of the angular range. Legendre polynomial fits to the data are presented.

* Now at Atomic Energy Board, Pelindaba, Pretoria, R.S.A.

† Now at Fermi National Accelerator Laboratory, Batavia, Illinois, U.S.A.

** Now at the Home Office, London, England.

†† Now at Science Research Council, London, England.

## 1. INTRODUCTION

In earlier papers[1-4] we have presented measurements and preliminary interpretations of the differential cross-sections for the reactions $\bar{p}p \to \pi^-\pi^+$ and $\bar{p}p \to K^-K^+$. The measurements were made at 20 incident antiproton momenta in the range 0.79 to 2.43 GeV/c. Typically, 2000 $\pi^-\pi^+$ and 300 $K^-K^+$ events were obtained at each momentum. We report here the results of a subsequent experiment, also done at the CERN proton synchrotron, in which a transversely polarized proton target was used to make measurements of the asymmetry parameter P in the same two reactions. Because of beam and cross-section limitations, results are restricted to 11 incident momenta in the range 1.0 to 2.2 GeV/c. The electronic trigger logic of the experiment was designed to optimise the signal from $\pi\pi$ events, and this resulted in the loss of some KK events (see 4.7). At each momentum typically several thousand $\pi^-\pi^+$ and several hundred $K^-K^+$ events were detected. The one previous experiment in this range, done by Ehrlich et al.[5], collected 350 $\pi\pi$ events at 1.64 GeV/c. The present experiment has therefore overwhelmingly increased the amount of polarization data available on these reactions.

The usefulness of asymmetry measurements in the analysis of elastic scattering of $0^-$ mesons on $\frac{1}{2}^+$ nucleons is well known. The amplitude complexity for the annihilation process $(\frac{1}{2}^+\frac{1}{2}^-) \to (0^-0^-)$ is comparable to that describing the elastic scattering process $(0^-\frac{1}{2}^+) \to (0^-\frac{1}{2}^+)$. From the present data one might therefore hope for clarification analogous to that obtained from early asymmetry measurements in $\pi N$ elastic scattering. To this end we have performed an amplitude analysis of the channel $\bar{p}p \to \pi^-\pi^+$ which combines the differential cross-sections of our previous experiment[2] and the polarization data presented here. This analysis is described elsewhere[6] - the present paper is concerned with the methods and results

of the polarization measurement.

In section 2 we describe the experimental apparatus and method of taking data, with particular emphasis on those aspects which differ from our earlier experiment. The reader is referred to (2) for constructional and other details not considered here. Section 3 comprises a brief description of the Monte Carlo program used to calculate the acceptance and resolution of the apparatus. In section 4 we discuss the data-handling and analysis chain which produced the asymmetries and differential cross-sections presented in section 5.

## 2. EXPERIMENTAL APPARATUS

### 2.1 General Description

A plan view of the experiment is shown in figure 1. Incident anti-protons passed through the time-of-flight scintillation counters C12 and C34, multiwire proportional chambers M1-4, and the final defining counter C5, whose diameter was 30 mm. The position of this counter could be altered to accommodate the variation of the incident trajectory as a function of beam momentum. The beam was steered onto the target by the magnet NP39, whose field was set to compensate the effect of the polarized target magnet. Non-interacting beam particles continued downstream, bending to the right and finally hitting the veto counter BV. Above and below the target, covering the magnet pole faces, were veto counters consisting of 3 mm Tantalum converter (radiation length = 4.1 mm) and 6 mm of scintillator. The solid angle covered by these counters was 63% of $4\pi$. Reaction products emerging from the target passed first through the 4-gap wire spark chamber J. After traversing the field of the polarizing magnet ($\int Bdl$ = 0.7 T m) the particles were detected by the scintillation counter hodoscope planes H3, H4 and H5. In front of these counters were large arrays - A3, A4, A5 -

of wire spark chambers with ferrite core read-out. Each array was 2.70 m wide x 0.75 m high. In A3 the area in front of BV was made insensitive by placing a mylar 'spoiler' in each gap.

## 2.2 The Beam

The beam line was originally built for our earlier experiment; ref. (7) contains a full description of the design and main characteristics. For this experiment it was necessary to reduce the size of the final beam spot. The last quadrupole triplet was therefore moved 2 m downstream, reducing the magnification by a factor 2. The beam was run with a momentum bite of ± 2%.

The trajectories of the incident beam particles were measured by the proportional chambers M1-4, which recorded x, y, y, x co-ordinates respectively. The chambers were of standard construction, with 2 mm wire spacing, and were filled with 'magic gas'[8]. Pre-amplifiers were mounted on the chambers and signals were taken along twisted-pair lines to CERN-design 'RTM' modules[9], each channel of which contained a delay and strobed latch. The 'RTM' modules were read out and encoded by a CAMAC module.

Because of the lack of redundancy in this arrangement (two x, two y co-ordinates) it was usually necessary to reject those events with either missing or extra information in any of these chambers. This limited the sustainable instantaneous beam flux to about 50,000 particles per acclerator burst of 400 msecs.

## 2.3 The Polarized Target

The polarized target consisted of a cylindrical microwave cavity, 97 mm long and 35 mm in diameter, containing small spheres ($\sim$ 3 mm diameter)

of 1-2 propanediol ($C_3H_8O_2$) doped with $Cr^V$ complexes. The packing fraction of the spheres was $\sim 0.7$, giving an effective polarized proton density of 66 kg $m^{-3}$ (c.f. liquid hydrogen, $\rho$ = 71 kg $m^{-3}$). Refrigeration was achieved using a two-stage (separated) $He_3/He_4$ system, operating at a temperature of $\sim 0.4^{\circ}$ K. The polarizing magnetic field of 2.5 T was provided by a conventional C-magnet. A field uniformity of ± 0.5 mT over the projected area of the target was achieved by shimming the pole faces, which were 250 mm in diameter and 102 mm apart. The outer diameter of the cryostat vessel was 84 mm.

Microwave power at 70 GHz was supplied to the cavity from a carcinotron oscillator. Typical polarization values, averaged over a run of a few hours, were around 80%. Reversal of polarization direction took about an hour. The instantaneous value of the polarization was sampled and read out on each accelerator pulse by a computerized NMR system using a resonance signal from one of several coils in and around the target volume. The presence of more than one coil enabled checks to be made on the uniformity of the polarization throughout the sample. The linearity of the system was checked periodically and absolute calibrations were made using the thermal equilibrium signal from the target protons.

## 2.4 The J-Chamber

Because of its shape the wire spark chamber in the central field region around the cryostat was named J. As shown in figure 2 it consisted of a set of 4 gaps, each 10 mm deep. The wires consisted of vertical strips printed on a substrate of Kapton. Each strip was 0.75 mm wide with a gap between strips of 0.75 mm, giving a pitch of 1.5 mm. The Kapton was glued onto preformed moulds of expanded polystyrene to give the required shape, gap uniformity and overall mechanical strength. The

gas used was the usual Ne/He mixture bubbled through 1-propanol at $0^{\circ}$ C. The information from the chamber was obtained from a capacity read-out system based on a design by Pizer[10, 11]. This system had the advantage of being compatible with the magnetic core read-out used on the large arrays: the same logic was used for both sets of chambers. The 4 gaps were separated into 2 pairs. The high voltage pulse was applied to the adjacent inner walls of each pair of gaps, the outer walls remaining at ground. The clearing field directions were also opposed, and the values were higher than normal ($\sim$ 200 V/cm) to enable the chamber to work in the high magnetic field with good efficiency and acceptable memory time[12]. Because of the opposing senses of both high voltage and clearing field, spark drifts in each member of a pair were in opposite directions.

## 2.5 The Trigger

The trigger was based on the simple requirement that, following the production of an antiproton signal by the beam time-of-flight system, two charged particles should emerge from the target, one on each side of the beam. However, this requirement on its own would have resulted in an unacceptably high trigger rate because of the large elastic scattering and multipion annihilation cross-sections ($\sigma_{tot} \sim 100$ mb, but $\sigma_{\pi\pi} \sim 100$ $\mu$b). Interactions could also occur off the more abundant bound nucleons in the target material. The rate was therefore reduced by applying the following further conditions:

a) No signal came from the beam veto counter.

b) No signal came from the pole-face veto counters.

c) One and only one hodoscope element was struck on each side of the beam.

d) A hodoscope matrix coincidence requirement was satisfied.

This last requirement was based on the kinematics of the channel $\bar{p}p \to \pi^-\pi^+$. Coincidences were formed of the type H3.H4, H3.H5 or H4.H5, where e.g. H3.H4 means an element of H3 in coincidence with an element of H4. A set of matrix coincidence units was used to allow triggers to be produced only by those combinations of hodoscope elements which were kinematically consistent with the process $\bar{p}p \to \pi^-\pi^+$. A simplified scheme of the logic is shown in figure 3. Even with all these conditions included in the logic, only about 1% of the triggers recorded were genuine $\pi\pi$ or KK events. The final trigger rate of 1-10 events/burst (dependent on momentum) was tolerable, both as regards the load on the spark chamber high voltage system and the rate at which magnetic tapes were written.

Triggers generated by this logic activated the proportional and spark chamber read-out systems, and all information from the chambers, together with scaler readings, trigger status bits, and the value of target polarization, were read into the on-line computer. As in our earlier experiment, no on-line data reduction was done and all the data were written in raw form onto magnetic tape. Extensive on-line monitoring was done, both of the data and the performance of the equipment, and little time was lost from undetected faults.

A typical run lasted 2-5 hours, depending on incident momentum and hence on event rate. A full data tape contained about 30,000 events, usually corresponding to 1 or 2 runs. The direction of polarization of the target was reversed every 6-24 hours, again depending on event rate. In addition, some runs were done with a 'dummy target' containing vitrified carbon. This simulated the properties of the normal target, except that it did not contain free protons. The data obtained were used to establish the level of the background of events from bound nucleons in the target (see section 4.6).

# 3. ACCEPTANCE

## 3.1 General

As indicated in the preceding section, the signal-to-noise ratio in the recorded data was very low ($\lesssim$ 1%). In order to be sure that the data processing chain to be described in section 4 was fully efficient (i.e. that no good events were rejected) and that the background in the final sample of good events was fully understood, it was decided to derive differential cross-sections from the data and compare the results with those obtained in our previous experiment[2]. It was therefore necessary to know the acceptance of the apparatus as a function of centre of mass scattering angle $\theta^*$ for each incident momentum. A Monte Carlo program was written to do this. The program also generated samples of events that were used to test the analysis programs and to estimate the experimental resolution.

## 3.2 Field Mapping

An essential input to the Monte Carlo program, and also to the analysis described in section 4, was a three-dimensional map of the magnetic field in the entire volume through which incident or outgoing particles could pass. This map was obtained using a set of Hall probes whose position was stepped automatically under computer control. Readings were taken on a three-dimensional grid of points and written onto magnetic tape[13].

These results showed that the azimuthal components of the field were negligible, so that the field was cylindrically symmetric and could therefore be represented by a two-dimensional model having only radial and vertical components. The map used was based on a grid-spacing of 20 mm in

both height and radius.

### 3.3 The Monte Carlo Program

The experimental arrangement described in section 2 could have produced a very non-uniform and incomplete geometrical acceptance. However, each of the three hodoscope pairings (H3.H4, H3.H5, H4.H5) contributed to the total acceptance in two different ranges of $\cos \theta^*$. This was because the range of $\theta^*$ subtended by each hodoscope depended on the sign of the charge of the pion or kaon entering it. We call left-handed events those in which the $\pi^-(K^-)$ was emitted on the left-hand side of the beam, and similarly for right-handed events. By judicious placing of the large arrays the holes in, say, the left-handed event acceptance function could be filled in by the right-handed acceptance, resulting in a fairly complete coverage of the range of $\cos \theta^*$. The filling-in was, of course, momentum dependent, and therefore with fixed geometry could not be optmized for all incident momenta. Figure 4 shows how the acceptance at a typical momentum was built up of its component parts.

In outline, the procedure used to generate the acceptance functions was as follows. For each value of the incident momentum the beam phase space and momentum distributions determined from the experimental data were represented by a set of Gaussian distributions. Using these distributions, incident beam trajectories were generated and tracked to an interaction point in the target volume. The effects of multiple scattering, energy loss and nuclear absorption were calculated. Pions or kaons emerging from the target were tracked through the magnetic field and the spark chambers to the trigger hodoscopes. Again, allowance was made for losses from absorption and also decay. The distribution of events at the hodoscope

planes was used to generate the pattern of valid matrix combinations, i.e. those corresponding to $\pi\pi$ events. These combinations were wired into the trigger logic as discussed in 2.5.

# 4. ANALYSIS

## 4.1 General

The main data analysis chain, which produced both the asymmetries and differential cross-sections, had four stages. Each of the first three of these stages eliminated a large proportion of the events it was given, so that only a small number of events containing a high proportion of $\pi\pi$ and KK remained at the end.

Before this, the raw data were 'stacked' from approximately 350 7-track 556 bpi tapes written by the on-line computer onto 9-track 1600 bpi tapes. The first three stages of the analysis were then run under the control of the book-keeping and automatic job submission system TRIAB[14]. Each stage produced a data summary tape (DSTn) which was read by the subsequent stage. The first two programs in the chain processed one run at a time so that dubious runs could be eliminated. At the third stage all data for a given momentum and polarized target sign were combined into one file.

Early development of the programs was done on the CERN CDC computers; later work and the production runs on the IBM 360-195 at the Rutherford Laboratory.

## 4.2 First Stage (WALRUS)

The first program, WALRUS, was developed from SCARP, which was written for our earlier experiment and is described in (2). Its main function was to decode the raw data, check for errors and calculate vectors and

co-ordinates from the spark chamber information.

Data from the beam proportional chambers were used to derive an incident beam trajectory, which was tracked to a fiducial area at the centre of the target. If more than one incident vector could be constructed because of the presence of extra signals in the chambers, then all possible vectors were tracked. An event was retained if one and only one vector was inside the fiducial region. About 10% of all triggers were rejected in this way and a further 10% because of missing information in the beam chambers. In all therefore about 20% of the events were rejected because of bad data on the incident beam trajectory. When an event was rejected on these grounds correct normalization was preserved by discarding the associated incident antiprotons.

Vectors in the large spark chambers were found by making straight line least squares fits to the vertical and horizontal co-ordinates separately and then combining these to give a three-dimensional vector, resolving any ambiguities in this operation using the information from the diagonal planes. Tracks were required to contain at least three sparks in both the vertical and horizontal projections, inside a 'road' width of ± 5 to 7 mm depending on the angle of the track. A check was then made that these vectors intersected a struck hodoscope counter.

The event was required to have only one vector in each of two different spark chamber arrays, unless one additional vector was less than 5 mm away. This was to allow for the fact that the pattern recognition procedure could find an extra track in association with a particle trajectory if there were spurious sparks in a chamber close to the correct one.

The information from the J-chamber was converted to spark co-ordinates in the laboratory frame of reference after a correction had been applied for the drift of the spark position caused by the magnetic field. Following

(12), the correction d was given by the expression

$$d = kB^{3/2} + \frac{aE}{B}\left(\frac{1}{1+\frac{f^2}{e^2B^2}}\right)$$

The first term corresponds to the drift during the application of the high voltage pulse and the formation of the spark, and the second term describes the effect of the clearing field. The values of the constants used were:

$k = -0.65$ mm/T$^{3/2}$

$a = 0.68$ μsec

$f = 1.97 \times 10^{-19}$ kg/sec for the inner pair of gaps

$= 2.05 \times 10^{-19}$ kg/sec for the outer pair of gaps

E is the clearing field in V/mm

e is the electronic charge in Coulombs

B is the magnetic flux density in Tesla

Because of the orientation of the chamber relative to the magnetic field, the value of B varied along each gap. This variation was parametrized in a simple way and local values of d calculated for each individual spark.

At this stage a simple check was made for correlations between J-chamber sparks and vectors in the large arrays. It was required that the vectors in each of the two arrays corresponding to the trigger, when projected into the J-chamber, had inside a wide 'road' at least one spark in the inner pair of J-gaps and one spark in the outer pair. Of those 80% of the events which survived the beam requirements discussed above, 50 - 60% satisfied the 2-prong requirement in the large arrays and 50 - 70% passed the J-chamber wide 'road' test. The pass rates were all momentum dependent, and there was overlap between the 2-prong and J-chamber requirements.

Typically WALRUS, which took about two minutes of CPU time to process a run of 30,000 events, passed 25% of all triggers. The accepted events were written to DST1.

For all surviving events the program calculated the efficiencies of the large spark chambers on a grid 400 mm wide x 200 mm high. It also gave individual array efficiencies and overall efficiencies for each trigger mode. Typical overall efficiencies were between 98% and 99%. Finally, for each run 25 quantities were written into a TRIAB data-set. These included normalization data, polarization averages, chamber efficiencies and various quantities monitoring the performance of both the apparatus and the analysis.

### 4.3 Second Stage (SCOUR)

The second stage program SCOUR read events from DST1 and reconstructed the three vectors at the interaction vertex. Wide kinematic cuts were made on the vectors before evaluating an error matrix and writing the events on DST2.

The procedure for associating the information from the J-chamber and the large arrays was complex and is described in detail in (15); we give here an outline of the method.

For each array vector, combinations of the J-chamber sparks inside the 'road' were used as candidates to form a track. All combinations were tried in turn, subject always to the condition that there be at least one inner and one outer spark. The often large number of possibilities emerging from this process was reduced by applying a simple constraint based on the necessary curvature of the track in the magnetic field. Successful spark combinations were then used to evaluate the $\chi^2$ for a two-parameter fit to the array vector in the horizontal plane. The

parameters used were $1/p$ and $\psi$, where p is the particle momentum and $\psi$ is the azimuthal angle of the trajectory outside the magnetic field; the trajectory was constrained to intersect the array vector at the 'centre of gravity' of the sparks in the array. Any combination of J sparks which gave a $\chi^2$ probability greater than $10^{-6}$ was retained as a possible trajectory. This led to the possibility of multiple 'versions' of an event. Fitting was then repeated using three parameters, the extra parameter being the lateral displacement of the trajectory from the large array vector.

Using the parameters from the above fitting procedure, the program then reconstructed all the outgoing trajectories at the edge of the uniform field region; the beam vector was also extrapolated to the uniform region. An iterative procedure employing circular orbits was then used to attempt to find a vertex. All possible combinations of trajectories were tried, and if the vertex parameters obtained satisfied some very loose conditions then this version of the event was checked for consistency with $\bar{p}p \to \pi^-\pi^+$ and $\bar{p}p \to K^-K^+$ kinematics. Again, loose cuts were applied and all successful versions of each event were written on DST2. SCOUR took about two minutes to process a run of 30,000 triggers, passing about 3% of the original triggers.

Successful events were used to measure the efficiency of the J-chamber. For this purpose each gap was divided into three regions (two straight sections and one curved) and the efficiency for each region calculated separately. Each gap had an efficiency of about 95%, giving an overall chamber efficiency of 99.5%. As in WALRUS, these efficiencies and other data were written into the book-keeping system at the end of each run.

The overall reliability of SCOUR was checked using events generated by the Monte Carlo program. About 1% of the simulated events failed on

the WALRUS wide 'road' cuts, and less than 0.1% in the track finding and broad kinematic cuts. The track finding in the J-chamber was further debugged and checked using visual displays of many real events.

4.4 Third Stage (FULFIT)

In this experiment, where the interaction vertex is at the centre of the polarized target magnet and measurements of outgoing angles and momenta are highly correlated, it is not possible to perform a simple sequence of cuts on angles and momenta. We have therefore chosen to use the $\chi^2$-probability for each of the two kinematic hypotheses as a means of event selection. To this end, in FULFIT the events on DST2 were submitted to a fit with four kinematic constraints plus the requirement that the three tracks should intersect at a point vertex, giving eight constraints altogether. If an event satisfied either of the two kinematic hypotheses with a probability greater than $10^{-6}$ then the fitted information was written to DST3, otherwise only a summary was recorded of why the event failed. Apart from the probability cut, an event could fail a hypothesis for the following reasons: the starting values gave a missing mass more than four standard deviations from zero, the $\chi^2$ or constraint errors diverged, or too many iterations were required. No other cuts were imposed on events in this program. The program took about 100 msecs to process a fitted event. The pass rate through FULFIT was about 30%, resulting in about 1% of the original triggers being written onto DST3.

Figure 5 shows the $\chi^2$-probability distribution for a typical sample of real events which have been passed by FULFIT. The excess at low values of probability shows that some background was still present in the events on DST3. Since the distribution is fairly flat we conclude that the error matrix is being estimated correctly - no adjustments of errors were made to obtain this.

Monte Carlo-generated events were also passed through FULFIT. None of them failed at this stage, and the $\chi^2$-probability distribution produced by such events was flat. The data produced from Monte Carlo events were used to estimate the error and statistical uncertainty in the centre of mass scattering angle, $\theta^*$, and to compare the latter with that calculated from the error matrix for real events. The standard deviation was found to be about 10 mrads, independent of angle, and the mean error about 7 mrads; binning of events in intervals of 0.02 in $\cos\theta^*$ was therefore considered to be optimum.

The resolution in various other parameters after the constrained fit is of interest for judging the precision of our event separation and also the usefulness of the constrained fit itself. The vertical and lateral vertex position resolution is limited by the 2 mm wire spacing of the beam proportional chambers, but the longitudinal vertex position is determined to better than ± 0.5 mm by the J-chamber when constraints are applied. The resolution in laboratory scattering angles is between ± 15 mrad (backward particle) and ± 5 mrad (forward particle), compared to ± 15 mrad without constraints. The unfitted momentum resolution for a single track is of the order of ± 8% $(\text{GeV/c})^{-1}$, but this decreases to ± 0.7% $(\text{GeV/c})^{-1}$ using the constraints. For the separation of $\pi\pi$ events from KK events the $\chi^2$ is weighted mainly by the momentum of the backward particle for extreme values of $\theta^*$, mainly by the opening angle near $\theta^* = 90^\circ$, and by varying proportions of the two in between.

## 4.5 Fourth Stage (MERGE)

The function of MERGE was to read the successful events from DST3, cut on probability to get a final sample of $\pi\pi$ and KK events, use normalization data and acceptances to derive polarization and differential

cross-section results, and to store these results on disc.

In section 4.3 it was mentioned that different 'versions' of the same event could arise in SCOUR. These different versions were retained through FULFIT. At each momentum there were only a few such multi-version events, and after the FULFIT stage it became apparent that for most of them the different versions satisfied the same hypothesis with essentially the same values of $\cos\theta^*$. Only about 1% of the total number of events had truly different versions, and so MERGE always selected the first version on DST3. It was checked that this procedure did not bias the angular distributions or the relative number of $\pi\pi$ and KK events by printing out the parameters of all versions of such events.

To exclude background, events were first subjected to a further cut on $\chi^2$-probability: > 1% for the $\pi\pi$ hypothesis and > 5% for the KK. Only about 3% of the final sample of $\pi\pi$ and KK events passed <u>both</u> cuts. For these ambiguous cases the hypothesis with the higher probability was chosen. Only for a very few events were the two probability values similar - this is illustrated in figure 6, where only the 3% of $\pi\pi$ and KK events at 1.6 GeV/c which were ambiguous are shown. It is clear that most of the events on this plot are $K^-K^+$. (Tests with Monte Carlo-generated events showed that $K^-K^+$ events often had probabilities for $\pi^-\pi^+$ just inside the cut, while $\pi^-\pi^+$ events tended to be excluded by the $K^-K^+$ probability cut.)

Using the events which passed the above cuts, the program then calculated differential cross-sections and polarization parameters for $\pi\pi$ and KK. This was done for left-handed and right-handed events separately, and also with the data combined. To perform these calculations the program extracted from the book-keeping system the numbers of incident beam particles, the mean polarization of the target, and the spark chamber efficiencies, forming means over the various runs weighted by the number

of incident antiprotons. The geometrical acceptances used to calculate differential cross-sections were taken from a disc data set produced by the Monte Carlo program (see 3.3). Bins on the edges of acceptance bands were not used in the calculations of the differential cross-sections. Some corrections were put into the program directly: namely the beam absorption which was calculated by the Monte Carlo program but not contained in the acceptances, and the background correction, taken to be a fixed fraction of the signal in each $\cos\theta^*$ bin and independent of target polarization. This latter correction was estimated using the dummy target data. (See 4.6 below.)

The results, binned in $\cos\theta^*$ intervals of 0.02 with left-handed and right-handed events combined, were stored on a disc data-set for later use, the program taking about 30 secs to perform these tasks for each momentum.

## 4.6 Background

The background from bound nuclei in the final data sample was measured directly in 'dummy target' runs at 1.23, 1.60 and 1.99 GeV/c. The data were subjected to the analysis chain described above. The backgrounds remaining were so low that the statistical errors on the points made it very difficult to define an angular distribution. Figure 7 shows these results. The curves are measured $\pi^-\pi^+$ angular distributions[2] smeared by the binning of 0.1 in $\cos\theta^*$. Since these are not inconsistent with the data, and since the data had to pass the standard set of cuts and constraints, it appeared that they were largely $\pi\pi$ and KK events from unpolarized but nearly stationary bound nucleons in the target. It was therefore assumed that the angular distribution of the background followed that of the unpolarized signal at an average level corresponding to that observed in the dummy target runs, and the necessary correction was made

by subtracting a fixed fraction of the signal in each angular bin. This fraction (noise:signal) was estimated to be 7 ± 1% for $\pi\pi$ events and 16 ± 6% for KK events for all momenta. The errors are the statistical uncertainty on the total number of events summed over all scattering angles.

Other possible sources of background in the $\pi\pi$ signal were the multi-pion annihilation channels, in particular the reaction $\bar{p}p \to \pi^+\pi^-\pi^o$. Any feed-through of these events into the final data sample would have produced a component of the background angular distribution which was not a fixed fraction of the $\pi\pi$ signal, invalidating the correction procedure described above. This problem was investigated by performing a simple Monte Carlo calculation. $\pi^+\pi^-\pi^o$ events were generated uniformly over phase-space and subjected to the equivalent of the kinematic cuts used for normal events. Taking the $\pi^+\pi^-\pi^o$ channel cross-section to be 10 times that of the $\pi^+\pi^-$ channel, and making reasonable assumptions on the effect of the Fermi motion, the background from $\pi^+\pi^-\pi^o$ events was found to be at most 1% of the signal. Some confirmation of this comes from the fact that the dips in the differential cross-sections agree with the results of (2), there being little evidence of filling-in from background processes.

## 4.7 Check on the Coincidence Matrix

The final samples of good events produced by MERGE were used to make an important check on the Monte Carlo program and spark chamber trigger. As discussed earlier, the program was used to generate a set of coincidence matrix combinations, and these formed part of the trigger requirement. Figure 8 shows a sample of $\pi\pi$ events superimposed on the matrix. Clearly, the edges of the distribution are not cut by the matrix requirement, and hence no bias was introduced into the acceptance by this part of the trigger

logic. For the KK channel the results are not so satisfactory. The slightly different kinematics produces a shift in the distribution of events, and some events fall outside the valid matrix region designed for the $\pi\pi$ channel. This is evident from figure 9 where the sharp edges of the distributions are caused by the matrix requirement. The loss of events limited the statistical precision of the $K^-K^+$ asymmetry measurement, gave rise to uncertainties in the acceptance for some regions of $\cos\theta^*$ which made it very difficult to calculate accurate $K^-K^+$ cross-sections and reduced the signal:background (see 4.6).

## 4.8 Consistency Checks

Several checks were carried out which lead us to believe that the results are correct to within the errors quoted in the tables:

a) At two momenta (1.23 and 1.60 GeV/c) the events on DST2 were re-analysed using the library program SUMX to apply conventional coplanarity, angle and momentum cuts. This involved setting up different cuts for several bands of $\cos\theta^*$, and the procedure was incapable of completely separating the two reactions because of the strong correlations between measured angles and momenta at the vertex; however, within the uncertainties that this caused, the results for the $\pi\pi$ channel agreed well with those obtained in the normal way.

b) At one momentum (1.60 GeV/c) the polarization parameter was re-calculated using a wide range of different values for the probability cut, and in all cases the results agreed within the statistical uncertainty.

c) Where there were both left- and right-handed events in a $\cos\theta^*$ bin (3.3) their associated asymmetries and differential cross-sections

were calculated separately and compared. Within the rather limited statistics the agreement was good.

d) The $\pi\pi$ differential cross-sections agreed well, both in shape and normalization, with the results of previous experiments (2, 16, 17).

A small amount of pp elastic scattering data was taken[18] and the polarization compared with previous measurements[19]. Because of the much larger cross-section ($\sim$ 30 mb) and lower background, a much simpler analysis technique was used. The good agreement with (19) provided an independent check of the target polarization measurements.

## 5. RESULTS

### 5.1 Number of events in final sample

The number of $\pi^-\pi^+$ and $K^-K^+$ events which passed through the analysis chain at each incident momentum and for each direction of target polarization is given in table 1. Three momenta (1.23, 1.60 and 1.99 GeV/c) have twice as many $\pi^-\pi^+$ events as the rest, while two (1.10 and 1.70 GeV/c) have somewhat fewer. The effect of $K^-K^+$ events being partly excluded by the coincidence matrix is to make the statistics more uneven, especially at the lower momenta.

### 5.2 Conventions and formulae

In all of our results we take $\cos\theta^*$ equal to + 1.0 for $\pi^-$ ($K^-$) going in the direction of the incident $\bar{p}$.

The asymmetry data use the following convention for the sign of the polarization parameter P. Positive P means that the $\pi^-$ ($K^-$) is preferentially scattered to the left when the target spin is up, i.e. at a given $\cos\theta^*$

the quantity

$$(\hat{K}_{\bar{p}} \times \hat{K}_{\pi^-}) \cdot \hat{S}_p$$

is positive more often than it is negative, where $\hat{K}_{\bar{p}}$, $\hat{K}_{\pi^-}$ are unit vectors in the $\bar{p}$, $\pi^-$ directions and $\hat{S}_p$ is the direction of the proton spin. However, rather than compare left-scattered events with right-scattered events for one target spin orientation, which requires precise knowledge of the experimental acceptance, what one normally compares is the number of events scattered to one side for each of the two target spin directions. For example,

$$P(\cos\theta^*) = \frac{1}{\cos\phi} \frac{N_L^+(\cos\theta^*) - N_L^-(\cos\theta^*)}{N_L^+(\cos\theta^*) + N_L^-(\cos\theta^*)}$$

where $N_L^+$ and $N_L^-$ are the numbers of events per incident antiproton for left-handed events (see 3.3). For right-handed events the sign of P is reversed. This formula assumes that the target is 100% polarized and neglects background. $\phi$ is the mean angle between the normal to the reaction plane and the target polarization direction; in this experiment the mean value of $\cos\phi$ was 0.99. Taking account of the actual target polarization and background, and the presence of both left- and right-handed events, the formula becomes

$$P(\cos\theta^*) = \frac{(1+F)}{\cos\phi} \frac{N_R^-(\cos\theta^*) + N_L^+(\cos\theta^*) - N_R^+(\cos\theta^*) - N_L^-(\cos\theta^*)}{P^- [N_R^+(\cos\theta^*) + N_L^+(\cos\theta^*)] + P^+ [N_R^-(\cos\theta^*) + N_L^-(\cos\theta^*)]}$$

The subscripts on N refer to left- and right-handed events, and the superscripts + and - to target spin up or down respectively. $P^+$ and $P^-$ are the target polarization values averaged over all runs of the specified sign according to incident beam flux. F is the ratio of the background per incident antiproton (assumed to show no polarization effect) to the

unpolarized signal, i.e.

$$F = \frac{N_B}{\frac{N^+ + N^-}{2} - N_B}$$

where $N^{\pm} = N_L^{\pm} + N_R^{\pm}$ and we assume $P^+ \simeq P^-$ (which it was to the accuracy needed).

The formula used to obtain the differential cross-section is

$$\frac{d\sigma}{d\Omega}(\cos\theta^*) = \frac{P^-N^+(\cos\theta^*) + P^+N^-(\cos\theta^*)}{\rho_H L d\Omega(\cos\theta^*)(P^+ + P^-)(1 + F)}$$

$\rho_H$ is the density of hydrogen nuclei in the target, L is the target length, and $d\Omega(\cos\theta^*)$ is the total solid angle (left plus right) calculated by the Monte Carlo program for each $\cos\theta^*$ bin.

## 5.3 Differential cross-sections for $\bar{p}p \to \pi^-\pi^+$

Although the systematics of an asymmetry measurement are somewhat different from those of a measurement of a differential cross-section, it is a very severe test of a polarized target experiment to compare its results with those from a cross-section measurement which used a hydrogen target. We have done this using our earlier experiment[2], binning the new results in intervals of 0.04 in $\cos\theta^*$ to match the older data. The results of this comparison are shown in figure 10. The error bars on the new results incorporate statistical uncertainties on the data, on the Monte Carlo acceptance (quite small) and on the overall level of the background correction. The major systematic uncertainty, which could be as high as ± 10%, is on $\rho_H$ due to the unknown packing fraction of the spheroids making up the target.

The agreement between the two experiments, both in shape and overall normalization, is excellent. We stress that we did not adjust the normalization of our new results in any way, and given the large uncertainty in the amount of material in the polarized target the agreement in normalization is better than one might expect.

The only discrepancy occurs in the backward direction at 1.23 GeV/c and below. We have tried very hard to find the cause of this disagreement, but we have failed to do so. We also compared both sets of data to that of Nicholson et al.[17] and it is interesting that in this region their data lies between our two sets.

It is also evident that our new experiment does not measure the very forward and backward regions of the angular distribution quite as well as the older one because of poorer and uncertain acceptance in these regions. In the extreme forward bins especially there is a large and sensitive absorption correction in the Monte Carlo program. Since the regions near $\cos\theta^* = \pm 1$ have a strong influence on fits to the data we use the older cross-sections for these[6], even though our new data has rather better statistics at several momenta.

## 5.4 Asymmetries for $\bar{p}p \to \pi^-\pi^+$

The results for the asymmetry parameter P in the $\pi^-\pi^+$ channel are shown in figure 11. The errors include statistical uncertainties on both the signal and background. For purposes of presentation the data are shown with a binning of 0.04 in $\cos\theta^*$. In table 2 we give the complete data set in its original binning of 0.02 in $\cos\theta^*$; this binning was used in all fits.

We have compared our data at 1.60 GeV/c with the only previous measurement, that of Ehrlich et al. at 1.64 GeV/c. Within their very limited

statistics the agreement is quite good.

The asymmetry data are extremely striking. The polarization is close to + 1 over a significant part of the angular range. As the momentum increases the maximum polarization remains near 1 and much of the structure disappears.

Fits to the data at all momenta (see 5.6) produce unphysical maximum asymmetries of + 1.05 ± 0.01. We consider two main systematic errors. The largest uncertainty is the absolute value of the target polarization. This is estimated to be $\sim$ ± 3%. (Relative values are good to < 1%.) Another uncertainty is the background angular distribution. We assumed this to be that of $\bar{p}p \to \pi^-\pi^+$ with a stationary target (3.6), with no allowance for either Fermi motion or contamination from other reactions. This is very hard to check experimentally without an order of magnitude more dummy target data, but if we arbitrarily assume that in any one angular bin we only know the background to $\sim$ ± 50% this corresponds to an uncertainty on the asymmetry of $\sim$ 3 – 4%. It would then be possible to explain the asymmetry error by a combination of the target polarization being higher and the background lower than we thought. However, we cannot just scale the values of P down by 5%. There is no region in which we can check that P also goes to - 1.05, and if part of the discrepancy is due to background considerations it will vary with cos $\theta^*$. We have therefore not attempted to correct the data in any way for these effects.

## 5.5 Asymmetries for $\bar{p}p \to K^-K^+$

The asymmetry parameter P for the $K^-K^+$ channel is shown in figure 12. This is the first measurement of P in this channel. The binning chosen is 0.1 in cos $\theta^*$ because of the limited statistics. All the data, in the original binning of 0.02, is given in table 2. Care must be taken in binning it up because many bins do not contain any events, so properly

weighted values of $\cos\theta^*$ must be used. (This is also true for the end bins of the $\pi^-\pi^+$ data.)

The most striking feature of the $K^-K^+$ data is its remarkable similarity to $\pi^-\pi^+$, despite the presence of amplitudes for G-parity = - 1 as well as + 1.

## 5.6 Legendre polynomial fits

We combined each of the sets of cross-section data with our $\pi^-\pi^+$ and $K^-K^+$ asymmetries to carry out Legendre polynomial fits to the data for each channel. The data for P and $d\sigma/d\Omega$ at each momentum were parametrized as

$$\frac{d\sigma}{d\Omega}(\cos\theta^*) = \sum_{\ell=0}^{\ell_{max}} a_\ell P_\ell^0 (\cos\theta^*)$$

$$P(\cos\theta^*).\frac{d\sigma}{d\Omega}(\cos\theta^*) = \sum_{\ell=1}^{\ell_{max}} b_\ell P_\ell^1 (\cos\theta^*)$$

where $P_\ell^0$ and $P_\ell^1$ are normal and associated Legendre polynomials. The values of $a_\ell$ and $b_\ell$ were determined simultaneously by an optimization of the $\chi^2$ for the overall data set, with P obtained by

$$P(\cos\theta^*) = \frac{\Sigma\, b_\ell P_\ell^1 (\cos\theta^*)}{\Sigma\, a_\ell P_\ell^0 (\cos\theta^*)}$$

There is nothing to constrain these fits within the physical bounds $d\sigma/d\Omega \geq 0$ and $|P| \leq 1$, and it was occasionally found necessary to penalize the $\chi^2$ artificially in order to do this. Since P actually goes to 1.05 in the data the penalties were only imposed one standard deviation above this value.

The values of $\ell_{max}$ needed for good fits to both P and $d\sigma/d\Omega$ at each

momentum are given in table 1. For $\pi^-\pi^+$ they ranged from 6 to 10 over the momentum range; by way of contrast the $K^-K^+$ data, partly because of its poorer statistics, could be fitted satisfactorily at all momenta with $\ell_{max} = 6$. Although the $\chi^2$ per degree of freedom for good fits varied somewhat from momentum to momentum, typical values are $\sim 1.3$ for both $\pi^-\pi^+$ and $K^-K^+$.

The Legendre fits to P in the $\pi^-\pi^+$ channel, using our older cross-section data, are shown with the data in figure 11. The fit to P in $K^-K^+$ is shown in figure 12. The coefficients $a_\ell$ and $b_\ell$ for these fits are plotted as a function of incident momentum in figure 13 ($\pi^-\pi^+$) and 14 ($K^-K^+$). In the $\pi^-\pi^+$ case we also show Legendre coefficients for fits using only the differential cross-sections from this experiment. There is little difference between the two fits.

The $\pi^-\pi^+$ Legendre coefficients show some striking features. $a_6$ has a large negative peak below 1.6 GeV/c. $a_8$ and $a_{10}$ are very large in the upper part of the momentum range. $b_1$ dominates the b-coefficients, but $b_5$, $b_6$, $b_7$ and $b_9$ all show interesting behaviour. Although these features cannot be uniquely interpreted, it is clear that total angular momenta of 3, 4 and 5 dominate this channel at certain momenta. This is confirmed in the amplitude analysis[6] which we have performed on the $\pi^-\pi^+$ channel.

ACKNOWLEDGEMENTS

We are above all deeply indebted to the CERN polarized target group, led by M. Borghini, for providing and operating the polarized target whose excellent performance and reliability was a large factor in the success of this experiment. O. Runolfsson provided us with the equipment and technical expertise to map the field of our magnet. D.V. Bugg and M.A.R. Kemp encouraged us to do this experiment and assisted in the early

stages. We are grateful to D. Quarrie for writing the kinematic fitting program and to Mrs. E.E. Smith for 'stacking' the data tapes and making drawings. This experiment benefited greatly from the services of the Rutherford, Daresbury and CERN laboratories. CF and DRJ acknowledge SRC studentships.

REFERENCES


1. E. Eisenhandler et al., Physics Letters 47B (1973) 531.
2. E. Eisenhandler et al., Nuclear Physics B96 (1975) 109.
3. E. Eisenhandler et al., Physics Letters 47B (1973) 536.
4. E. Eisenhandler et al., Physics Letters 49B (1974) 201.
5. R.D. Ehrlich et al., Physical Review Letters 28 (1972) 1147.
6. A.A. Carter et al., to be published in Physics Letters.
7. P.I.P. Kalmus et al., CERN Report 71-25 (1971).
8. R. Bouclier et al., Nuclear Instruments and Methods 88 (1970) 149.
9. J.C. Tarlé and H. Verweij, Nuclear Instruments and Methods 102 (1972) 131.
10. G.T.J. Arnison, Rutherford Laboratory Internal Report 74-094 (1974).
11. G.T.J. Arnison, Nuclear Instruments and Methods 108 (1973) 135; I.H. Pizer, Nuclear Instruments and Methods 93 (1971) 249.
12. F. Bradamante et al., Nuclear Instruments and Methods 112 (1973) 513 and CERN-Trieste Group Internal Note; I.A. Radkevich and I.A. Dukhovskoi, SLAC Translation 140 from ITEP Report 884 (1971).
13. J. Adams and O. Runolfsson, CERN Internal Report NP-DHG-74 (1974).
14. J. Hart, Rutherford Laboratory Notice.
15. M. Coupland, Rutherford Laboratory Report RL-77-007/A (1977).
16. D. Fong, Ph.D. Thesis, California Inst. of Technology (1968).
17. H. Nicholson et al., Phys. Rev. 7D (1973) 2572.
18. C.B. Franklyn, "Proton-Proton Elastic Polarization Measurements at 1.385 GeV/c", M.Phil Thesis, University of London, Oct. 1974.
19. F. Betz et al., Phys. Rev. 148 (1966) 1289; G. Cozzika et al., Phys. Rev. 164 (1967) 1672.

TABLE CAPTIONS

1. Numbers of events in final sample at each incident momentum, and maximum order Legendre polynomial used in fit to the data.

2. Asymmetries for $\bar{p}p \to \pi^-\pi^+$ and $\bar{p}p \to K^-K^+$. Under each heading the first column is the asymmetry and the second the error. Entries of $0.0 \pm 0.0$ mean there were no events in that bin.

FIGURE CAPTIONS

1. Plan view of the apparatus. The two circular pole-face veto counters, above and below the target, are not shown.

2. The J-shaped spark chamber which surrounded the target cryostat.

3. Schematic representation of the trigger logic.

4. Experimental acceptance for $\bar{p}p \to \pi^-\pi^+$ as a function of cos $\theta^*$. The total acceptance is the sum of that with the $\pi^-$ on left of beam and $\pi^-$ on right of beam.

5. Histogram of $\chi^2$-probability for the hypothesis $\bar{p}p \to \pi^-\pi^+$ in 0.01 bins. All events at 1.23 GeV/c having $\pi^-\pi^+$ probability > $10^{-6}$ and > $K^-K^+$ probability are included in the plot. The final cut used was 0.01.

6. Scatter plot of $\chi^2$-probability for the hypothesis $\bar{p}p \to K^-K^+$ versus $\chi^2$-probability for the hypothesis $\bar{p}p \to \pi^-\pi^+$ at 1.60 GeV/c. Note that only the 3% of all fitted events satisfying <u>both</u> hypotheses above the cuts 0.01 for $\pi^-\pi^+$ and 0.05 for $K^-K^+$ are included in the plot. 97% of the final sample of events are unambiguous and do not appear.

7. Background 'differential cross-sections' derived from a pure carbon target for events passing the $\pi^-\pi^+$ cuts. The curves indicate the shape of the angular distributions for $\bar{p}p \to \pi^-\pi^+$ (ref. 2) smeared to the cos $\theta^*$ binning used. The scale is arbitrary.

8. A representation of the kinematic coincidence matrix used in the trigger at 1.60 GeV/c - labels refer to hodoscope counters. Numbers in the scatter plot represent all $\pi^-\pi^+$ events at this momentum.

9. As fig. 8 but events shown are all $K^-K^+$ events at 1.60 GeV/c.

10. Differential cross-sections for $\bar{p}p \to \pi^-\pi^+$. Crosses are results from this experiment using a propanediol target, while x's are from our previous experiment (ref. 2) using a hydrogen target. The overall normalization has not been adjusted in any way.

11. Asymmetry parameter P for the reaction $\bar{p}p \to \pi^-\pi^+$. The curves are Legendre polynomial fits to both P and $d\sigma/d\Omega$; see text for details.

12. Asymmetry parameter P for the reaction $\bar{p}p \to K^-K^+$. The curves are Legendre polynomial fits to both P and $d\sigma/d\Omega$; see text for details.

13. Coefficients $a_\ell$ and $b_\ell$ for Legendre polynomial fits to both P and $d\sigma/d\Omega$ for $\bar{p}p \to \pi^-\pi^+$. Open circles used $d\sigma/d\Omega$ from ref. 2, dots used $d\sigma/d\Omega$ from this experiment. All coefficients are normalized to $a_o$.

14. Coefficients $a_\ell$ and $b_\ell$ for Legendre polynomial fits to $\bar{p}p \to K^-K^+$. See caption of fig. 13 for details.

Table 1

| Incident Momentum (GeV/c) | Target Polarization Sign | $\pi^-\pi^+$ Events | $K^-K^+$ Events | Order of Legendre Fit to $\pi^-\pi^+$ | Order of Legendre Fit to $K^-K^+$ |
|---|---|---|---|---|---|
| 1.00 | + | 1379 | 178 | 6 | 6 |
| | - | 1013 | 115 | | |
| 1.10 | + | 884 | 98 | 7 | 6 |
| | - | 620 | 40 | | |
| 1.23 | + | 2680 | 331 | | |
| | - | 2638 | 289 | 7 | 6 |
| | dummy | 54 | 19 | | |
| 1.36 | + | 1091 | 157 | 9 | 6 |
| | - | 1068 | 91 | | |
| 1.43 | + | 1097 | 186 | 9 | 6 |
| | - | 1147 | 145 | | |
| 1.60 | + | 2120 | 515 | | |
| | - | 2611 | 509 | 10 | 6 |
| | dummy | 68 | 19 | | |
| 1.70 | + | 515 | 118 | 10 | 6 |
| | - | 525 | 110 | | |
| 1.80 | + | 1310 | 310 | 10 | 6 |
| | - | 1079 | 167 | | |
| 1.90 | + | 1105 | 316 | 10 | 6 |
| | - | 1059 | 224 | | |
| 1.99 | + | 2739 | 766 | | |
| | - | 2409 | 558 | 10 | 6 |
| | dummy | 50 | 27 | | |
| 2.20 | + | 1141 | 286 | 10 | 6 |
| | - | 1063 | 215 | | |

INCIDENT MOMENTUM 1.00 GEV/C

Table 2

| COS(θ*) | PIPI POLN | | KK POLN | | COS(θ*) | PIPI POLN | | KK POLN | |
|---|---|---|---|---|---|---|---|---|---|
| -.99 | 0.0 | 0.0 | 0.0 | 0.0 | .01 | 0.79 | 0.19 | 0.0 | 0.0 |
| -.97 | 0.0 | 0.0 | -1.52 | 0.97 | .03 | 1.24 | 0.14 | 0.64 | 0.62 |
| -.95 | 0.58 | 0.23 | 0.85 | 0.50 | .05 | 0.51 | 0.21 | 1.52 | 0.44 |
| -.93 | 0.63 | 0.18 | -1.07 | 0.37 | .07 | 0.83 | 0.18 | 0.37 | 0.74 |
| -.91 | 0.34 | 0.14 | 0.85 | 0.50 | .09 | 1.08 | 0.16 | -0.85 | 0.50 |
| -.89 | 0.42 | 0.14 | 1.49 | 0.57 | .11 | 0.97 | 0.18 | 0.81 | 0.52 |
| -.87 | 0.48 | 0.14 | -1.52 | 0.69 | .13 | 1.20 | 0.16 | -1.49 | 0.57 |
| -.85 | 0.47 | 0.16 | 0.85 | 0.35 | .15 | 0.72 | 0.22 | 0.64 | 0.62 |
| -.83 | 0.34 | 0.16 | 0.85 | 0.50 | .17 | 0.64 | 0.22 | 0.37 | 0.53 |
| -.81 | -0.05 | 0.17 | 0.15 | 0.90 | .19 | 0.73 | 0.20 | -0.15 | 0.90 |
| -.79 | 0.27 | 0.16 | 0.0 | 0.0 | .21 | 1.03 | 0.19 | 0.0 | 0.0 |
| -.77 | 0.65 | 0.14 | 1.49 | 0.79 | .23 | 0.91 | 0.20 | 1.52 | 0.40 |
| -.75 | 0.22 | 0.18 | 0.0 | 0.0 | .25 | 0.94 | 0.19 | 0.37 | 0.74 |
| -.73 | 0.33 | 0.19 | 0.0 | 0.0 | .27 | 0.26 | 0.22 | 1.52 | 0.40 |
| -.71 | 0.04 | 0.23 | 0.0 | 0.0 | .29 | 1.13 | 0.19 | 0.52 | 0.48 |
| -.69 | -0.00 | 0.18 | 0.0 | 0.0 | .31 | 0.80 | 0.22 | 0.92 | 0.45 |
| -.67 | -0.13 | 0.23 | 0.0 | 0.0 | .33 | 1.01 | 0.19 | 1.52 | 0.40 |
| -.65 | 0.22 | 0.30 | 0.0 | 0.0 | .35 | 0.89 | 0.24 | 1.52 | 0.38 |
| -.63 | -0.12 | 0.28 | 0.0 | 0.0 | .37 | 0.92 | 0.20 | -0.15 | 0.90 |
| -.61 | -0.02 | 0.43 | 0.0 | 0.0 | .39 | 0.97 | 0.18 | 1.52 | 0.69 |
| -.59 | 0.14 | 0.64 | 0.0 | 0.0 | .41 | 0.85 | 0.22 | 0.37 | 0.53 |
| -.57 | 0.14 | 0.90 | 0.0 | 0.0 | .43 | 0.63 | 0.21 | 1.00 | 0.40 |
| -.55 | 0.0 | 0.0 | 0.0 | 0.0 | .45 | 1.10 | 0.19 | 1.00 | 0.40 |
| -.53 | 0.0 | 0.0 | 0.0 | 0.0 | .47 | 0.72 | 0.24 | 0.37 | 0.53 |
| -.51 | 0.0 | 0.0 | 0.0 | 0.0 | .49 | 0.81 | 0.23 | 1.50 | 0.38 |
| -.49 | -1.38 | 0.74 | 0.0 | 0.0 | .51 | 1.23 | 0.19 | 0.07 | 0.64 |
| -.47 | -1.38 | 0.37 | 1.52 | 0.56 | .53 | 0.98 | 0.20 | 1.51 | 0.52 |
| -.45 | -0.58 | 0.64 | 1.52 | 0.69 | .55 | 0.05 | 0.37 | 1.51 | 0.39 |
| -.43 | 0.34 | 0.53 | 1.52 | 0.97 | .57 | 0.90 | 0.18 | 1.12 | 0.34 |
| -.41 | -0.14 | 0.64 | 1.52 | 0.97 | .59 | 0.28 | 0.24 | 0.83 | 0.36 |
| -.39 | 1.40 | 0.53 | 0.0 | 0.0 | .61 | -0.03 | 0.29 | 0.96 | 0.30 |
| -.37 | -0.14 | 0.90 | 1.52 | 0.49 | .63 | -0.09 | 0.28 | 0.63 | 0.59 |
| -.35 | 0.76 | 0.36 | 0.37 | 0.53 | .65 | -0.37 | 0.38 | 0.0 | 0.0 |
| -.33 | 0.26 | 0.57 | -0.15 | 0.90 | .67 | 0.05 | 0.31 | 0.0 | 0.0 |
| -.31 | 0.19 | 0.41 | 0.64 | 0.62 | .69 | -0.59 | 0.35 | 1.49 | 0.57 |
| -.29 | 1.24 | 0.20 | -0.15 | 0.64 | .71 | -0.11 | 0.32 | 0.85 | 0.50 |
| -.27 | 0.33 | 0.29 | 0.0 | 0.0 | .73 | 0.04 | 0.33 | 1.49 | 0.79 |
| -.25 | 0.57 | 0.32 | -0.50 | 0.69 | .75 | -0.45 | 0.24 | 0.0 | 0.0 |
| -.23 | 0.39 | 0.28 | -0.11 | 0.45 | .77 | -1.03 | 0.23 | 0.0 | 0.0 |
| -.21 | 0.90 | 0.19 | 0.95 | 0.43 | .79 | -0.18 | 0.31 | 0.63 | 0.65 |
| -.19 | 0.92 | 0.23 | -0.63 | 0.65 | .81 | -0.91 | 0.20 | -1.52 | 0.97 |
| -.17 | 1.04 | 0.15 | 0.94 | 0.44 | .83 | -0.74 | 0.37 | 0.0 | 0.0 |
| -.15 | 1.02 | 0.16 | 0.57 | 0.68 | .85 | -0.87 | 0.22 | 0.0 | 0.0 |
| -.13 | 0.89 | 0.19 | 0.98 | 0.40 | .87 | -0.34 | 0.37 | 0.0 | 0.0 |
| -.11 | 0.77 | 0.19 | -0.63 | 0.65 | .89 | 0.0 | 0.0 | -1.52 | 0.56 |
| -.09 | 1.13 | 0.15 | 0.55 | 0.47 | .91 | 0.0 | 0.0 | 0.0 | 0.0 |
| -.07 | 1.31 | 0.14 | 0.0 | 0.90 | .93 | 0.0 | 0.0 | 0.0 | 0.0 |
| -.05 | 0.96 | 0.16 | 0.85 | 0.49 | .95 | 0.0 | 0.0 | 0.0 | 0.0 |
| -.03 | 0.69 | 0.18 | 1.49 | 0.79 | .97 | 0.0 | 0.0 | 0.0 | 0.0 |
| -.01 | 1.12 | 0.12 | -0.32 | 0.56 | .99 | 0.0 | 0.0 | 0.0 | 0.0 |

POINTS GIVEN AS 0.0+-0.0 HAVE NO DATA

INCIDENT MOMENTUM 1.10 GEV/C

Table 2 contd.

| COS(θ*) | PIPI | POLN | KK | POLN | COS(θ*) | PIPI | POLN | KK | POLN |
|---|---|---|---|---|---|---|---|---|---|
| -.99 | 0.0 | 0.0 | 0.0 | 0.0 | .01 | 0.68 | 0.24 | 1.53 | 0.53 |
| -.97 | -1.38 | 0.81 | 0.0 | 0.0 | .03 | 0.73 | 0.20 | 0.74 | 0.56 |
| -.95 | 0.18 | 0.31 | -0.49 | 0.71 | .05 | 1.11 | 0.22 | 1.50 | 0.51 |
| -.93 | -0.34 | 0.21 | 1.61 | 0.96 | .07 | 0.84 | 0.23 | 1.50 | 0.62 |
| -.91 | 0.45 | 0.21 | -1.50 | 0.87 | .09 | 0.45 | 0.25 | 0.0 | 0.0 |
| -.89 | 0.53 | 0.22 | 0.0 | 0.0 | .11 | 1.12 | 0.20 | 1.50 | 0.62 |
| -.87 | 0.14 | 0.22 | 1.61 | 0.69 | .13 | 0.94 | 0.19 | -0.02 | 0.94 |
| -.85 | 0.12 | 0.20 | 0.0 | 0.0 | .15 | 0.72 | 0.24 | 1.50 | 0.51 |
| -.83 | 0.06 | 0.20 | 0.0 | 0.0 | .17 | 0.69 | 0.25 | 0.90 | 0.47 |
| -.81 | 0.02 | 0.22 | 1.61 | 0.96 | .19 | 0.89 | 0.24 | 1.50 | 0.51 |
| -.79 | 0.10 | 0.22 | 1.61 | 0.69 | .21 | 1.04 | 0.22 | 0.0 | 0.0 |
| -.77 | 0.31 | 0.26 | -1.50 | 0.87 | .23 | 0.80 | 0.24 | 0.49 | 0.71 |
| -.75 | 0.15 | 0.28 | 0.0 | 0.0 | .25 | 0.94 | 0.19 | -0.55 | 0.73 |
| -.73 | -0.24 | 0.25 | 1.61 | 0.96 | .27 | 0.69 | 0.21 | -0.55 | 0.73 |
| -.71 | 0.02 | 0.23 | 0.02 | 0.94 | .29 | 0.45 | 0.36 | 1.50 | 0.62 |
| -.69 | 0.02 | 0.27 | 0.0 | 0.0 | .31 | 0.53 | 0.24 | 1.50 | 0.87 |
| -.67 | 0.18 | 0.26 | 0.0 | 0.0 | .33 | 0.45 | 0.27 | 1.50 | 0.62 |
| -.65 | -0.14 | 0.31 | 1.61 | 0.96 | .35 | 0.77 | 0.25 | 0.0 | 0.0 |
| -.63 | 0.99 | 0.24 | 0.0 | 0.0 | .37 | 1.25 | 0.20 | -1.61 | 0.96 |
| -.61 | 1.49 | 0.33 | 1.61 | 0.96 | .39 | 0.87 | 0.25 | 0.64 | 0.45 |
| -.59 | -0.59 | 0.44 | 0.0 | 0.0 | .41 | 1.19 | 0.24 | 1.50 | 0.44 |
| -.57 | 0.02 | 0.66 | -1.50 | 0.87 | .43 | 1.26 | 0.23 | 0.65 | 0.45 |
| -.55 | 0.50 | 0.73 | 0.55 | 0.73 | .45 | 0.98 | 0.26 | 0.0 | 0.90 |
| -.53 | 1.49 | 0.92 | 0.0 | 0.0 | .47 | 1.44 | 0.21 | 1.50 | 0.87 |
| -.51 | 0.0 | 0.0 | 0.0 | 0.0 | .49 | 1.09 | 0.23 | 1.50 | 0.62 |
| -.49 | -0.02 | 0.94 | 0.0 | 0.0 | .51 | 0.78 | 0.26 | 1.50 | 0.62 |
| -.47 | 0.45 | 0.71 | 1.50 | 0.87 | .53 | 0.86 | 0.34 | 1.50 | 0.62 |
| -.45 | -1.49 | 0.92 | 0.0 | 0.0 | .55 | 0.33 | 0.36 | 1.50 | 0.87 |
| -.43 | -0.02 | 0.94 | 0.0 | 0.0 | .57 | -0.16 | 0.44 | 1.50 | 0.34 |
| -.41 | 1.38 | 0.58 | -1.61 | 0.96 | .59 | -0.01 | 0.68 | 1.50 | 0.87 |
| -.39 | -1.49 | 0.92 | 0.0 | 0.0 | .61 | -0.15 | 0.43 | -1.61 | 0.96 |
| -.37 | -0.02 | 0.94 | 1.50 | 0.87 | .63 | 0.88 | 0.48 | 0.0 | 0.0 |
| -.35 | 1.38 | 0.58 | 0.0 | 0.0 | .65 | -0.33 | 0.45 | 1.61 | 0.96 |
| -.33 | 0.83 | 0.46 | 0.0 | 0.0 | .67 | 0.02 | 0.54 | 0.0 | 0.0 |
| -.31 | 1.38 | 0.47 | -0.02 | 0.94 | .69 | 0.23 | 0.50 | 0.0 | 0.0 |
| -.29 | 1.41 | 0.43 | 0.0 | 0.0 | .71 | -0.83 | 0.33 | 0.0 | 0.0 |
| -.27 | 0.59 | 0.44 | 1.50 | 0.62 | .73 | -0.45 | 0.50 | 0.0 | 0.0 |
| -.25 | 1.38 | 0.41 | 0.49 | 0.71 | .75 | -0.69 | 0.40 | 1.61 | 0.96 |
| -.23 | 0.48 | 0.36 | 1.50 | 0.62 | .77 | 0.02 | 0.47 | 0.0 | 0.0 |
| -.21 | 0.74 | 0.27 | -0.02 | 0.94 | .79 | -0.55 | 0.38 | -1.50 | 0.62 |
| -.19 | 0.67 | 0.30 | -0.02 | 0.94 | .81 | -1.10 | 0.27 | 1.61 | 0.96 |
| -.17 | 0.68 | 0.31 | 0.51 | 0.73 | .83 | -1.04 | 0.31 | 0.0 | 0.0 |
| -.15 | 0.52 | 0.28 | -0.50 | 0.70 | .85 | -0.99 | 0.34 | 0.0 | 0.0 |
| -.13 | 0.47 | 0.29 | 1.55 | 0.65 | .87 | -0.74 | 0.30 | 0.0 | 0.0 |
| -.11 | 0.80 | 0.26 | 0.0 | 0.0 | .89 | -0.33 | 0.45 | -1.50 | 0.87 |
| -.09 | 0.74 | 0.22 | 1.50 | 0.62 | .91 | 0.0 | 0.0 | -1.50 | 0.62 |
| -.07 | 0.81 | 0.20 | 0.49 | 0.71 | .93 | 0.0 | 0.0 | 0.0 | 0.0 |
| -.05 | 0.64 | 0.20 | 1.50 | 0.87 | .95 | 0.0 | 0.0 | 0.0 | 0.0 |
| -.03 | 0.95 | 0.18 | 1.50 | 0.87 | .97 | 0.0 | 0.0 | 0.0 | 0.0 |
| -.01 | 1.12 | 0.21 | 0.0 | 0.0 | .99 | 0.0 | 0.0 | 0.0 | 0.0 |

POINTS GIVEN AS 0.0+-0.0 HAVE NO DATA

INCIDENT MOMENTUM 1.23 GEV/C

| COS(θ*) | PIPI POLN | | KK POLN | | COS(θ*) | PIPI POLN | | KK POLN | |
|---|---|---|---|---|---|---|---|---|---|
| -.99 | 0.0 | 0.0 | 0.0 | 0.0 | .01 | 0.70 | 0.10 | 0.06 | 0.57 |
| -.97 | 0.0 | 0.0 | -0.09 | 0.70 | .03 | 0.74 | 0.12 | 1.08 | 0.31 |
| -.95 | 0.35 | 0.28 | 1.67 | 0.49 | .05 | 0.89 | 0.11 | 0.62 | 0.42 |
| -.93 | 0.25 | 0.15 | 0.94 | 0.55 | .07 | 0.85 | 0.12 | 0.62 | 0.72 |
| -.91 | 0.08 | 0.16 | 0.47 | 0.80 | .09 | 0.78 | 0.12 | 0.98 | 0.29 |
| -.89 | 0.07 | 0.13 | 0.76 | 0.65 | .11 | 1.00 | 0.12 | 0.41 | 0.42 |
| -.87 | 0.08 | 0.14 | -0.09 | 0.98 | .13 | 0.72 | 0.13 | 1.29 | 0.34 |
| -.85 | 0.62 | 0.12 | 0.47 | 0.80 | .15 | 0.89 | 0.13 | 1.25 | 0.36 |
| -.83 | 0.51 | 0.13 | 1.06 | 0.48 | .17 | 1.07 | 0.11 | 1.61 | 0.27 |
| -.81 | 0.42 | 0.13 | 0.0 | 0.0 | .19 | 1.00 | 0.12 | 0.76 | 0.45 |
| -.79 | 0.46 | 0.13 | 1.67 | 0.76 | .21 | 0.57 | 0.15 | 1.61 | 0.42 |
| -.77 | 0.33 | 0.13 | 1.14 | 0.44 | .23 | 0.50 | 0.17 | 1.25 | 0.36 |
| -.75 | 0.43 | 0.13 | 0.0 | 0.0 | .25 | 1.01 | 0.14 | 0.76 | 0.45 |
| -.73 | 0.27 | 0.14 | 1.14 | 0.44 | .27 | 0.64 | 0.17 | 0.87 | 0.40 |
| -.71 | 0.73 | 0.14 | 1.42 | 0.29 | .29 | 0.92 | 0.14 | 1.12 | 0.42 |
| -.69 | 0.57 | 0.15 | 1.36 | 0.33 | .31 | 0.79 | 0.17 | 0.76 | 0.45 |
| -.67 | 0.67 | 0.14 | 1.66 | 0.47 | .33 | 0.89 | 0.14 | 1.12 | 0.42 |
| -.65 | 0.93 | 0.14 | 1.67 | 0.49 | .35 | 1.12 | 0.12 | 1.19 | 0.28 |
| -.63 | 0.72 | 0.15 | 1.14 | 0.44 | .37 | 1.22 | 0.13 | 0.39 | 0.42 |
| -.61 | 0.53 | 0.21 | 1.38 | 0.32 | .39 | 0.91 | 0.15 | 0.70 | 0.34 |
| -.59 | 0.78 | 0.18 | 1.00 | 0.36 | .41 | 1.16 | 0.15 | 1.61 | 0.66 |
| -.57 | 0.70 | 0.21 | 0.47 | 0.56 | .43 | 1.01 | 0.13 | 1.25 | 0.36 |
| -.55 | 0.70 | 0.29 | 0.94 | 0.55 | .45 | 1.39 | 0.14 | 0.54 | 0.35 |
| -.53 | 0.90 | 0.26 | 1.67 | 0.62 | .47 | 0.93 | 0.15 | 0.74 | 0.38 |
| -.51 | -0.08 | 0.44 | 1.06 | 0.48 | .49 | 0.87 | 0.15 | -0.45 | 0.48 |
| -.49 | 0.0 | 0.0 | 1.67 | 0.62 | .51 | 0.93 | 0.15 | 1.44 | 0.26 |
| -.47 | -0.08 | 0.98 | 0.0 | 1.01 | .53 | 0.91 | 0.17 | 1.23 | 0.27 |
| -.45 | 1.50 | 0.54 | 1.67 | 1.07 | .55 | 1.12 | 0.22 | 1.67 | 1.07 |
| -.43 | -0.43 | 0.80 | 1.02 | 0.47 | .57 | 0.66 | 0.24 | 1.67 | 1.07 |
| -.41 | 0.57 | 0.51 | 1.61 | 0.66 | .59 | 0.56 | 0.33 | 0.76 | 0.65 |
| -.39 | 0.38 | 0.59 | 0.09 | 0.70 | .61 | -0.25 | 0.32 | 1.67 | 0.54 |
| -.37 | 0.25 | 0.45 | 0.62 | 0.51 | .63 | 0.54 | 0.25 | 1.06 | 0.48 |
| -.35 | 0.33 | 0.39 | 0.09 | 0.57 | .65 | 0.04 | 0.22 | -1.61 | 0.66 |
| -.33 | 0.27 | 0.34 | 0.09 | 0.70 | .67 | 0.49 | 0.31 | 1.67 | 1.07 |
| -.31 | 0.19 | 0.27 | 0.62 | 0.51 | .69 | 0.73 | 0.24 | -1.61 | 0.93 |
| -.29 | 0.66 | 0.27 | 0.36 | 0.39 | .71 | 0.29 | 0.23 | -0.09 | 0.98 |
| -.27 | -0.36 | 0.26 | 1.29 | 0.34 | .73 | -0.31 | 0.26 | 0.94 | 0.55 |
| -.25 | 0.49 | 0.21 | 1.12 | 0.42 | .75 | 0.00 | 0.23 | -0.09 | 0.98 |
| -.23 | 0.27 | 0.22 | 1.61 | 0.47 | .77 | 0.03 | 0.22 | 0.0 | 0.0 |
| -.21 | 0.22 | 0.19 | 0.72 | 0.38 | .79 | -0.32 | 0.24 | 1.67 | 0.76 |
| -.19 | 0.58 | 0.19 | 0.87 | 0.40 | .81 | -0.38 | 0.21 | -0.87 | 0.56 |
| -.17 | 0.21 | 0.16 | 1.19 | 0.40 | .83 | -0.55 | 0.18 | 1.67 | 0.45 |
| -.15 | 0.64 | 0.13 | 0.76 | 0.46 | .85 | -0.02 | 0.27 | 1.67 | 0.62 |
| -.13 | 0.38 | 0.15 | 1.62 | 0.38 | .87 | -0.87 | 0.19 | 0.0 | 0.0 |
| -.11 | 0.41 | 0.13 | 0.50 | 0.39 | .89 | -0.85 | 0.20 | 1.67 | 0.62 |
| -.09 | 0.55 | 0.13 | 0.17 | 0.36 | .91 | 0.70 | 0.65 | 0.24 | 0.63 |
| -.07 | 0.71 | 0.13 | 1.17 | 0.29 | .93 | 0.0 | 0.0 | 0.0 | 0.0 |
| -.05 | 0.22 | 0.14 | 0.34 | 0.36 | .95 | 0.0 | 0.0 | 0.0 | 0.0 |
| -.03 | 0.78 | 0.11 | 0.59 | 0.37 | .97 | 0.0 | 0.0 | 0.0 | 0.0 |
| -.01 | 0.75 | 0.11 | 1.19 | 0.38 | .99 | 0.0 | 0.0 | 0.0 | 0.0 |

POINTS GIVEN AS 0.0+-0.0 HAVE NO DATA

INCIDENT MOMENTUM 1.36 GEV/C

Table 2 contd.

| COS(θ*) | PIPI POLN | | KK POLN | | COS(θ*) | PIPI POLN | | KK POLN | |
|---|---|---|---|---|---|---|---|---|---|
| -.99 | 0.0 | 0.0 | 0.0 | 0.0 | .01 | 0.75 | 0.15 | 0.0 | 0.0 |
| -.97 | 0.0 | 0.0 | 1.57 | 0.92 | .03 | 0.70 | 0.16 | 0.47 | 0.70 |
| -.95 | 0.14 | 0.36 | 1.57 | 0.92 | .05 | 1.11 | 0.14 | 0.72 | 0.56 |
| -.93 | 0.61 | 0.20 | 1.57 | 0.92 | .07 | 0.65 | 0.19 | 1.48 | 0.44 |
| -.91 | 0.12 | 0.23 | 0.0 | 0.0 | .09 | 1.04 | 0.15 | 1.48 | 0.50 |
| -.89 | 0.07 | 0.22 | 1.57 | 0.92 | .11 | 1.04 | 0.17 | 0.0 | 0.0 |
| -.87 | 0.29 | 0.25 | -1.48 | 0.86 | .13 | 0.67 | 0.21 | 1.48 | 0.39 |
| -.85 | 0.40 | 0.24 | 1.57 | 0.92 | .15 | 0.63 | 0.20 | 0.88 | 0.46 |
| -.83 | 0.45 | 0.21 | 1.57 | 0.92 | .17 | 1.04 | 0.15 | 1.48 | 0.86 |
| -.81 | 0.93 | 0.18 | 1.57 | 0.65 | .19 | 0.94 | 0.15 | 1.48 | 0.86 |
| -.79 | 0.68 | 0.18 | 1.57 | 0.92 | .21 | 0.86 | 0.21 | 0.98 | 0.46 |
| -.77 | 0.52 | 0.19 | -1.48 | 0.86 | .23 | 0.69 | 0.21 | 1.48 | 0.61 |
| -.75 | 0.60 | 0.20 | 1.57 | 0.47 | .25 | 0.90 | 0.18 | 1.48 | 0.86 |
| -.73 | 0.76 | 0.22 | 0.0 | 0.0 | .27 | 0.75 | 0.21 | 0.72 | 0.56 |
| -.71 | 1.13 | 0.17 | 1.55 | 0.45 | .29 | 1.05 | 0.16 | 0.62 | 0.44 |
| -.69 | 0.72 | 0.18 | 0.0 | 0.95 | .31 | 0.84 | 0.22 | 1.48 | 0.61 |
| -.67 | 0.94 | 0.15 | 1.52 | 0.45 | .33 | 0.39 | 0.30 | 0.72 | 0.56 |
| -.65 | 0.63 | 0.24 | 1.51 | 0.52 | .35 | 0.79 | 0.24 | 1.48 | 0.50 |
| -.63 | 0.89 | 0.17 | 0.78 | 0.56 | .37 | 0.83 | 0.23 | 1.48 | 0.86 |
| -.61 | 0.95 | 0.18 | 0.52 | 0.70 | .39 | 0.89 | 0.20 | 1.51 | 0.52 |
| -.59 | 1.00 | 0.22 | 1.57 | 0.47 | .41 | 1.01 | 0.19 | -0.30 | 0.57 |
| -.57 | 0.55 | 0.28 | 0.54 | 0.50 | .43 | 0.86 | 0.22 | 1.52 | 0.63 |
| -.55 | 0.91 | 0.26 | 0.03 | 0.65 | .45 | 0.87 | 0.22 | 1.48 | 0.34 |
| -.53 | 0.56 | 0.30 | 0.80 | 0.57 | .47 | 1.41 | 0.22 | 1.48 | 0.61 |
| -.51 | 0.50 | 0.32 | 1.13 | 0.38 | .49 | 0.58 | 0.38 | 1.48 | 0.61 |
| -.49 | 1.04 | 0.36 | 1.57 | 0.47 | .51 | 0.59 | 0.38 | 0.0 | 0.0 |
| -.47 | 0.30 | 0.58 | 0.0 | 0.0 | .53 | 0.74 | 0.40 | 0.0 | 0.0 |
| -.45 | 1.45 | 0.87 | 0.0 | 0.0 | .55 | 0.74 | 0.40 | 0.0 | 0.0 |
| -.43 | 1.36 | 0.57 | 1.48 | 0.61 | .57 | 1.13 | 0.31 | 0.0 | 0.0 |
| -.41 | 0.81 | 0.46 | 0.0 | 0.0 | .59 | 0.55 | 0.28 | 0.0 | 0.0 |
| -.39 | 0.90 | 0.39 | 1.48 | 0.61 | .61 | 1.13 | 0.22 | 0.0 | 0.0 |
| -.37 | 0.32 | 0.44 | 0.0 | 0.0 | .63 | 0.31 | 0.40 | 0.0 | 0.0 |
| -.35 | -0.03 | 0.53 | -0.03 | 0.92 | .65 | 0.31 | 0.40 | -1.48 | 0.86 |
| -.33 | -0.16 | 0.39 | 1.48 | 0.50 | .67 | 0.50 | 0.29 | 0.0 | 0.0 |
| -.31 | -0.50 | 0.41 | 0.72 | 0.40 | .69 | 1.09 | 0.33 | 0.0 | 0.0 |
| -.29 | 0.67 | 0.39 | 1.48 | 0.39 | .71 | 0.50 | 0.29 | -1.48 | 0.86 |
| -.27 | 0.17 | 0.49 | 0.72 | 0.56 | .73 | 0.64 | 0.32 | 1.52 | 0.63 |
| -.25 | 0.12 | 0.30 | 1.48 | 0.61 | .75 | 0.82 | 0.20 | 1.52 | 0.63 |
| -.23 | -0.36 | 0.35 | -0.03 | 0.53 | .77 | 0.61 | 0.24 | 1.52 | 0.63 |
| -.21 | 0.20 | 0.37 | 0.18 | 0.49 | .79 | -0.72 | 0.30 | 1.48 | 0.86 |
| -.19 | 1.18 | 0.23 | 1.48 | 0.61 | .81 | -0.67 | 0.39 | 1.57 | 0.92 |
| -.17 | 0.07 | 0.24 | 1.48 | 0.86 | .83 | 0.88 | 0.33 | 0.0 | 0.0 |
| -.15 | -0.01 | 0.40 | 1.05 | 0.36 | .85 | -0.29 | 0.35 | 0.54 | 0.71 |
| -.13 | 0.20 | 0.22 | 0.27 | 0.57 | .87 | -0.60 | 0.35 | 0.0 | 0.0 |
| -.11 | 0.40 | 0.17 | 1.05 | 0.36 | .89 | 0.31 | 0.57 | 0.0 | 0.0 |
| -.09 | 0.56 | 0.16 | 0.88 | 0.46 | .91 | -0.81 | 0.46 | 0.03 | 0.92 |
| -.07 | 0.48 | 0.17 | -0.03 | 0.53 | .93 | -1.36 | 0.80 | 1.57 | 0.92 |
| -.05 | 0.14 | 0.18 | 0.98 | 0.40 | .95 | 0.0 | 0.0 | 0.0 | 0.0 |
| -.03 | 0.85 | 0.14 | 0.28 | 0.57 | .97 | 0.0 | 0.0 | 0.0 | 0.0 |
| -.01 | 0.62 | 0.16 | 0.19 | 0.48 | .99 | 0.0 | 0.0 | 0.0 | 0.0 |

POINTS GIVEN AS 0.0+-0.0 HAVE NO DATA

Table 2 contd.

INCIDENT MOMENTUM 1.43 GEV/C

| COS(θ*) | PIPI POLN | | KK POLN | | COS(θ*) | PIPI POLN | | KK POLN | |
|---|---|---|---|---|---|---|---|---|---|
| -.99 | 0.0 | 0.0 | 0.0 | 0.0 | .01 | 0.44 | 0.20 | -0.01 | 1.02 |
| -.97 | 0.0 | 0.0 | 0.0 | 0.0 | .03 | 0.68 | 0.19 | -0.01 | 0.51 |
| -.95 | -0.14 | 0.44 | 0.01 | 1.02 | .05 | 0.71 | 0.19 | 0.56 | 0.56 |
| -.93 | 0.32 | 0.32 | 0.0 | 0.0 | .07 | 1.08 | 0.18 | -0.57 | 0.79 |
| -.91 | -0.08 | 0.33 | 0.0 | 0.0 | .09 | 0.96 | 0.22 | -0.01 | 0.72 |
| -.89 | 0.28 | 0.26 | 0.0 | 0.0 | .11 | 1.24 | 0.20 | -0.01 | 0.51 |
| -.87 | 0.43 | 0.24 | -1.69 | 1.04 | .13 | 0.57 | 0.23 | -0.35 | 0.63 |
| -.85 | 0.48 | 0.31 | 1.70 | 0.74 | .15 | 0.54 | 0.21 | 0.33 | 0.64 |
| -.83 | 0.76 | 0.24 | -1.69 | 1.04 | .17 | 1.18 | 0.19 | 1.69 | 0.61 |
| -.81 | 0.07 | 0.30 | 1.70 | 0.74 | .19 | 1.21 | 0.20 | 0.56 | 0.56 |
| -.79 | 0.74 | 0.23 | 1.70 | 0.74 | .21 | 0.63 | 0.25 | 0.84 | 0.63 |
| -.77 | 0.81 | 0.20 | 1.70 | 0.74 | .23 | 1.13 | 0.20 | -0.57 | 0.79 |
| -.75 | 0.68 | 0.25 | 0.57 | 0.79 | .25 | 1.21 | 0.25 | -0.35 | 0.63 |
| -.73 | 0.97 | 0.22 | 1.70 | 0.53 | .27 | 0.60 | 0.26 | -0.19 | 0.48 |
| -.71 | 0.94 | 0.17 | 0.84 | 0.63 | .29 | 0.82 | 0.30 | 0.0 | 0.0 |
| -.69 | 0.71 | 0.20 | 1.70 | 0.44 | .31 | 0.67 | 0.29 | 0.39 | 0.39 |
| -.67 | 1.01 | 0.18 | 0.57 | 0.79 | .33 | 0.74 | 0.29 | 0.85 | 0.63 |
| -.65 | 1.01 | 0.17 | -0.85 | 0.63 | .35 | 1.15 | 0.22 | 1.02 | 0.52 |
| -.63 | 0.98 | 0.20 | 0.00 | 0.72 | .37 | 1.10 | 0.21 | -0.00 | 0.59 |
| -.61 | 1.24 | 0.17 | 1.70 | 0.74 | .39 | 1.14 | 0.23 | 0.56 | 0.79 |
| -.59 | 1.57 | 0.22 | 1.03 | 0.52 | .41 | 0.99 | 0.22 | 0.72 | 0.50 |
| -.57 | 1.07 | 0.22 | 1.70 | 0.53 | .43 | 0.81 | 0.25 | 1.70 | 1.05 |
| -.55 | 0.88 | 0.28 | 1.70 | 0.53 | .45 | 0.97 | 0.25 | 0.0 | 1.03 |
| -.53 | 0.86 | 0.26 | 1.70 | 1.05 | .47 | 0.63 | 0.42 | 1.70 | 1.05 |
| -.51 | 0.61 | 0.37 | 1.70 | 1.05 | .49 | 0.95 | 0.37 | 0.0 | 0.0 |
| -.49 | 0.53 | 0.32 | 0.86 | 0.63 | .51 | 0.95 | 0.26 | 0.0 | 0.0 |
| -.47 | 0.01 | 0.51 | 0.01 | 1.02 | .53 | 1.12 | 0.29 | 0.0 | 0.0 |
| -.45 | -0.22 | 0.54 | 0.57 | 0.79 | .55 | 0.90 | 0.32 | -1.69 | 1.04 |
| -.43 | 0.31 | 0.63 | 0.0 | 0.0 | .57 | 0.48 | 0.31 | 0.0 | 0.0 |
| -.41 | -1.57 | 0.50 | 1.70 | 0.61 | .59 | 0.79 | 0.31 | 0.0 | 0.0 |
| -.39 | -1.12 | 0.41 | 0.0 | 1.02 | .61 | 1.24 | 0.24 | 0.0 | 0.0 |
| -.37 | 0.93 | 0.52 | 1.69 | 1.04 | .63 | 0.35 | 0.33 | 0.0 | 0.0 |
| -.35 | 0.52 | 0.56 | 1.70 | 0.61 | .65 | 0.65 | 0.32 | 1.70 | 1.05 |
| -.33 | -0.01 | 0.34 | 0.56 | 0.56 | .67 | 1.05 | 0.32 | 0.0 | 0.0 |
| -.31 | 0.38 | 0.50 | 1.69 | 0.61 | .69 | 0.28 | 0.35 | 0.0 | 0.0 |
| -.29 | 0.22 | 0.38 | 1.21 | 0.43 | .71 | 0.48 | 0.29 | 1.69 | 0.74 |
| -.27 | 0.62 | 0.42 | 0.72 | 0.50 | .73 | 0.64 | 0.23 | 1.13 | 0.47 |
| -.25 | -0.11 | 0.37 | 0.56 | 0.79 | .75 | 0.71 | 0.22 | 1.32 | 0.38 |
| -.23 | -0.01 | 0.34 | 1.69 | 0.74 | .77 | 0.58 | 0.31 | 0.84 | 0.45 |
| -.21 | -0.16 | 0.32 | -0.20 | 0.48 | .79 | -0.22 | 0.38 | 0.0 | 1.02 |
| -.19 | 0.07 | 0.32 | 0.33 | 0.64 | .81 | -0.31 | 0.45 | 0.0 | 0.0 |
| -.17 | 0.38 | 0.29 | -0.01 | 1.02 | .83 | -0.25 | 0.41 | 0.0 | 0.0 |
| -.15 | 0.61 | 0.28 | 1.12 | 0.47 | .85 | -0.22 | 0.54 | 0.69 | 0.42 |
| -.13 | 0.81 | 0.25 | 1.12 | 0.47 | .87 | 0.15 | 0.43 | 0.0 | 0.0 |
| -.11 | 0.14 | 0.25 | 0.33 | 0.64 | .89 | -0.78 | 0.44 | 0.01 | 1.02 |
| -.09 | 0.44 | 0.20 | 1.01 | 0.52 | .91 | 0.53 | 0.46 | 0.57 | 0.56 |
| -.07 | 0.52 | 0.18 | 0.84 | 0.63 | .93 | 0.01 | 1.02 | -0.56 | 0.56 |
| -.05 | 0.46 | 0.19 | 0.94 | 0.41 | .95 | 0.0 | 0.0 | 0.0 | 0.0 |
| -.03 | 0.52 | 0.17 | 1.01 | 0.37 | .97 | 0.0 | 0.0 | 0.0 | 0.0 |
| -.01 | 0.56 | 0.19 | 1.69 | 1.04 | .99 | 0.0 | 0.0 | 0.0 | 0.0 |

POINTS GIVEN AS 0.0+-0.0 HAVE NO DATA

INCIDENT MOMENTUM 1.60 GEV/C

Table 2 contd.

| COS(θ*) | PIPI POLN | | KK POLN | | COS(θ*) | PIPI POLN | | KK POLN | |
|---|---|---|---|---|---|---|---|---|---|
| -.99 | 0.0 | 0.0 | 0.0 | 0.0 | .01 | 0.70 | 0.12 | 0.71 | 0.29 |
| -.97 | -1.46 | 0.83 | -1.58 | 0.88 | .03 | 0.65 | 0.14 | 0.79 | 0.30 |
| -.95 | -0.60 | 0.40 | 0.0 | 0.0 | .05 | 0.72 | 0.15 | 0.00 | 0.41 |
| -.93 | -0.49 | 0.44 | 0.39 | 0.77 | .07 | 0.60 | 0.15 | 1.39 | 0.26 |
| -.91 | -0.13 | 0.33 | 1.57 | 1.01 | .09 | 0.59 | 0.16 | 0.73 | 0.32 |
| -.89 | 0.45 | 0.28 | 1.57 | 1.01 | .11 | 0.66 | 0.15 | 1.10 | 0.24 |
| -.87 | 0.65 | 0.25 | 1.57 | 0.59 | .13 | 0.85 | 0.13 | 1.10 | 0.24 |
| -.85 | 1.13 | 0.16 | 0.39 | 0.77 | .15 | 0.67 | 0.14 | 0.50 | 0.35 |
| -.83 | 0.85 | 0.22 | 0.39 | 0.77 | .17 | 0.64 | 0.17 | 0.75 | 0.36 |
| -.81 | 1.03 | 0.15 | 0.0 | 0.0 | .19 | 1.08 | 0.15 | 0.82 | 0.27 |
| -.79 | 1.30 | 0.15 | 1.57 | 0.72 | .21 | 0.89 | 0.15 | 0.83 | 0.34 |
| -.77 | 0.98 | 0.13 | 0.85 | 0.54 | .23 | 1.16 | 0.14 | 0.45 | 0.57 |
| -.75 | 0.95 | 0.12 | 1.29 | 0.32 | .25 | 0.86 | 0.16 | 0.50 | 0.27 |
| -.73 | 1.02 | 0.10 | 1.04 | 0.30 | .27 | 0.75 | 0.16 | 0.98 | 0.33 |
| -.71 | 1.02 | 0.09 | 1.24 | 0.25 | .29 | 0.98 | 0.14 | 0.99 | 0.27 |
| -.69 | 1.18 | 0.09 | 0.57 | 0.42 | .31 | 0.94 | 0.12 | 0.60 | 0.32 |
| -.67 | 0.85 | 0.11 | 0.47 | 0.34 | .33 | 0.60 | 0.20 | 0.91 | 0.26 |
| -.65 | 0.90 | 0.10 | 0.79 | 0.34 | .35 | 0.83 | 0.15 | 0.78 | 0.34 |
| -.63 | 1.11 | 0.09 | 0.57 | 0.41 | .37 | 1.06 | 0.15 | 1.21 | 0.36 |
| -.61 | 1.04 | 0.12 | 0.66 | 0.47 | .39 | 0.94 | 0.17 | -0.12 | 0.39 |
| -.59 | 1.13 | 0.13 | 0.75 | 0.43 | .41 | 1.08 | 0.19 | 0.55 | 0.49 |
| -.57 | 0.76 | 0.16 | 1.58 | 0.50 | .43 | 0.67 | 0.23 | -0.14 | 0.67 |
| -.55 | 0.86 | 0.15 | 0.97 | 0.46 | .45 | 1.19 | 0.20 | 0.17 | 0.61 |
| -.53 | 0.58 | 0.15 | 1.57 | 0.39 | .47 | 0.62 | 0.24 | -0.45 | 0.57 |
| -.51 | 0.75 | 0.16 | 1.57 | 0.72 | .49 | 0.78 | 0.24 | 1.57 | 0.37 |
| -.49 | 0.88 | 0.17 | 1.57 | 1.01 | .51 | 0.50 | 0.24 | 0.39 | 0.55 |
| -.47 | 0.36 | 0.19 | -0.14 | 0.95 | .53 | 1.06 | 0.17 | 0.91 | 0.35 |
| -.45 | 0.64 | 0.20 | 1.57 | 1.01 | .55 | 0.67 | 0.18 | 1.16 | 0.36 |
| -.43 | 0.41 | 0.24 | 1.57 | 0.59 | .57 | 0.78 | 0.18 | 1.57 | 0.42 |
| -.41 | 0.32 | 0.27 | 1.05 | 0.42 | .59 | 0.83 | 0.18 | 0.17 | 0.43 |
| -.39 | 0.99 | 0.28 | 0.86 | 0.38 | .61 | 1.00 | 0.14 | 1.57 | 0.46 |
| -.37 | 0.40 | 0.30 | 1.00 | 0.31 | .63 | 0.79 | 0.17 | 1.01 | 0.31 |
| -.35 | 0.00 | 0.28 | 0.73 | 0.45 | .65 | 1.04 | 0.14 | 0.91 | 0.35 |
| -.33 | 0.22 | 0.23 | 0.66 | 0.47 | .67 | 0.94 | 0.15 | 0.88 | 0.31 |
| -.31 | 0.83 | 0.24 | 1.58 | 0.34 | .69 | 0.89 | 0.12 | 1.00 | 0.27 |
| -.29 | 0.56 | 0.27 | 0.99 | 0.27 | .71 | 1.03 | 0.10 | 0.89 | 0.19 |
| -.27 | 0.10 | 0.21 | 1.58 | 0.25 | .73 | 0.82 | 0.12 | 0.79 | 0.19 |
| -.25 | 0.13 | 0.22 | 0.53 | 0.44 | .75 | 0.86 | 0.14 | 0.94 | 0.21 |
| -.23 | -0.36 | 0.21 | 0.97 | 0.34 | .77 | 0.89 | 0.13 | 0.72 | 0.20 |
| -.21 | 0.13 | 0.20 | 0.95 | 0.29 | .79 | 1.27 | 0.23 | 1.05 | 0.30 |
| -.19 | 0.47 | 0.19 | 0.94 | 0.26 | .81 | -0.01 | 0.28 | 1.58 | 0.44 |
| -.17 | 0.86 | 0.14 | 0.45 | 0.40 | .83 | 0.84 | 0.35 | 0.88 | 0.26 |
| -.15 | 0.56 | 0.16 | 0.97 | 0.34 | .85 | 1.07 | 0.34 | 0.97 | 0.27 |
| -.13 | 0.84 | 0.13 | 0.90 | 0.38 | .87 | 0.16 | 0.61 | 1.08 | 0.29 |
| -.11 | 0.67 | 0.16 | 0.65 | 0.49 | .89 | 0.97 | 0.40 | -1.58 | 0.88 |
| -.09 | 0.77 | 0.14 | 0.65 | 0.35 | .91 | 0.08 | 0.36 | 0.39 | 0.77 |
| -.07 | 0.58 | 0.14 | 0.79 | 0.30 | .93 | 0.62 | 0.63 | 0.14 | 0.33 |
| -.05 | 0.72 | 0.13 | 1.10 | 0.24 | .95 | 0.0 | 0.0 | 0.55 | 0.49 |
| -.03 | 0.52 | 0.12 | 0.90 | 0.27 | .97 | 0.0 | 0.0 | 0.0 | 0.0 |
| -.01 | 0.73 | 0.11 | 1.39 | 0.26 | .99 | 0.0 | 0.0 | 0.0 | 0.0 |

POINTS GIVEN AS 0.0+-0.0 HAVE NO DATA

INCIDENT MOMENTUM 1.70 GEV/C

Table 2 contd.

| COS(θ*) | PIPI POLN | | KK POLN | | COS(θ*) | PIPI POLN | | KK POLN | |
|---|---|---|---|---|---|---|---|---|---|
| -.99 | 0.0 | 0.0 | 0.0 | 0.0 | .01 | 0.80 | 0.24 | 0.45 | 0.67 |
| -.97 | 0.0 | 0.0 | 0.0 | 0.0 | .03 | 0.80 | 0.24 | -1.41 | 0.55 |
| -.95 | 0.0 | 0.0 | -1.41 | 0.57 | .05 | 0.54 | 0.30 | 1.41 | 0.80 |
| -.93 | 1.30 | 0.70 | 1.41 | 0.77 | .07 | 0.63 | 0.27 | -0.03 | 0.60 |
| -.91 | 0.0 | 0.0 | -1.41 | 0.80 | .09 | 1.05 | 0.17 | 1.41 | 0.47 |
| -.89 | 1.30 | 0.70 | 0.0 | 0.0 | .11 | 0.92 | 0.19 | 0.83 | 0.44 |
| -.87 | 0.0 | 0.0 | 0.03 | 0.85 | .13 | 0.94 | 0.22 | 1.41 | 0.57 |
| -.85 | 1.30 | 0.41 | 0.0 | 0.0 | .15 | 1.17 | 0.17 | -0.86 | 0.42 |
| -.83 | 0.99 | 0.27 | 0.0 | 0.0 | .17 | 0.19 | 0.35 | 0.45 | 0.67 |
| -.81 | 0.67 | 0.51 | 0.0 | 0.0 | .19 | 0.48 | 0.31 | 1.41 | 0.80 |
| -.79 | 0.80 | 0.30 | 0.03 | 0.85 | .21 | 0.41 | 0.30 | -0.03 | 0.60 |
| -.77 | 0.67 | 0.36 | -1.41 | 0.80 | .23 | 0.59 | 0.28 | 0.69 | 0.53 |
| -.75 | 1.04 | 0.17 | 1.41 | 0.77 | .25 | 0.63 | 0.31 | 1.41 | 0.80 |
| -.73 | 0.95 | 0.18 | 1.41 | 0.77 | .27 | 0.54 | 0.30 | -0.29 | 0.53 |
| -.71 | 0.80 | 0.19 | 1.41 | 0.57 | .29 | 0.92 | 0.33 | -0.49 | 0.65 |
| -.69 | 0.81 | 0.21 | 0.0 | 0.0 | .31 | 0.41 | 0.33 | 0.0 | 0.0 |
| -.67 | 0.83 | 0.20 | 0.46 | 0.66 | .33 | 0.20 | 0.34 | 1.41 | 0.46 |
| -.65 | 1.09 | 0.15 | 1.41 | 0.80 | .35 | 0.54 | 0.42 | 1.41 | 0.80 |
| -.63 | 0.71 | 0.28 | 1.41 | 0.77 | .37 | 0.66 | 0.51 | 1.41 | 0.55 |
| -.61 | 0.94 | 0.22 | 1.41 | 0.77 | .39 | 0.94 | 0.31 | 0.0 | 0.0 |
| -.59 | 0.74 | 0.23 | 0.72 | 0.51 | .41 | 0.46 | 0.37 | -1.41 | 0.80 |
| -.57 | 0.96 | 0.21 | 0.72 | 0.51 | .43 | 0.94 | 0.31 | 0.0 | 0.0 |
| -.55 | 1.02 | 0.25 | 1.41 | 0.55 | .45 | 1.30 | 0.29 | 1.41 | 0.55 |
| -.53 | 0.80 | 0.24 | 0.49 | 0.65 | .47 | 0.84 | 0.27 | 0.0 | 0.0 |
| -.51 | 1.13 | 0.19 | 1.41 | 0.77 | .49 | 0.99 | 0.27 | 0.0 | 0.0 |
| -.49 | 0.46 | 0.37 | 0.0 | 0.0 | .51 | 1.30 | 0.27 | -1.41 | 0.57 |
| -.47 | 1.07 | 0.22 | 0.0 | 0.0 | .53 | 0.80 | 0.42 | 0.31 | 0.52 |
| -.45 | 1.05 | 0.23 | 1.41 | 0.77 | .55 | 0.54 | 0.34 | 0.0 | 0.0 |
| -.43 | 1.30 | 0.29 | 1.41 | 0.55 | .57 | 0.54 | 0.34 | 0.0 | 0.0 |
| -.41 | 0.17 | 0.40 | 0.0 | 0.0 | .59 | 1.30 | 0.20 | 0.0 | 0.0 |
| -.39 | 0.66 | 0.37 | 1.41 | 0.77 | .61 | 1.15 | 0.18 | 0.0 | 0.0 |
| -.37 | 0.19 | 0.45 | 1.41 | 0.77 | .63 | 0.78 | 0.31 | 0.48 | 0.65 |
| -.35 | 1.30 | 0.42 | 1.41 | 0.77 | .65 | 1.00 | 0.19 | 1.41 | 0.36 |
| -.33 | 1.30 | 0.52 | 1.41 | 0.80 | .67 | 0.87 | 0.18 | 1.41 | 0.77 |
| -.31 | 0.0 | 0.0 | 1.41 | 0.33 | .69 | 0.84 | 0.22 | 0.45 | 0.67 |
| -.29 | 1.30 | 0.33 | 0.45 | 0.67 | .71 | 0.97 | 0.16 | 0.93 | 0.38 |
| -.27 | 0.41 | 0.38 | -0.03 | 0.85 | .73 | 0.78 | 0.22 | 0.16 | 0.40 |
| -.25 | -0.17 | 0.40 | 0.45 | 0.67 | .75 | 1.11 | 0.21 | 0.60 | 0.29 |
| -.23 | 0.92 | 0.33 | 0.0 | 0.0 | .77 | 1.07 | 0.23 | 0.84 | 0.31 |
| -.21 | 0.19 | 0.35 | 1.41 | 0.47 | .79 | 1.30 | 0.36 | 0.46 | 0.66 |
| -.19 | -0.17 | 0.40 | 0.0 | 0.0 | .81 | 1.30 | 0.70 | -1.41 | 0.77 |
| -.17 | 0.33 | 0.35 | 0.69 | 0.53 | .83 | 0.46 | 0.65 | 1.41 | 0.77 |
| -.15 | -0.12 | 0.33 | 0.83 | 0.44 | .85 | 1.30 | 0.70 | 0.49 | 0.65 |
| -.13 | 0.68 | 0.29 | 1.41 | 0.57 | .87 | 0.02 | 0.85 | 0.31 | 0.52 |
| -.11 | 0.30 | 0.42 | 0.69 | 0.53 | .89 | 1.30 | 0.70 | 1.41 | 0.77 |
| -.09 | 0.59 | 0.28 | 1.41 | 0.80 | .91 | 1.30 | 0.50 | 1.02 | 0.32 |
| -.07 | 0.41 | 0.30 | 0.83 | 0.44 | .93 | 0.80 | 0.42 | 0.86 | 0.42 |
| -.05 | 1.06 | 0.23 | 1.41 | 0.47 | .95 | 0.0 | 0.0 | -1.41 | 0.80 |
| -.03 | 0.42 | 0.30 | -0.03 | 0.85 | .97 | 0.0 | 0.0 | 0.0 | 0.0 |
| -.01 | 0.52 | 0.21 | 0.83 | 0.44 | .99 | 0.0 | 0.0 | 0.0 | 0.0 |

POINTS GIVEN AS 0.0+-0.0 HAVE NO DATA

INCIDENT MOMENTUM 1.80 GEV/C

Table 2 contd.

| COS(θ*) | PIPI POLN | | KK POLN | | COS(θ*) | PIPI POLN | | KK POLN | |
|---|---|---|---|---|---|---|---|---|---|
| -.99 | 0.0 | 0.0 | 0.0 | 0.0 | .01 | 0.44 | 0.22 | 0.07 | 0.57 |
| -.97 | 0.0 | 0.0 | 0.0 | 0.0 | .03 | 0.63 | 0.22 | 0.81 | 0.39 |
| -.95 | 0.0 | 0.0 | 1.74 | 1.00 | .05 | 0.49 | 0.26 | 0.42 | 0.50 |
| -.93 | 0.16 | 0.74 | -1.74 | 0.83 | .07 | 0.43 | 0.28 | 0.51 | 0.41 |
| -.91 | -1.60 | 1.13 | 0.0 | 0.0 | .09 | 1.03 | 0.19 | -1.74 | 0.71 |
| -.89 | 0.0 | 0.0 | 0.0 | 0.0 | .11 | 0.76 | 0.25 | 0.92 | 0.60 |
| -.87 | -1.60 | 0.80 | 0.18 | 1.04 | .13 | 1.14 | 0.19 | 1.22 | 0.45 |
| -.85 | 1.61 | 0.68 | 0.0 | 0.0 | .15 | 1.06 | 0.21 | 0.92 | 0.60 |
| -.83 | 1.61 | 0.56 | 0.18 | 0.74 | .17 | 0.77 | 0.26 | -0.18 | 0.52 |
| -.81 | 1.10 | 0.27 | 1.74 | 1.00 | .19 | 0.25 | 0.31 | 0.54 | 0.46 |
| -.79 | 1.16 | 0.25 | 0.0 | 1.05 | .21 | 0.81 | 0.22 | 1.22 | 0.45 |
| -.77 | 1.03 | 0.18 | -1.74 | 0.71 | .23 | 0.71 | 0.28 | 0.73 | 0.71 |
| -.75 | 1.17 | 0.19 | 0.66 | 0.78 | .25 | 0.59 | 0.31 | 1.74 | 1.17 |
| -.73 | 1.00 | 0.16 | 1.74 | 1.17 | .27 | 0.39 | 0.38 | 0.92 | 0.60 |
| -.71 | 0.84 | 0.18 | -1.74 | 1.17 | .29 | 0.32 | 0.29 | 1.74 | 0.83 |
| -.69 | 1.12 | 0.15 | 1.74 | 0.83 | .31 | 0.43 | 0.30 | 1.74 | 0.45 |
| -.67 | 1.13 | 0.14 | 1.74 | 0.71 | .33 | 0.99 | 0.30 | 1.74 | 1.17 |
| -.65 | 1.09 | 0.16 | 0.06 | 0.61 | .35 | 0.41 | 0.34 | 1.74 | 1.00 |
| -.63 | 1.18 | 0.13 | 1.74 | 0.55 | .37 | 0.68 | 0.38 | 0.0 | 0.0 |
| -.61 | 1.16 | 0.18 | 1.74 | 0.55 | .39 | 0.77 | 0.39 | 1.74 | 1.00 |
| -.59 | 0.82 | 0.19 | 1.38 | 0.40 | .41 | 0.92 | 0.26 | -1.74 | 1.17 |
| -.57 | 1.11 | 0.21 | 0.08 | 0.74 | .43 | 0.47 | 0.36 | 0.73 | 0.75 |
| -.55 | 0.92 | 0.21 | 1.74 | 0.71 | .45 | 1.06 | 0.24 | 0.0 | 0.0 |
| -.53 | 0.98 | 0.22 | 0.0 | 0.0 | .47 | 1.31 | 0.34 | -1.74 | 1.17 |
| -.51 | 0.88 | 0.20 | 1.74 | 1.00 | .49 | 1.01 | 0.23 | 0.0 | 0.0 |
| -.49 | 0.64 | 0.24 | 1.74 | 1.00 | .51 | 0.92 | 0.29 | 0.0 | 0.0 |
| -.47 | 1.26 | 0.22 | 1.74 | 1.00 | .53 | 0.92 | 0.22 | 1.00 | 0.58 |
| -.45 | 0.77 | 0.28 | -1.74 | 1.17 | .55 | 0.47 | 0.31 | 0.0 | 0.0 |
| -.43 | 1.20 | 0.23 | 0.0 | 0.0 | .57 | 0.83 | 0.24 | 0.0 | 0.0 |
| -.41 | 1.02 | 0.29 | 1.74 | 0.71 | .59 | 0.68 | 0.28 | 0.58 | 0.81 |
| -.39 | 0.97 | 0.27 | 0.0 | 0.0 | .61 | 0.86 | 0.19 | 1.74 | 0.42 |
| -.37 | 0.45 | 0.39 | 0.18 | 1.04 | .63 | 1.07 | 0.16 | 0.73 | 0.50 |
| -.35 | 0.57 | 0.39 | 1.74 | 0.59 | .65 | 0.70 | 0.18 | 1.21 | 0.35 |
| -.33 | 0.26 | 0.43 | 1.74 | 0.71 | .67 | 0.79 | 0.17 | 1.32 | 0.31 |
| -.31 | 1.60 | 0.31 | 0.78 | 0.69 | .69 | 0.96 | 0.16 | 1.42 | 0.34 |
| -.29 | 0.85 | 0.34 | 0.73 | 0.71 | .71 | 0.92 | 0.19 | 0.22 | 0.47 |
| -.27 | 1.31 | 0.33 | 0.92 | 0.60 | .73 | 1.08 | 0.20 | 0.44 | 0.44 |
| -.25 | 1.25 | 0.36 | 1.74 | 0.40 | .75 | 0.42 | 0.31 | 0.11 | 0.30 |
| -.23 | 1.60 | 0.36 | 0.07 | 0.57 | .77 | 0.91 | 0.26 | 0.64 | 0.30 |
| -.21 | 1.11 | 0.25 | 0.07 | 0.57 | .79 | 0.96 | 0.39 | 1.00 | 0.33 |
| -.19 | 0.58 | 0.27 | 1.74 | 0.40 | .81 | 1.61 | 0.56 | 1.74 | 0.83 |
| -.17 | 0.90 | 0.33 | 1.06 | 0.52 | .83 | 0.0 | 0.0 | -1.74 | 1.17 |
| -.15 | 0.55 | 0.27 | 1.06 | 0.52 | .85 | -1.60 | 1.13 | 0.33 | 0.43 |
| -.13 | 0.79 | 0.24 | 1.22 | 0.45 | .87 | -0.16 | 0.67 | 0.93 | 0.37 |
| -.11 | 1.02 | 0.24 | 1.39 | 0.36 | .89 | -1.60 | 1.13 | 0.18 | 1.04 |
| -.09 | 0.80 | 0.26 | 1.74 | 0.42 | .91 | -1.60 | 0.51 | 0.0 | 0.0 |
| -.07 | 0.59 | 0.25 | 1.15 | 0.48 | .93 | 0.47 | 0.62 | -0.42 | 0.61 |
| -.05 | 0.65 | 0.22 | -0.18 | 0.47 | .95 | 0.82 | 0.46 | -0.02 | 0.50 |
| -.03 | 0.76 | 0.22 | 0.73 | 0.71 | .97 | 0.0 | 0.0 | 0.0 | 0.0 |
| -.01 | 0.82 | 0.21 | 0.18 | 0.67 | .99 | 0.0 | 0.0 | 0.0 | 0.0 |

POINTS GIVEN AS 0.0+-0.0 HAVE NO DATA

INCIDENT MOMENTUM 1.90 GEV/C

Table 2 contd.

| COS(θ*) | PIPI POLN | | KK POLN | | COS(θ*) | PIPI POLN | | KK POLN | |
|---|---|---|---|---|---|---|---|---|---|
| -.99 | 0.0 | 0.0 | 0.0 | 0.0 | .01 | 0.86 | 0.22 | 0.90 | 0.47 |
| -.97 | 0.0 | 0.0 | 0.0 | 0.0 | .03 | 1.09 | 0.16 | 0.75 | 0.56 |
| -.95 | 1.47 | 0.64 | -1.50 | 0.88 | .05 | 0.75 | 0.21 | 1.07 | 0.36 |
| -.93 | -0.46 | 0.71 | 0.53 | 0.73 | .07 | 0.30 | 0.21 | 0.90 | 0.47 |
| -.91 | 1.47 | 0.64 | -1.50 | 0.88 | .09 | 0.61 | 0.19 | 1.13 | 0.34 |
| -.89 | 0.0 | 0.0 | 0.0 | 0.0 | .11 | 1.10 | 0.20 | -0.02 | 0.66 |
| -.87 | -0.46 | 0.71 | 1.59 | 0.95 | .13 | 0.98 | 0.16 | 1.50 | 0.40 |
| -.85 | 0.88 | 0.48 | -1.50 | 0.62 | .15 | 0.89 | 0.19 | 0.75 | 0.40 |
| -.83 | 0.49 | 0.42 | 0.02 | 0.93 | .17 | 0.87 | 0.25 | 1.07 | 0.36 |
| -.81 | 0.63 | 0.46 | 1.53 | 0.53 | .19 | 0.59 | 0.22 | 1.50 | 0.40 |
| -.79 | 1.19 | 0.28 | 0.0 | 0.0 | .21 | 0.64 | 0.23 | 0.75 | 0.40 |
| -.77 | 1.09 | 0.18 | 1.50 | 0.62 | .23 | 0.67 | 0.20 | -1.59 | 0.95 |
| -.75 | 1.11 | 0.13 | 1.50 | 0.88 | .25 | 0.69 | 0.23 | 1.50 | 0.51 |
| -.73 | 0.83 | 0.18 | 0.50 | 0.70 | .27 | 0.40 | 0.34 | 0.0 | 0.0 |
| -.71 | 1.15 | 0.13 | 1.55 | 0.46 | .29 | 0.63 | 0.35 | 0.01 | 0.67 |
| -.69 | 0.80 | 0.15 | 0.75 | 0.56 | .31 | 0.00 | 0.48 | 0.02 | 0.93 |
| -.67 | 0.88 | 0.14 | 0.31 | 0.58 | .33 | 0.82 | 0.37 | 1.59 | 0.67 |
| -.65 | 1.13 | 0.13 | 0.0 | 0.64 | .35 | 0.17 | 0.44 | 0.0 | 0.0 |
| -.63 | 0.93 | 0.13 | 0.0 | 0.0 | .37 | -0.31 | 0.35 | 0.0 | 0.0 |
| -.61 | 1.12 | 0.14 | 1.04 | 0.41 | .39 | 0.77 | 0.25 | 0.0 | 0.0 |
| -.59 | 0.92 | 0.16 | -0.02 | 0.66 | .41 | 0.88 | 0.24 | 0.0 | 0.0 |
| -.57 | 0.31 | 0.27 | 1.59 | 0.95 | .43 | 0.69 | 0.31 | 1.59 | 0.67 |
| -.55 | 1.19 | 0.19 | 0.0 | 0.0 | .45 | 1.07 | 0.25 | 0.02 | 0.93 |
| -.53 | 1.17 | 0.17 | 0.0 | 0.0 | .47 | 0.91 | 0.23 | 1.59 | 0.55 |
| -.51 | 0.96 | 0.19 | 1.59 | 0.95 | .49 | 1.09 | 0.17 | 0.80 | 0.58 |
| -.49 | 0.69 | 0.31 | 1.59 | 0.95 | .51 | 0.61 | 0.21 | 1.06 | 0.43 |
| -.47 | 1.07 | 0.25 | 1.59 | 0.55 | .53 | 0.62 | 0.22 | 1.59 | 0.48 |
| -.45 | 0.73 | 0.29 | 1.59 | 0.67 | .55 | 0.75 | 0.18 | 1.58 | 0.30 |
| -.43 | 0.49 | 0.36 | -1.50 | 0.88 | .57 | 1.12 | 0.16 | 1.06 | 0.43 |
| -.41 | 0.25 | 0.38 | 0.0 | 0.0 | .59 | 1.10 | 0.14 | 0.10 | 0.34 |
| -.39 | 0.88 | 0.48 | 0.0 | 0.0 | .61 | 0.63 | 0.15 | 0.42 | 0.27 |
| -.37 | 1.10 | 0.34 | 1.59 | 0.95 | .63 | 0.73 | 0.16 | 0.69 | 0.24 |
| -.35 | 1.18 | 0.27 | 0.02 | 0.93 | .65 | 0.80 | 0.15 | 0.57 | 0.28 |
| -.33 | 0.71 | 0.33 | 1.50 | 0.88 | .67 | 0.98 | 0.13 | 0.72 | 0.30 |
| -.31 | 0.85 | 0.27 | 0.50 | 0.71 | .69 | 0.82 | 0.19 | 1.23 | 0.29 |
| -.29 | 0.47 | 0.50 | 0.0 | 0.0 | .71 | 0.89 | 0.18 | 0.60 | 0.38 |
| -.27 | -0.01 | 0.66 | 0.75 | 0.56 | .73 | 0.83 | 0.17 | 1.27 | 0.26 |
| -.25 | 0.63 | 0.35 | 1.50 | 0.62 | .75 | 0.93 | 0.21 | 0.81 | 0.27 |
| -.23 | 0.77 | 0.36 | 1.50 | 0.45 | .77 | 1.43 | 0.33 | 0.98 | 0.21 |
| -.21 | 0.46 | 0.32 | 0.64 | 0.45 | .79 | 0.61 | 0.45 | 0.43 | 0.34 |
| -.19 | 0.34 | 0.45 | -0.53 | 0.73 | .81 | 1.47 | 0.90 | -0.26 | 0.38 |
| -.17 | 1.39 | 0.25 | 1.07 | 0.36 | .83 | -1.39 | 0.82 | 1.30 | 0.31 |
| -.15 | 0.77 | 0.25 | 0.64 | 0.45 | .85 | 0.01 | 0.93 | 0.20 | 0.26 |
| -.13 | 1.11 | 0.19 | 1.50 | 0.32 | .87 | -1.39 | 0.58 | 1.13 | 0.39 |
| -.11 | 0.80 | 0.24 | -0.02 | 0.54 | .89 | -0.19 | 0.35 | 0.33 | 0.58 |
| -.09 | 0.95 | 0.14 | 1.20 | 0.30 | .91 | -0.13 | 0.29 | 0.0 | 0.0 |
| -.07 | 0.61 | 0.23 | 0.16 | 0.44 | .93 | -0.63 | 0.35 | 0.02 | 0.66 |
| -.05 | 0.78 | 0.22 | 0.64 | 0.45 | .95 | 0.17 | 0.44 | -0.90 | 0.33 |
| -.03 | 0.53 | 0.24 | 1.15 | 0.24 | .97 | 0.0 | 0.0 | 0.0 | 0.0 |
| -.01 | 0.65 | 0.20 | 0.90 | 0.33 | .99 | 0.0 | 0.0 | 0.0 | 0.0 |

POINTS GIVEN AS 0.0+-0.0 HAVE NO DATA

INCIDENT MOMENTUM 1.99 GEV/C

Table 2 contd.

| COS(θ*) | PIPI POLN | | KK POLN | | COS(θ*) | PIPI POLN | | KK POLN | |
|---|---|---|---|---|---|---|---|---|---|
| -.99 | 0.0 | 0.0 | 0.0 | 0.0 | .01 | 0.59 | 0.17 | 1.12 | 0.28 |
| -.97 | 1.50 | 0.90 | -1.57 | 0.97 | .03 | 0.94 | 0.12 | 1.41 | 0.23 |
| -.95 | 0.87 | 0.26 | 1.63 | 0.95 | .05 | 0.76 | 0.13 | 0.38 | 0.36 |
| -.93 | 0.07 | 0.32 | 0.0 | 0.0 | .07 | 0.61 | 0.16 | 1.09 | 0.24 |
| -.91 | 0.94 | 0.33 | 0.08 | 0.96 | .09 | 0.69 | 0.15 | 0.90 | 0.23 |
| -.89 | -0.63 | 0.32 | -1.57 | 0.69 | .11 | 0.98 | 0.13 | 0.52 | 0.30 |
| -.87 | -0.18 | 0.28 | -1.57 | 0.57 | .13 | 0.74 | 0.16 | 1.23 | 0.24 |
| -.85 | -0.64 | 0.28 | -1.57 | 0.97 | .15 | 0.61 | 0.17 | 1.12 | 0.28 |
| -.83 | -0.02 | 0.33 | 0.0 | 0.0 | .17 | 0.73 | 0.16 | 1.41 | 0.23 |
| -.81 | 0.16 | 0.33 | 1.63 | 0.95 | .19 | 0.36 | 0.20 | 0.46 | 0.34 |
| -.79 | 0.66 | 0.19 | -1.63 | 0.67 | .21 | 1.04 | 0.14 | 0.73 | 0.43 |
| -.77 | 0.54 | 0.17 | -0.08 | 0.96 | .23 | 0.85 | 0.15 | 0.90 | 0.51 |
| -.75 | 0.85 | 0.13 | 1.57 | 0.97 | .25 | 1.01 | 0.27 | -0.08 | 0.96 |
| -.73 | 1.00 | 0.11 | 0.56 | 0.73 | .27 | 0.49 | 0.28 | 1.57 | 0.97 |
| -.71 | 0.96 | 0.11 | 0.04 | 0.68 | .29 | 0.67 | 0.33 | 1.63 | 0.95 |
| -.69 | 0.91 | 0.10 | 1.60 | 0.68 | .31 | 0.69 | 0.32 | 0.08 | 0.68 |
| -.67 | 1.13 | 0.10 | 0.48 | 0.54 | .33 | 1.02 | 0.18 | 1.63 | 0.43 |
| -.65 | 0.98 | 0.11 | 0.34 | 0.47 | .35 | 0.67 | 0.21 | 1.12 | 0.31 |
| -.63 | 1.00 | 0.09 | 0.46 | 0.76 | .37 | 0.64 | 0.18 | 0.09 | 0.48 |
| -.61 | 1.11 | 0.10 | -0.08 | 0.96 | .39 | 0.58 | 0.20 | 0.86 | 0.41 |
| -.59 | 1.09 | 0.11 | 0.97 | 0.35 | .41 | 0.57 | 0.16 | 0.60 | 0.42 |
| -.57 | 1.13 | 0.11 | 1.60 | 0.68 | .43 | 0.82 | 0.14 | 1.12 | 0.31 |
| -.55 | 1.12 | 0.16 | 0.86 | 0.41 | .45 | 0.64 | 0.15 | 0.86 | 0.58 |
| -.53 | 0.98 | 0.16 | 1.24 | 0.36 | .47 | 0.40 | 0.16 | 1.63 | 0.35 |
| -.51 | 1.05 | 0.15 | 0.25 | 0.45 | .49 | 0.62 | 0.15 | 0.71 | 0.39 |
| -.49 | 1.09 | 0.15 | 1.63 | 0.43 | .51 | 0.84 | 0.12 | 0.60 | 0.52 |
| -.47 | 1.02 | 0.18 | 0.60 | 0.73 | .53 | 0.60 | 0.15 | 1.33 | 0.30 |
| -.45 | 0.94 | 0.19 | 1.63 | 0.33 | .55 | 0.69 | 0.11 | 0.86 | 0.28 |
| -.43 | 0.87 | 0.21 | 0.08 | 0.68 | .57 | 0.70 | 0.10 | 0.69 | 0.27 |
| -.41 | 0.56 | 0.33 | 0.86 | 0.41 | .59 | 0.70 | 0.09 | 0.72 | 0.20 |
| -.39 | 0.85 | 0.31 | 1.63 | 0.48 | .61 | 0.67 | 0.10 | 1.20 | 0.18 |
| -.37 | 0.83 | 0.27 | 1.25 | 0.36 | .63 | 0.67 | 0.09 | 0.63 | 0.22 |
| -.35 | 1.16 | 0.19 | 1.63 | 0.55 | .65 | 0.80 | 0.10 | 0.84 | 0.20 |
| -.33 | 0.75 | 0.26 | 1.63 | 0.95 | .67 | 0.69 | 0.13 | 1.18 | 0.17 |
| -.31 | -0.03 | 0.29 | 0.25 | 0.60 | .69 | 0.69 | 0.11 | 1.15 | 0.20 |
| -.29 | 0.60 | 0.28 | 1.57 | 0.49 | .71 | 0.24 | 0.14 | 0.56 | 0.18 |
| -.27 | 1.03 | 0.25 | 1.23 | 0.33 | .73 | 0.75 | 0.13 | 0.44 | 0.18 |
| -.25 | 0.83 | 0.29 | 0.73 | 0.43 | .75 | 0.74 | 0.17 | 0.86 | 0.15 |
| -.23 | 0.89 | 0.19 | 0.90 | 0.30 | .77 | 0.44 | 0.22 | 1.17 | 0.17 |
| -.21 | 0.51 | 0.21 | 0.80 | 0.33 | .79 | 0.63 | 0.25 | 0.70 | 0.24 |
| -.19 | 0.70 | 0.20 | 0.85 | 0.31 | .81 | 0.18 | 0.41 | 1.12 | 0.23 |
| -.17 | 0.97 | 0.16 | 0.83 | 0.23 | .83 | 0.56 | 0.73 | 0.61 | 0.22 |
| -.15 | 0.82 | 0.17 | 1.12 | 0.28 | .85 | -1.45 | 0.41 | 0.25 | 0.26 |
| -.13 | 0.65 | 0.16 | 1.01 | 0.31 | .87 | -0.76 | 0.28 | 0.16 | 0.31 |
| -.11 | 0.92 | 0.18 | 0.85 | 0.31 | .89 | 0.22 | 0.25 | 0.75 | 0.46 |
| -.09 | 0.63 | 0.16 | 0.87 | 0.27 | .91 | -0.52 | 0.20 | 0.0 | 0.0 |
| -.07 | 0.50 | 0.16 | 1.33 | 0.21 | .93 | -0.34 | 0.18 | 0.03 | 0.29 |
| -.05 | 0.74 | 0.16 | 1.04 | 0.25 | .95 | -0.23 | 0.23 | -0.46 | 0.31 |
| -.03 | 0.68 | 0.16 | 0.62 | 0.28 | .97 | 1.50 | 0.90 | 0.08 | 0.96 |
| -.01 | 0.70 | 0.15 | 0.53 | 0.32 | .99 | 0.0 | 0.0 | 0.0 | 0.0 |

POINTS GIVEN AS 0.0+-0.0 HAVE NO DATA

INCIDENT MOMENTUM 2.20 GEV/C

| COS(θ*) | PIPI POLN | | KK POLN | | COS(θ*) | PIPI POLN | | KK POLN | |
|---|---|---|---|---|---|---|---|---|---|
| -.99 | 0.0 | 0.0 | -1.51 | 0.88 | .01 | 0.94 | 0.22 | 1.51 | 0.29 |
| -.97 | 0.49 | 0.51 | 0.0 | 0.0 | .03 | 0.68 | 0.23 | 0.74 | 0.40 |
| -.95 | 0.38 | 0.32 | 0.0 | 0.0 | .05 | 0.88 | 0.21 | 0.95 | 0.31 |
| -.93 | 0.41 | 0.38 | 1.56 | 0.92 | .07 | 0.79 | 0.29 | 0.74 | 0.40 |
| -.91 | -0.45 | 0.36 | 0.0 | 0.0 | .09 | 0.65 | 0.26 | 1.20 | 0.30 |
| -.89 | 0.63 | 0.45 | 0.0 | 0.0 | .11 | 0.96 | 0.18 | 1.51 | 0.37 |
| -.87 | 0.49 | 0.41 | -1.51 | 0.88 | .13 | 0.83 | 0.21 | 0.49 | 0.71 |
| -.85 | -0.68 | 0.40 | 1.53 | 0.64 | .15 | 0.87 | 0.20 | -0.33 | 0.57 |
| -.83 | 0.30 | 0.57 | 0.0 | 0.0 | .17 | 0.90 | 0.21 | 1.51 | 0.52 |
| -.81 | -0.28 | 0.57 | -1.56 | 0.54 | .19 | 1.04 | 0.31 | 0.0 | 0.0 |
| -.79 | -0.20 | 0.48 | 0.0 | 0.0 | .21 | 1.39 | 0.41 | 0.0 | 0.0 |
| -.77 | -0.47 | 0.50 | 1.56 | 0.92 | .23 | 0.0 | 0.0 | 1.56 | 0.38 |
| -.75 | 1.40 | 0.42 | -0.02 | 0.93 | .25 | 0.96 | 0.40 | 1.56 | 0.42 |
| -.73 | 1.04 | 0.24 | 1.51 | 0.88 | .27 | 0.02 | 0.93 | 0.95 | 0.47 |
| -.71 | 1.00 | 0.25 | 0.0 | 0.0 | .29 | 0.97 | 0.28 | -1.51 | 0.63 |
| -.69 | 0.77 | 0.23 | 1.00 | 0.41 | .31 | 1.25 | 0.23 | 1.56 | 0.92 |
| -.67 | 1.04 | 0.19 | -1.54 | 0.53 | .33 | -0.06 | 0.32 | 0.0 | 0.0 |
| -.65 | 0.96 | 0.22 | 0.49 | 0.71 | .35 | 0.09 | 0.29 | -1.51 | 0.88 |
| -.63 | 0.71 | 0.22 | 1.52 | 0.46 | .37 | 0.58 | 0.25 | -1.51 | 0.88 |
| -.61 | 0.68 | 0.22 | 1.51 | 0.88 | .39 | 0.68 | 0.23 | 0.54 | 0.71 |
| -.59 | 0.94 | 0.20 | 1.51 | 0.88 | .41 | 0.64 | 0.24 | 1.56 | 0.92 |
| -.57 | 0.83 | 0.22 | 1.51 | 0.88 | .43 | 0.84 | 0.19 | 0.0 | 0.0 |
| -.55 | 0.64 | 0.28 | 0.49 | 0.71 | .45 | 0.38 | 0.20 | 0.0 | 0.0 |
| -.53 | 1.02 | 0.20 | 0.66 | 0.46 | .47 | 0.53 | 0.18 | 1.51 | 0.88 |
| -.51 | 0.81 | 0.36 | 1.56 | 0.65 | .49 | 0.47 | 0.18 | 1.53 | 0.64 |
| -.49 | 0.81 | 0.36 | 1.56 | 0.65 | .51 | 0.60 | 0.13 | 0.67 | 0.45 |
| -.47 | 1.44 | 0.28 | 0.0 | 0.0 | .53 | 0.51 | 0.14 | 1.12 | 0.26 |
| -.45 | 1.22 | 0.25 | 0.0 | 0.0 | .55 | 0.52 | 0.13 | 0.91 | 0.47 |
| -.43 | 0.97 | 0.28 | 0.79 | 0.57 | .57 | 0.48 | 0.13 | 1.00 | 0.40 |
| -.41 | 0.97 | 0.40 | 0.54 | 0.71 | .59 | 0.63 | 0.12 | 1.51 | 0.37 |
| -.39 | 0.73 | 0.40 | 0.02 | 0.93 | .61 | 0.69 | 0.12 | 0.76 | 0.33 |
| -.37 | 1.44 | 0.39 | 1.56 | 0.92 | .63 | 0.80 | 0.12 | 0.91 | 0.28 |
| -.35 | 1.03 | 0.35 | 1.56 | 0.92 | .65 | 0.60 | 0.15 | 0.89 | 0.22 |
| -.33 | -0.26 | 0.57 | 0.54 | 0.71 | .67 | 0.41 | 0.16 | 0.56 | 0.31 |
| -.31 | 0.87 | 0.47 | 1.56 | 0.65 | .69 | 0.57 | 0.16 | 0.44 | 0.28 |
| -.29 | -0.27 | 0.57 | 1.54 | 0.53 | .71 | 0.43 | 0.20 | 0.91 | 0.28 |
| -.27 | 1.16 | 0.27 | -0.02 | 0.93 | .73 | 0.47 | 0.22 | 1.54 | 0.27 |
| -.25 | 1.00 | 0.34 | 1.52 | 0.46 | .75 | 1.08 | 0.22 | 0.46 | 0.30 |
| -.23 | 0.61 | 0.32 | 0.90 | 0.47 | .77 | 0.61 | 0.26 | 1.15 | 0.25 |
| -.21 | 0.83 | 0.27 | 1.51 | 0.45 | .79 | 0.77 | 0.31 | 0.67 | 0.28 |
| -.19 | 0.45 | 0.36 | -0.02 | 0.93 | .81 | 0.57 | 0.38 | 1.00 | 0.29 |
| -.17 | 0.68 | 0.28 | -0.02 | 0.65 | .83 | 0.40 | 0.38 | 0.20 | 0.49 |
| -.15 | 0.74 | 0.30 | 1.51 | 0.45 | .85 | 0.67 | 0.35 | 0.33 | 0.41 |
| -.13 | 0.30 | 0.35 | 0.49 | 0.71 | .87 | 0.49 | 0.32 | 1.12 | 0.38 |
| -.11 | 0.79 | 0.29 | 1.00 | 0.40 | .89 | -0.07 | 0.34 | 1.12 | 0.38 |
| -.09 | 0.35 | 0.29 | 1.51 | 0.34 | .91 | -0.48 | 0.23 | 1.56 | 0.54 |
| -.07 | 0.99 | 0.20 | 1.00 | 0.40 | .93 | -0.71 | 0.22 | 0.54 | 0.51 |
| -.05 | 1.04 | 0.31 | 1.20 | 0.30 | .95 | -0.66 | 0.22 | 0.72 | 0.36 |
| -.03 | 0.58 | 0.26 | 1.00 | 0.40 | .97 | -1.39 | 0.59 | 0.02 | 0.53 |
| -.01 | 0.73 | 0.27 | 0.15 | 0.43 | .99 | 0.0 | 0.0 | 0.0 | 0.0 |

POINTS GIVEN AS 0.0+-0.0 HAVE NO DATA

Figure 1

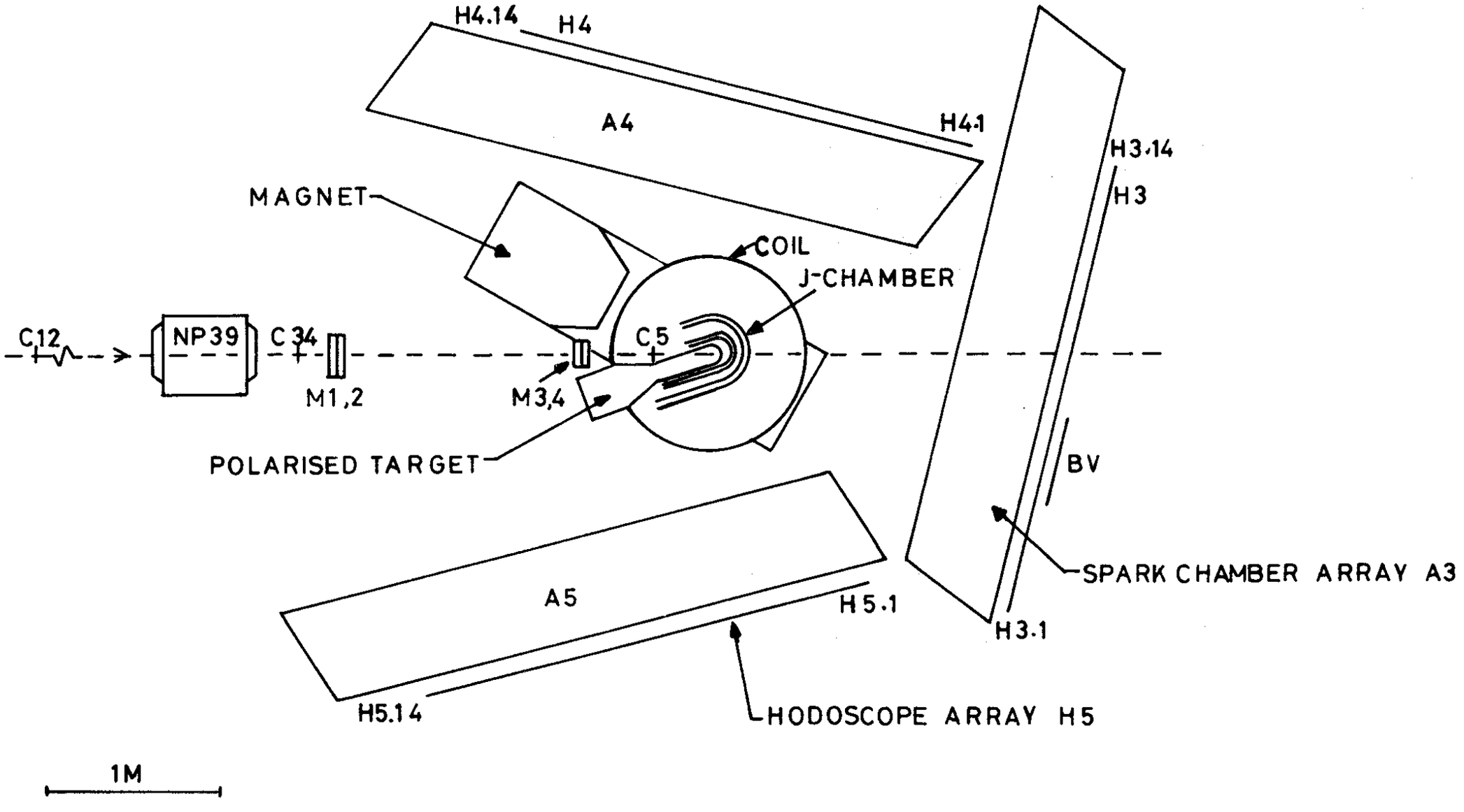
H4.14
H4
A4
H4.1
H3.14
H3
MAGNET
COIL
J-CHAMBER
C12
NP39
C34
C5
M1,2
M3,4
POLARISED TARGET
BV
SPARK CHAMBER ARRAY A3
A5
H5.1
H3.1
H5.14
HODOSCOPE ARRAY H5
1M

Figure 2

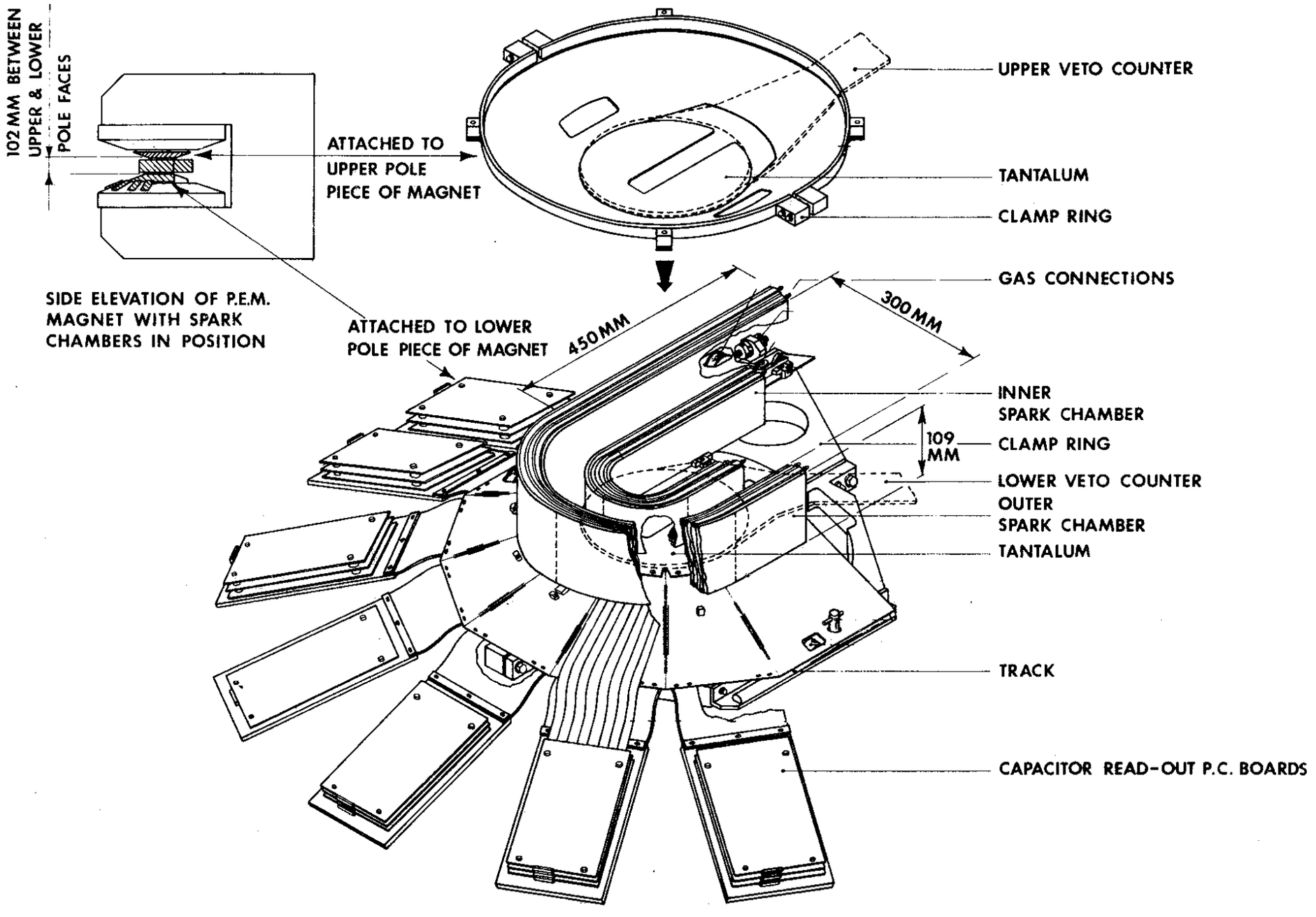
102 MM BETWEEN UPPER & LOWER POLE FACES
ATTACHED TO UPPER POLE PIECE OF MAGNET
SIDE ELEVATION OF P.E.M. MAGNET WITH SPARK CHAMBERS IN POSITION
ATTACHED TO LOWER POLE PIECE OF MAGNET
450 MM
300 MM
UPPER VETO COUNTER
TANTALUM
CLAMP RING
GAS CONNECTIONS
INNER SPARK CHAMBER
109 MM
CLAMP RING
LOWER VETO COUNTER
OUTER SPARK CHAMBER
TANTALUM
TRACK
CAPACITOR READ-OUT P.C. BOARDS

Figure 3

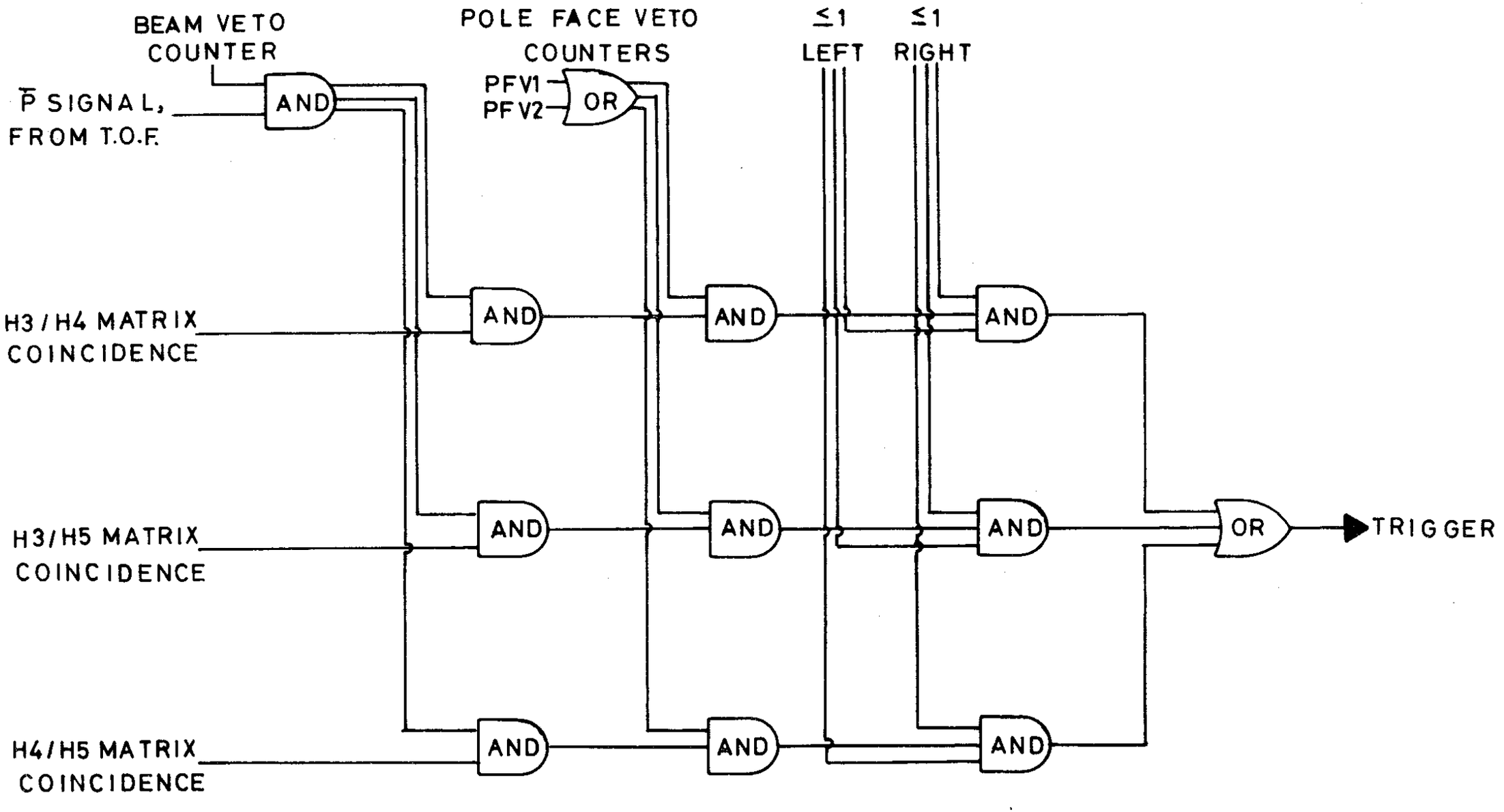
BEAM VETO COUNTER
POLE FACE VETO COUNTERS
≤1 LEFT
≤1 RIGHT
$\bar{P}$ SIGNAL, FROM T.O.F.
PFV1
PFV2
AND
OR
H3/H4 MATRIX COINCIDENCE
H3/H5 MATRIX COINCIDENCE
H4/H5 MATRIX COINCIDENCE
TRIGGER

Figure 4

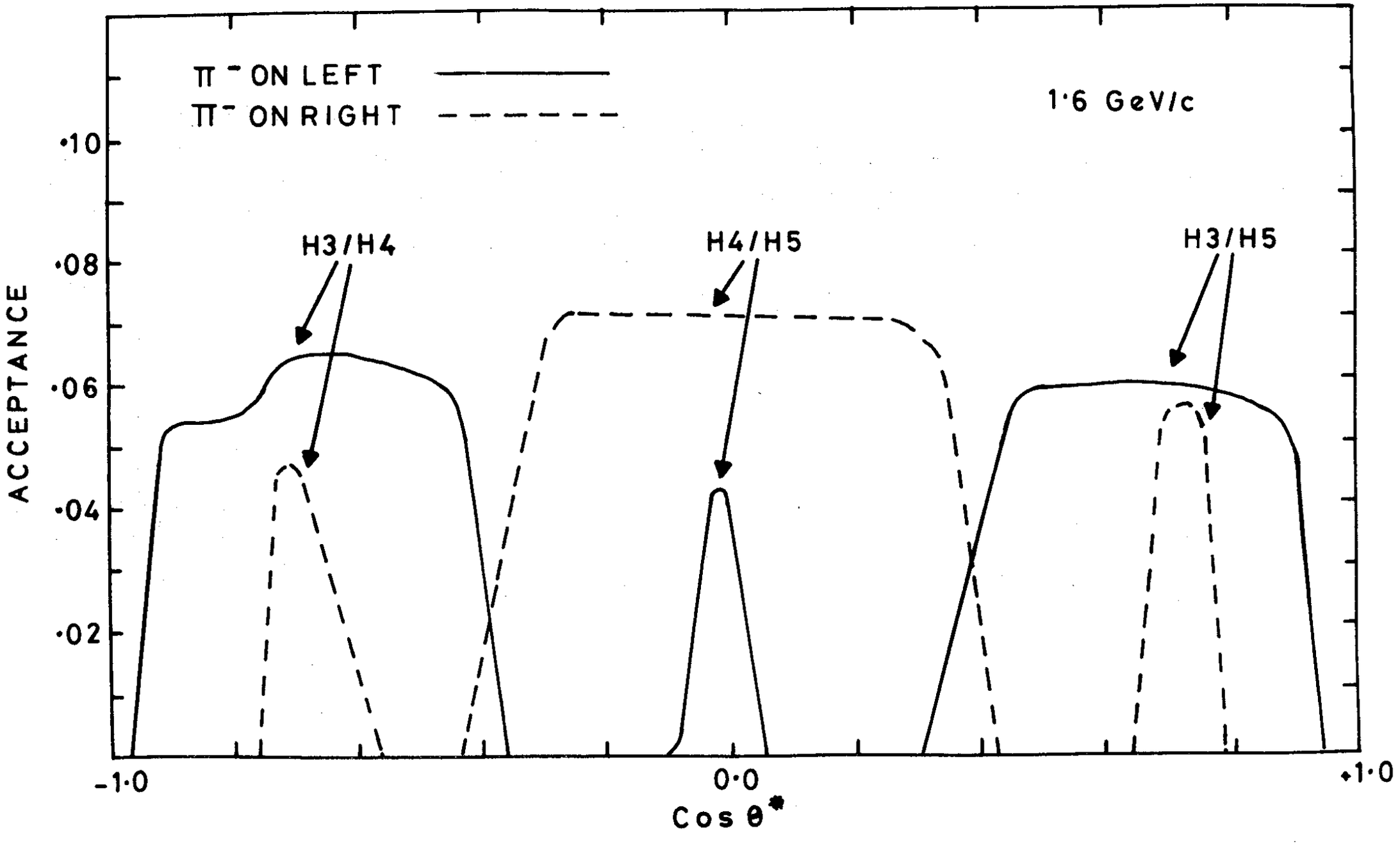
π⁻ ON LEFT
π⁻ ON RIGHT
1·6 GeV/c
H3/H4
H4/H5
H3/H5
ACCEPTANCE
·10
·08
·06
·04
·02
-1·0
0·0
+1·0
Cos θ*

Figure 5

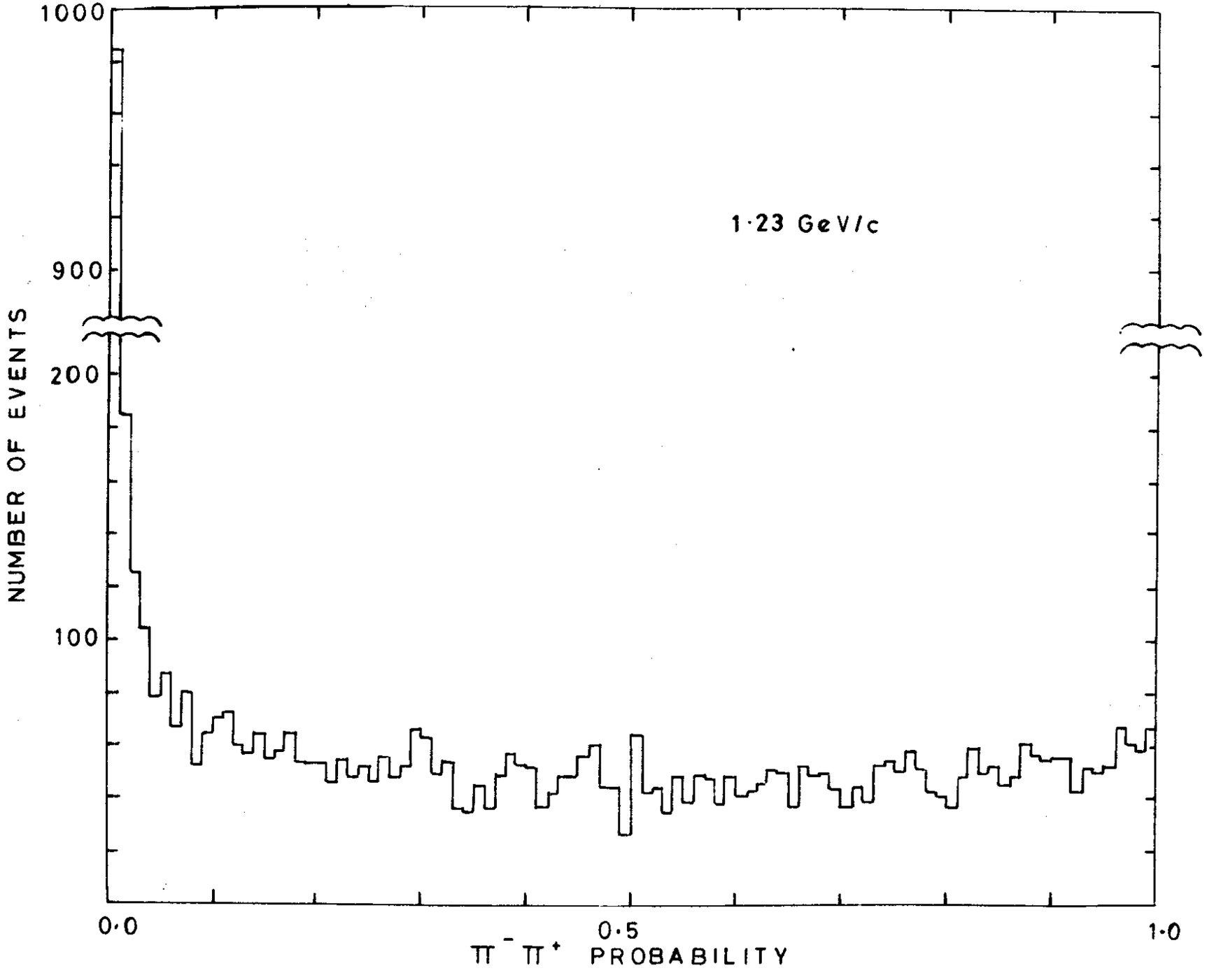
1000
900
200
100
NUMBER OF EVENTS
1·23 GeV/c
0·0
0·5
1·0
π⁻π⁺ PROBABILITY

Figure 6

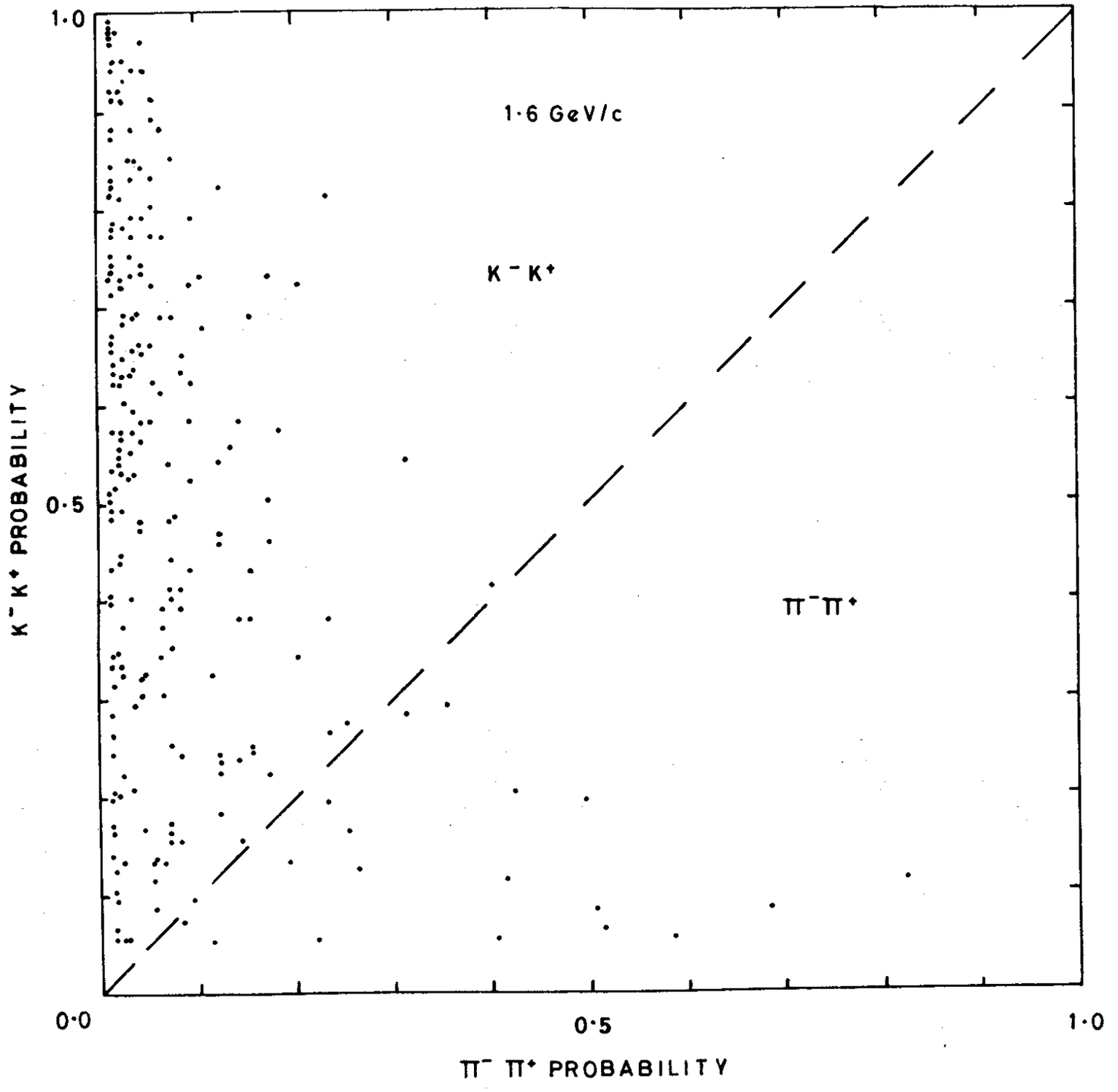

Figure 7

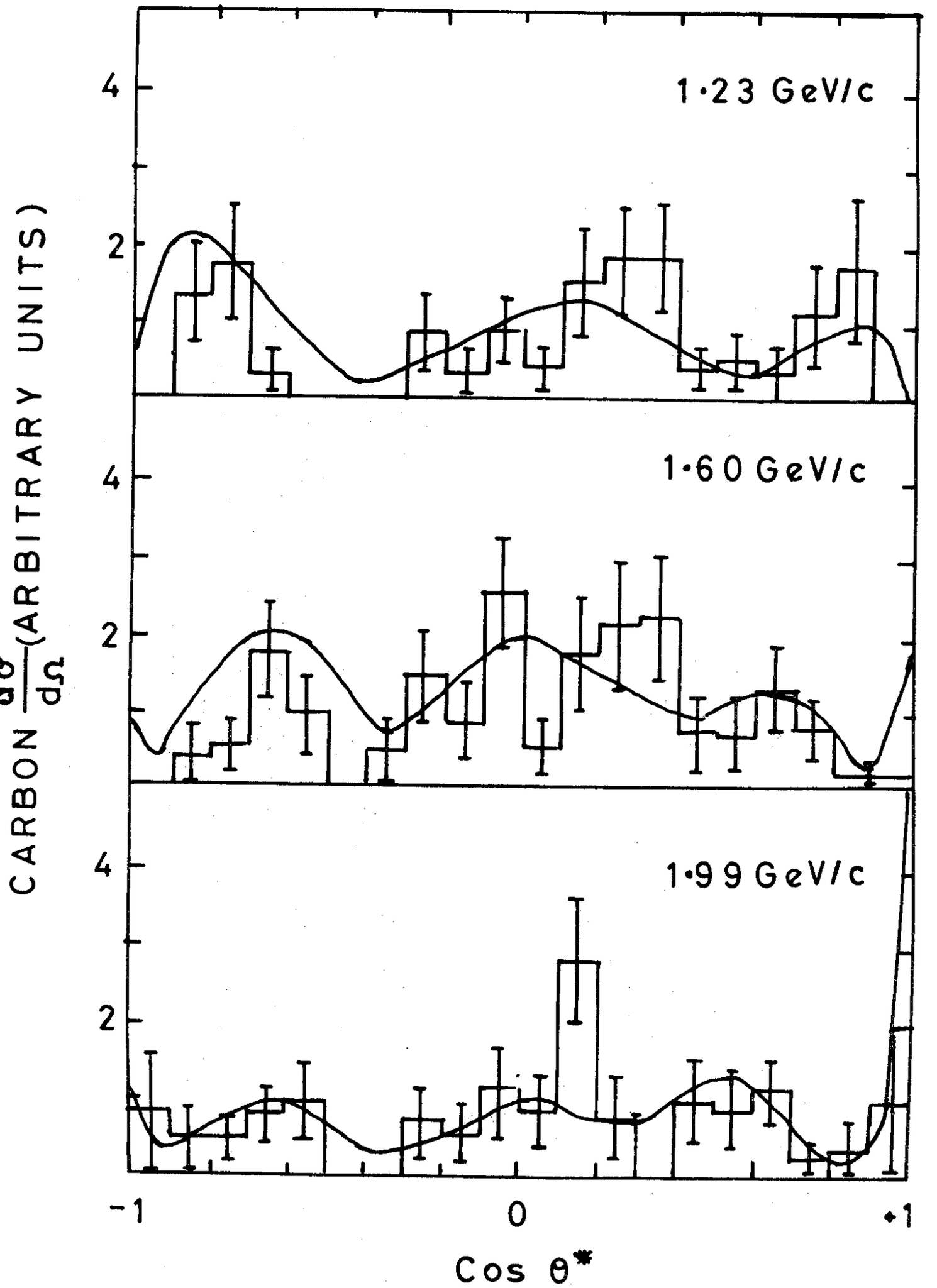
1·23 GeV/c
1·60 GeV/c
1·99 GeV/c
4
2
-1
0
+1
Cos θ*
CARBON dσ/dΩ (ARBITRARY UNITS)

Figure 8

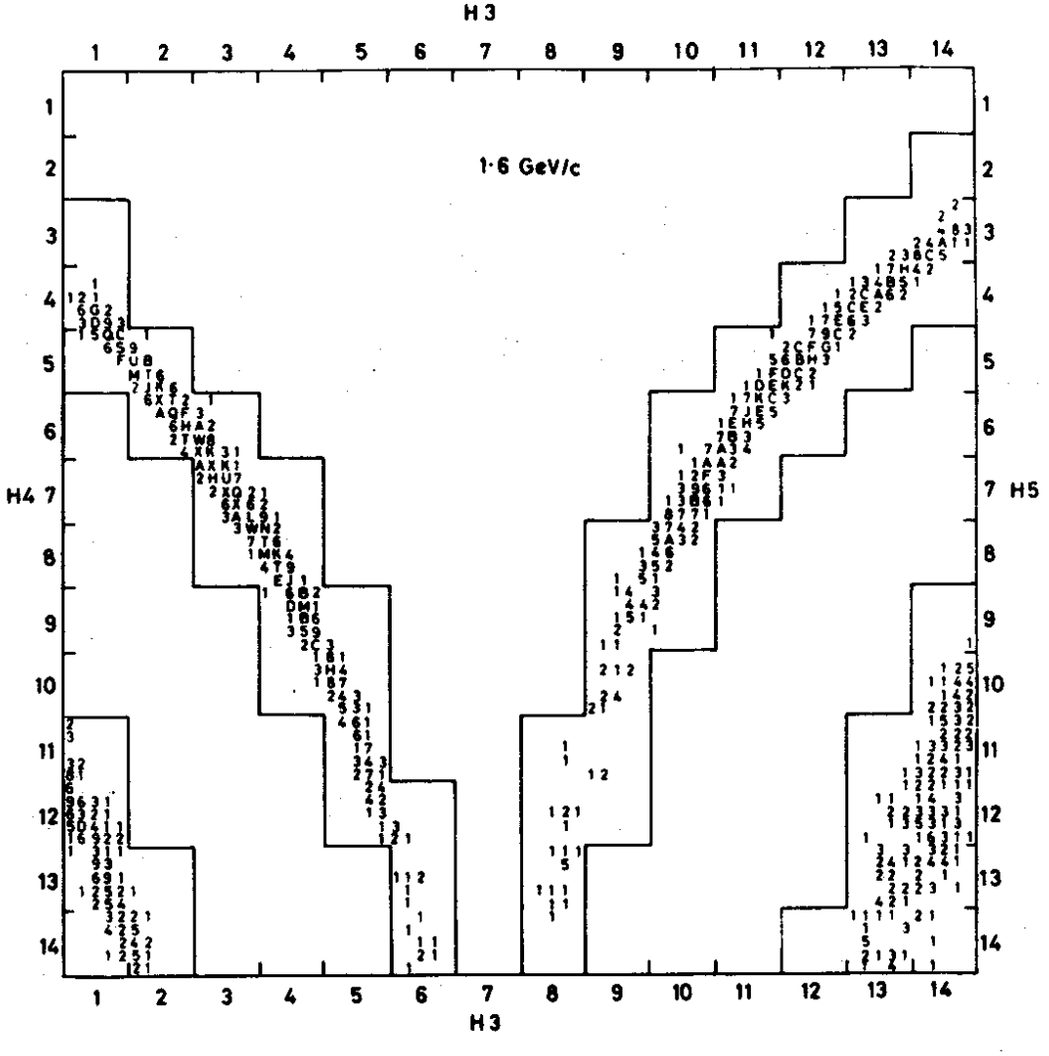

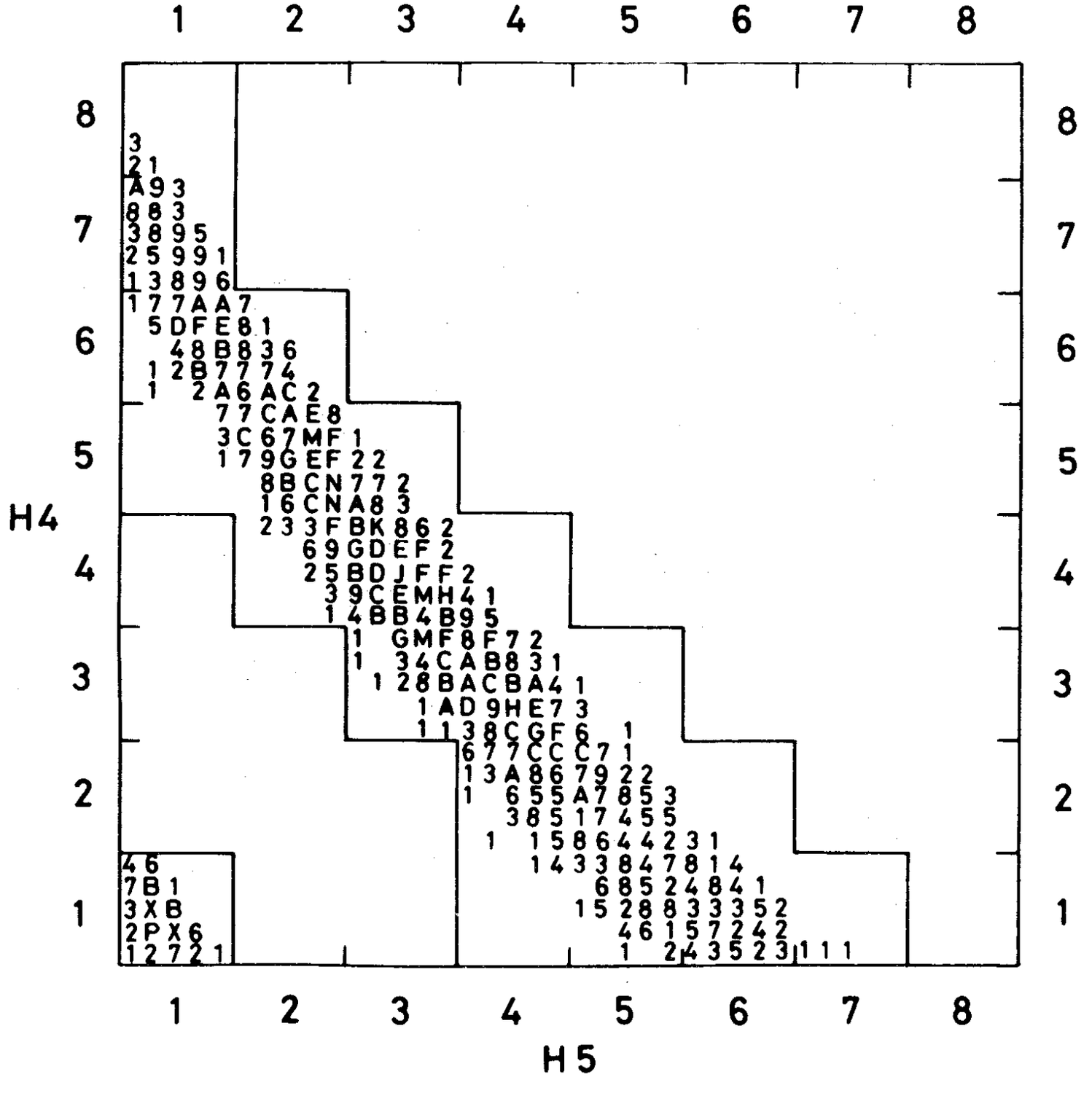


Figure 8 contd.

Figure 9

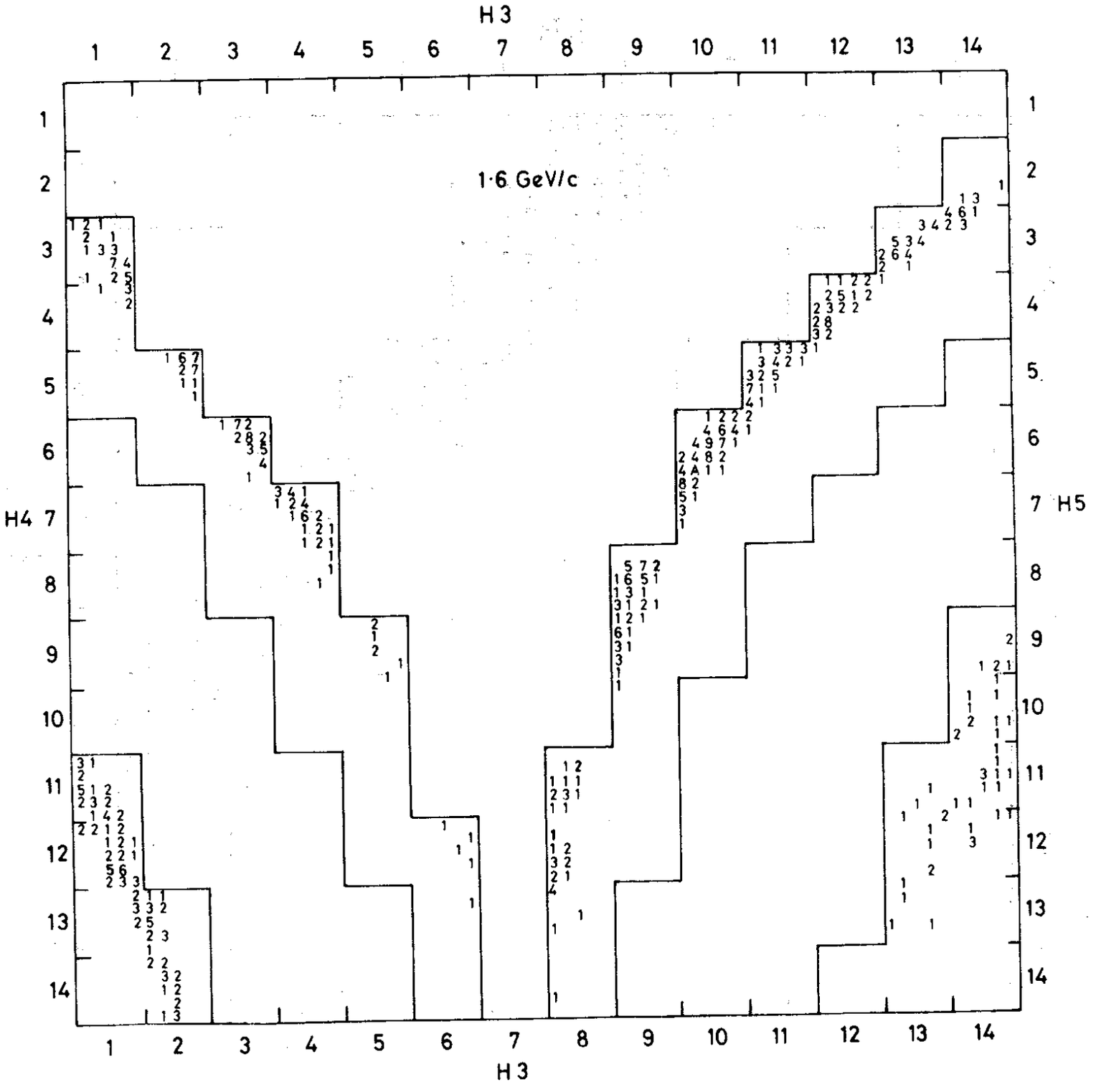

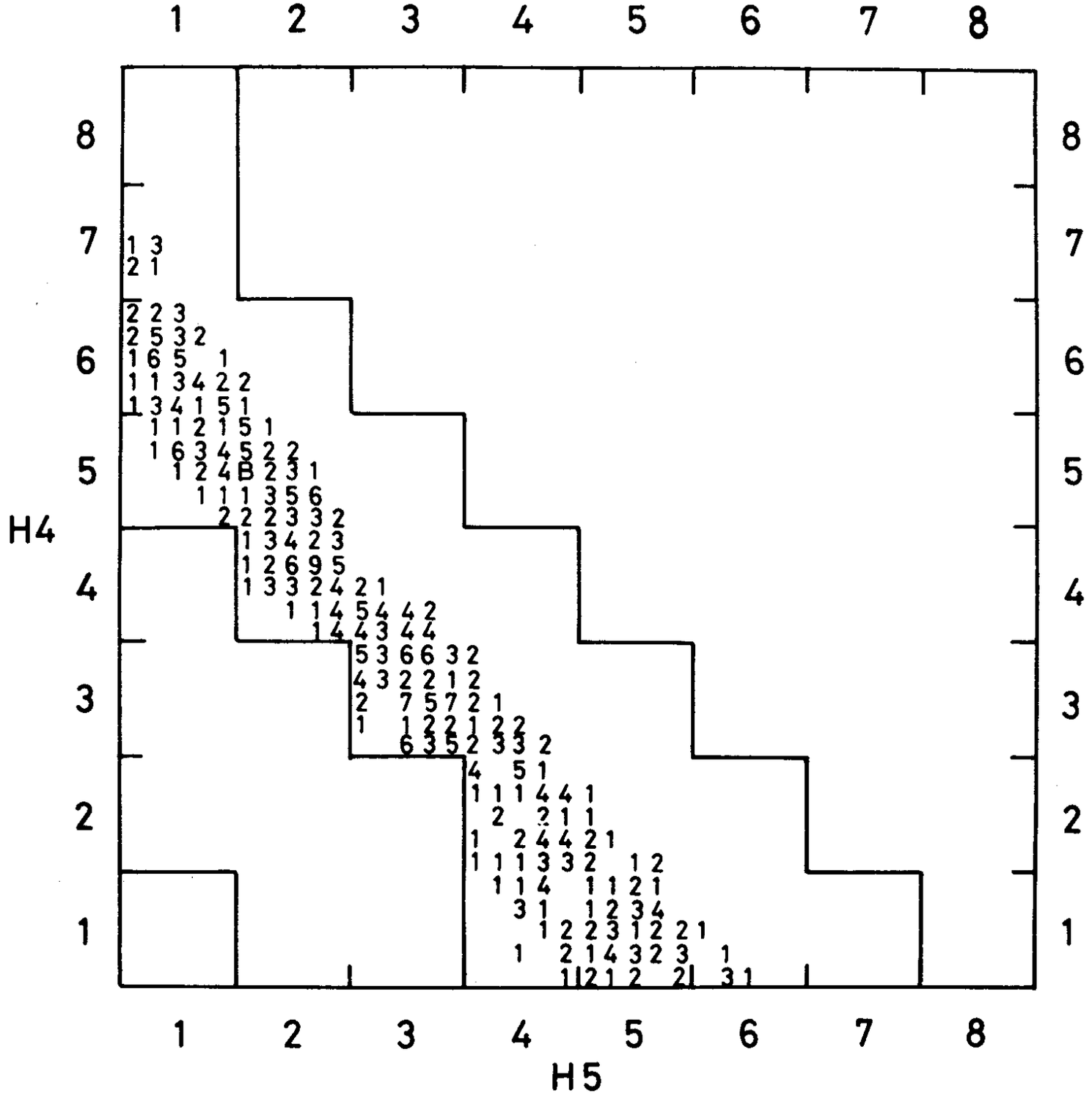


Figure 9 contd.

Figure 10

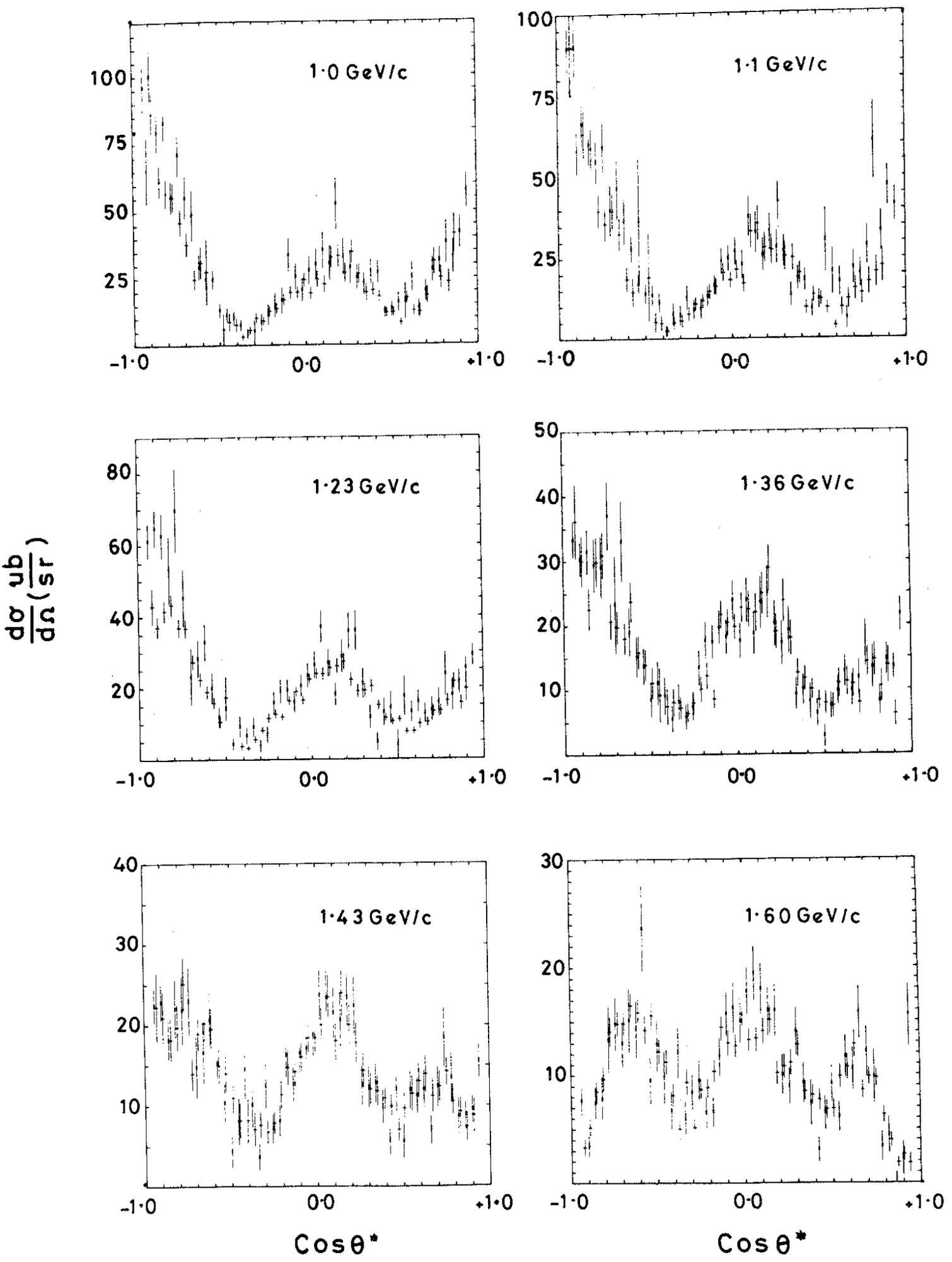
1·0 GeV/c
1·1 GeV/c
1·23 GeV/c
1·36 GeV/c
1·43 GeV/c
1·60 GeV/c
dσ/dΩ μb/(sr)
Cos θ*
Cos θ*

Figure 10 contd.

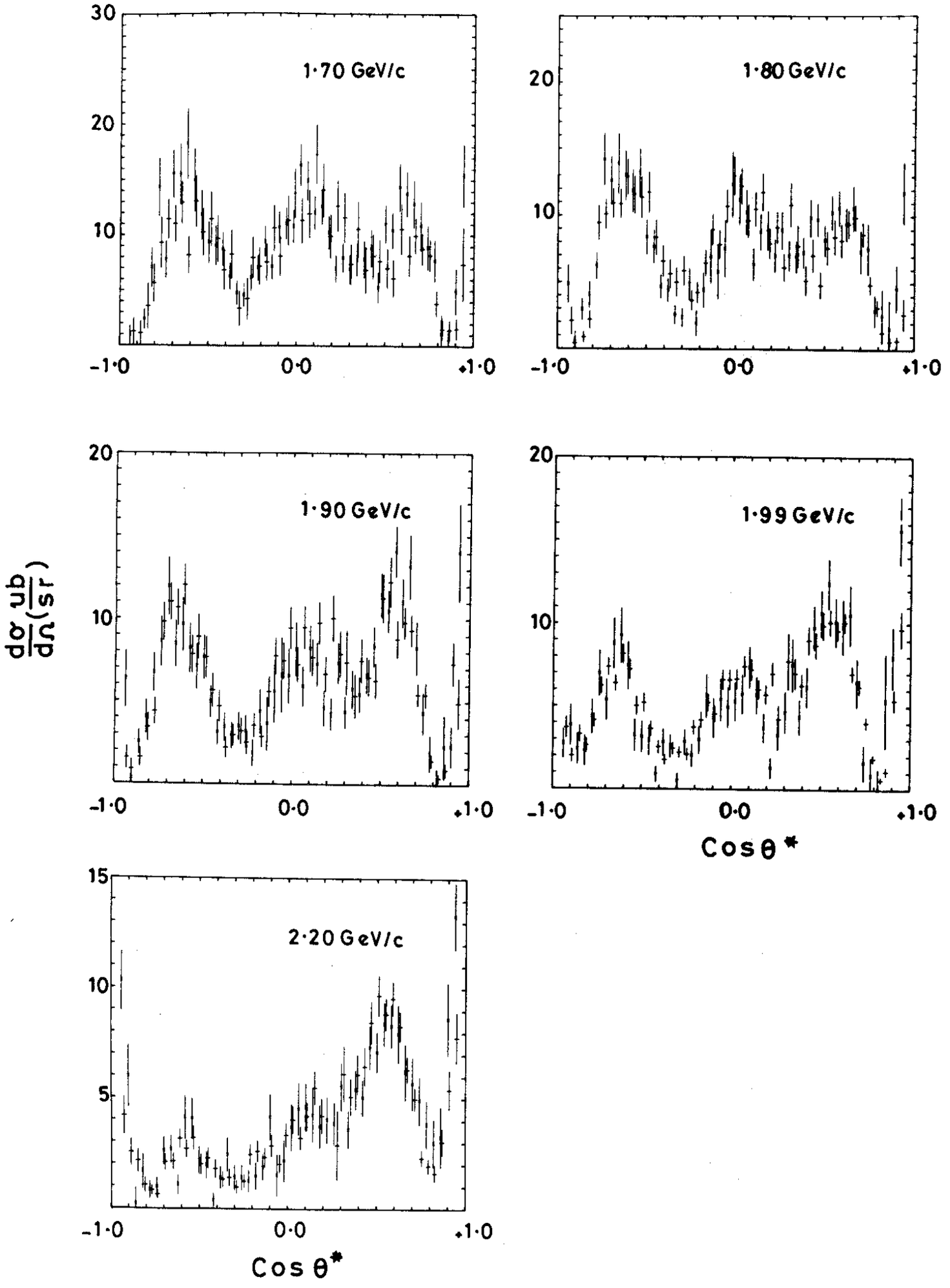

Figure 11

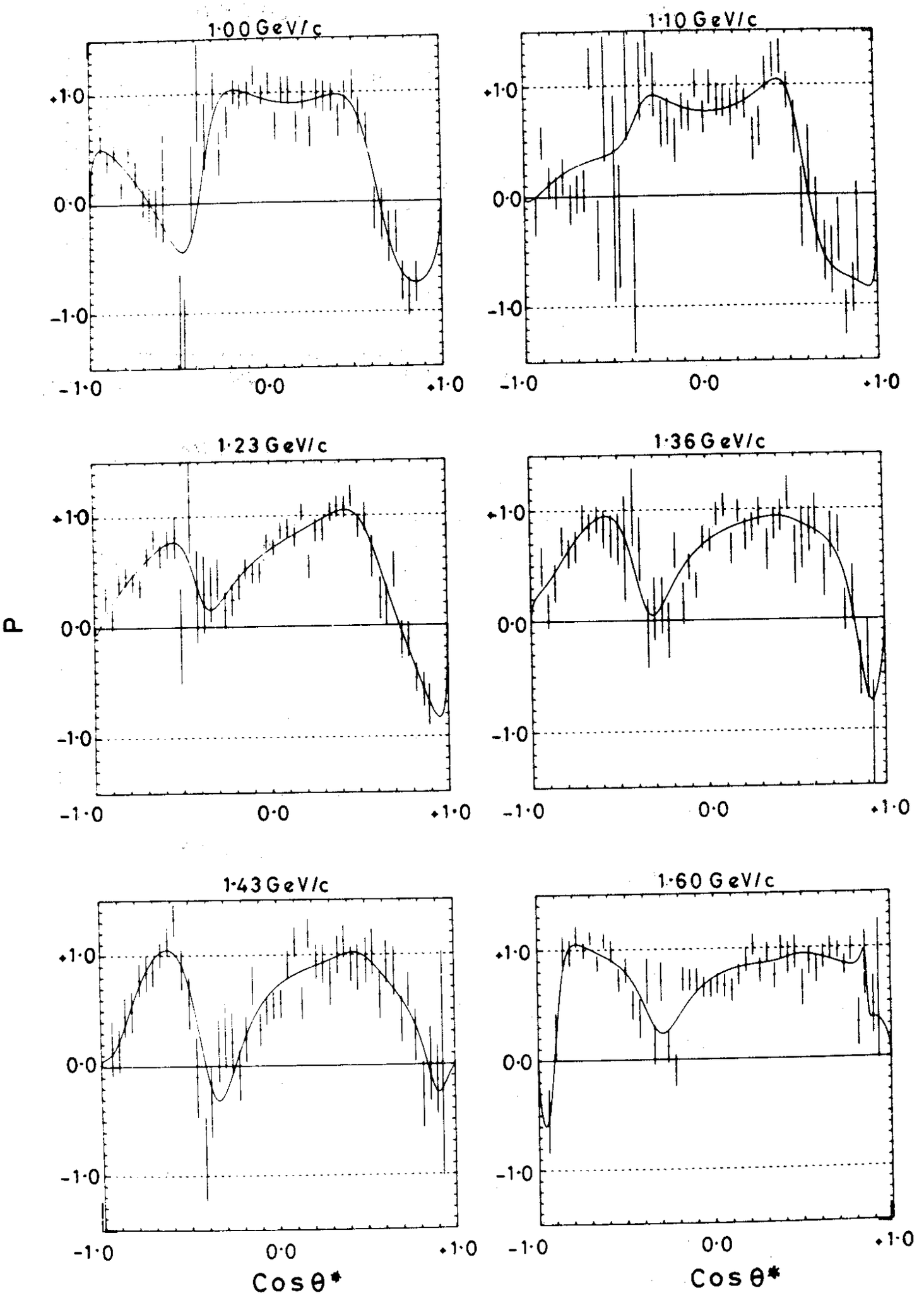
1·00 GeV/c
1·10 GeV/c
1·23 GeV/c
1·36 GeV/c
1·43 GeV/c
1·60 GeV/c
P
+1·0
0·0
-1·0
Cos θ*

Figure 11 contd.

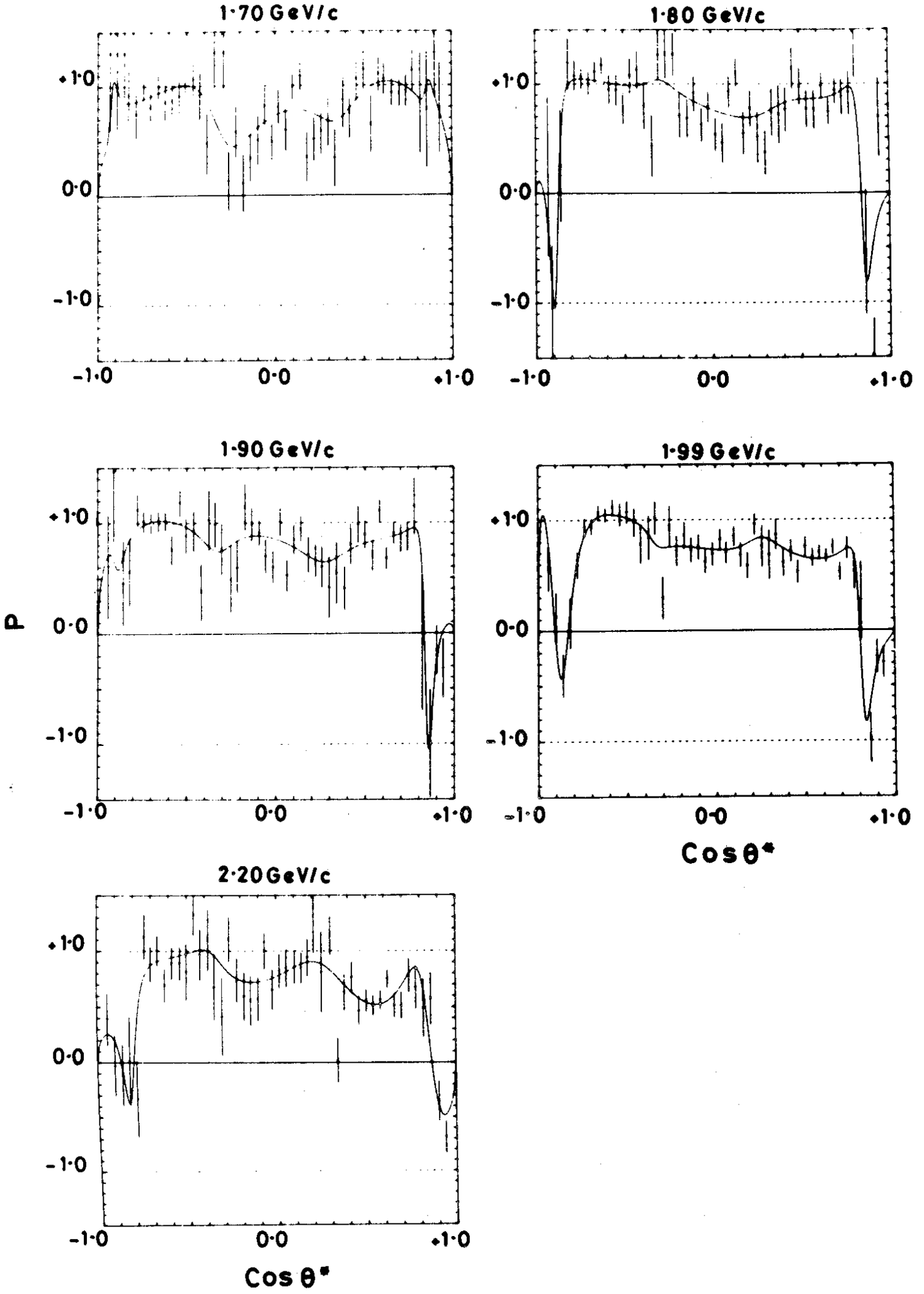

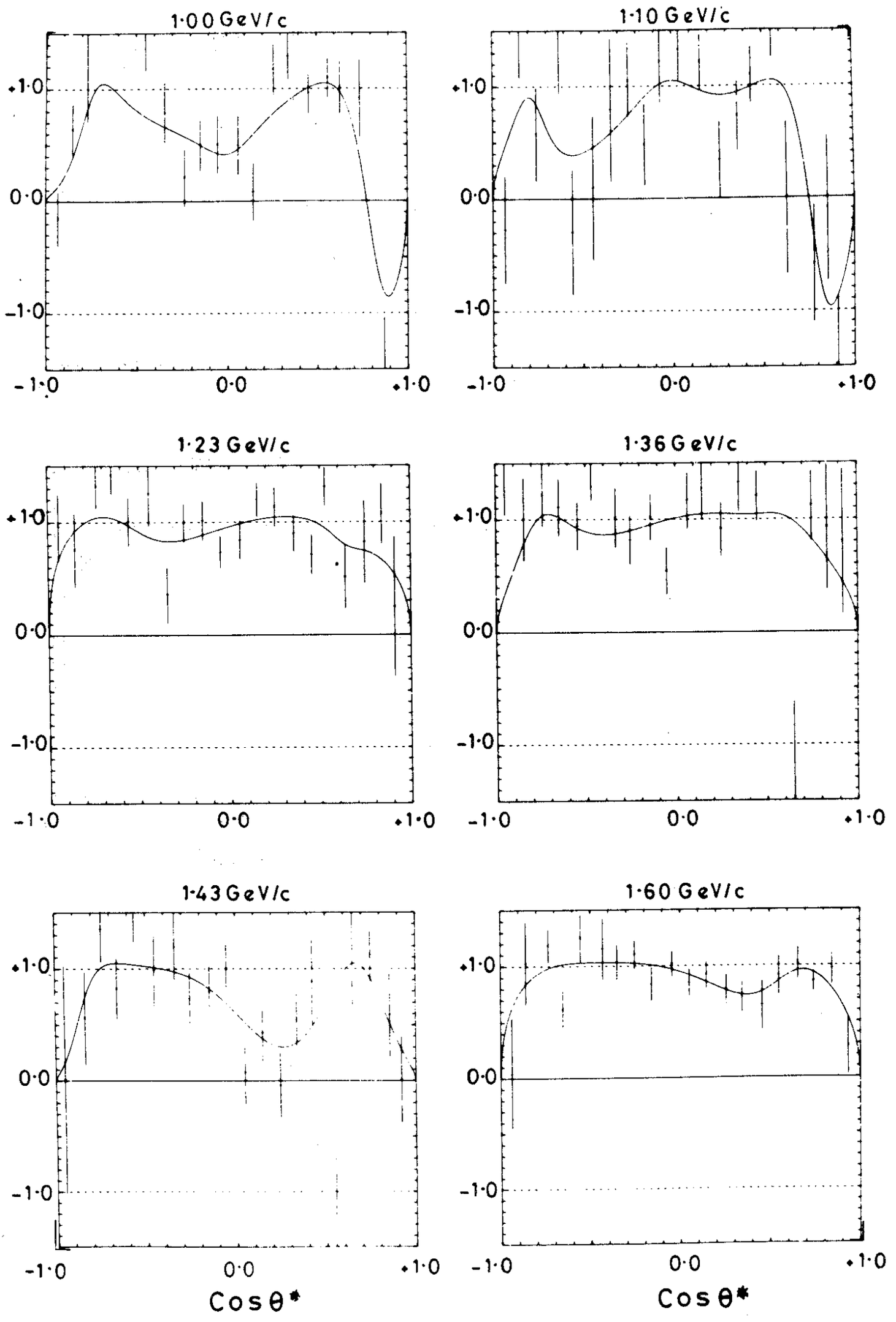
1·00 GeV/c
1·10 GeV/c
1·23 GeV/c
1·36 GeV/c
1·43 GeV/c
1·60 GeV/c
+1·0
0·0
-1·0
-1·0
0·0
+1·0
Cos θ*

Figure 12 contd.

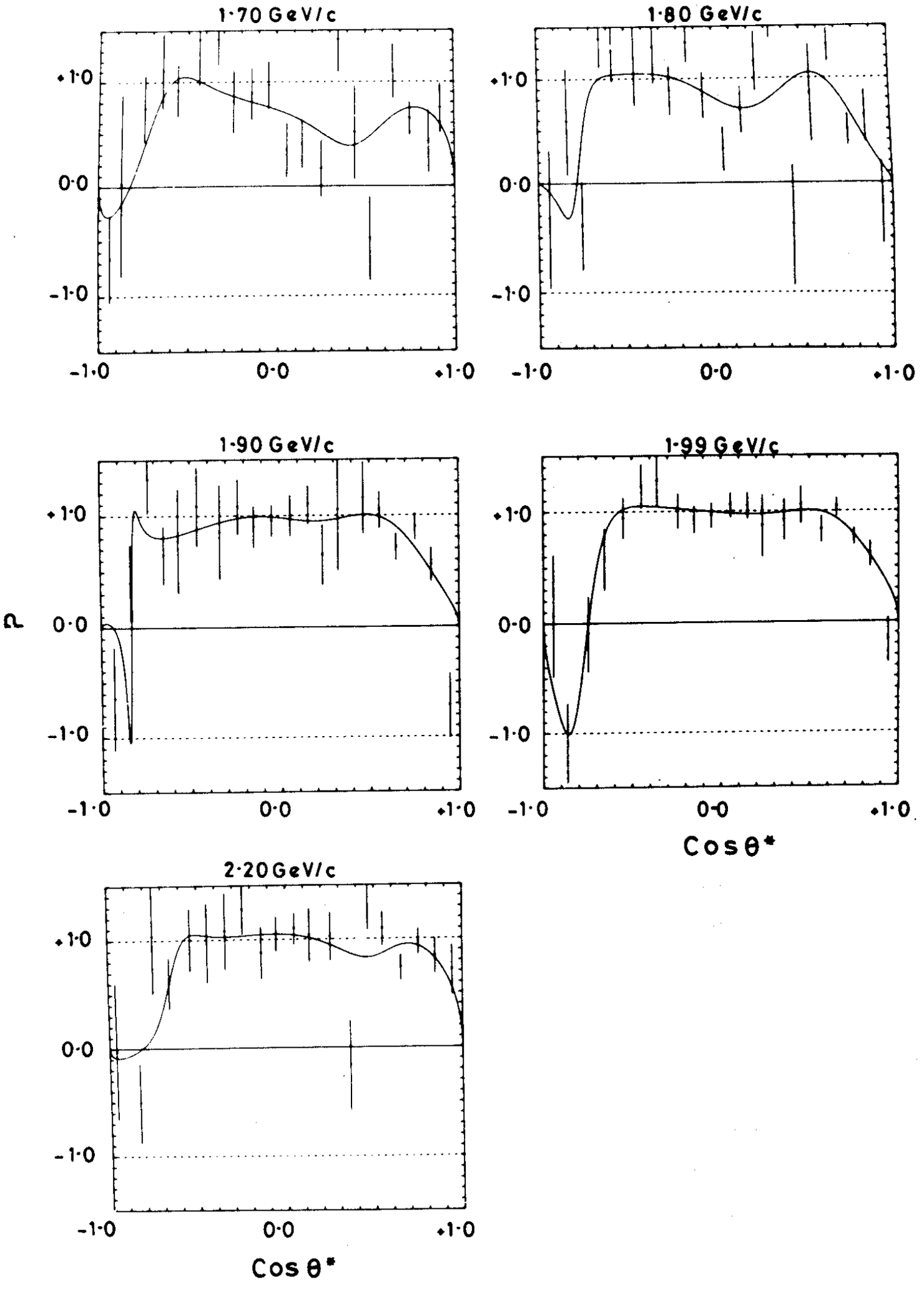

Figure 13

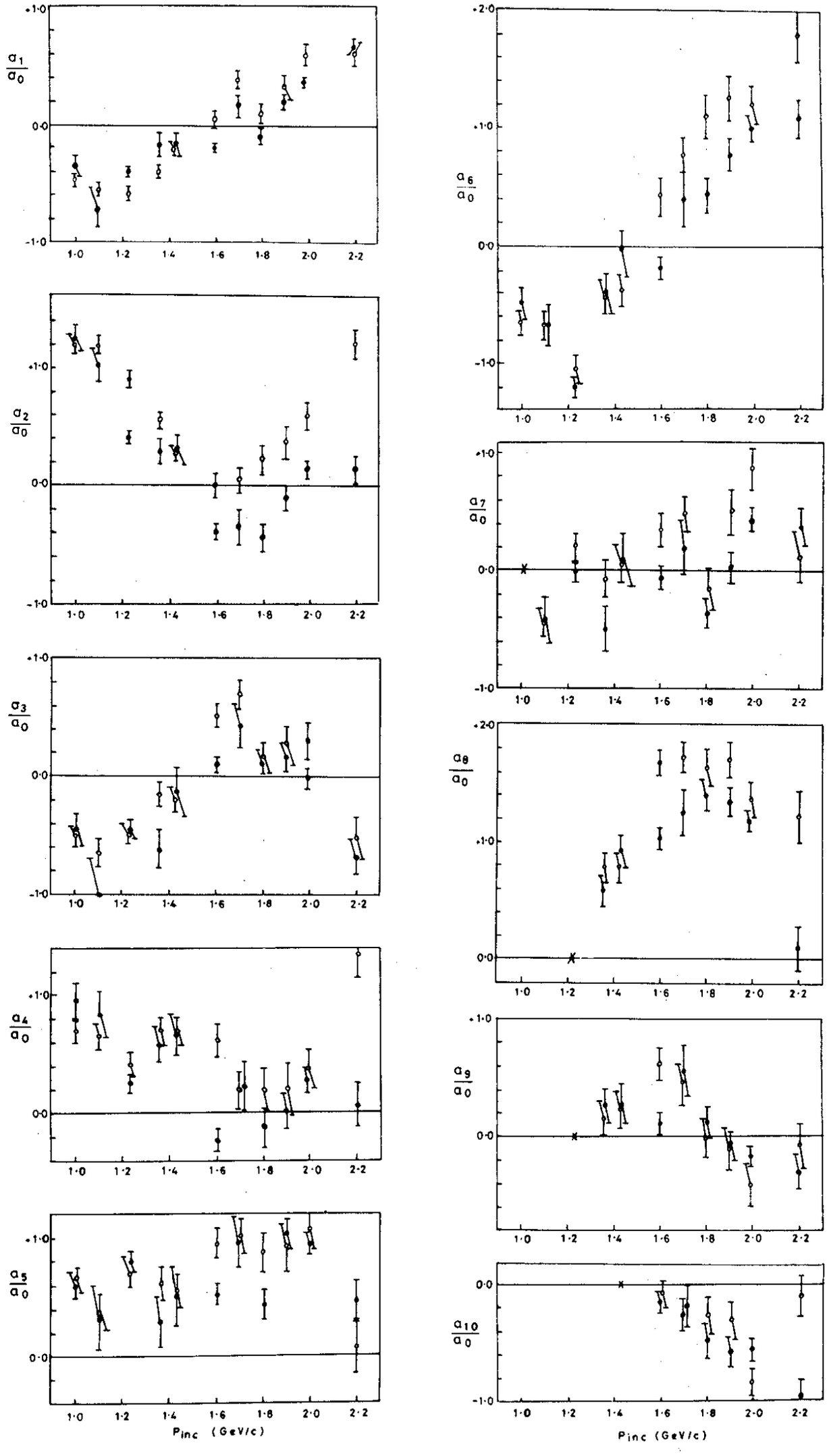
a1/a0
a2/a0
a3/a0
a4/a0
a5/a0
a6/a0
a7/a0
a8/a0
a9/a0
a10/a0
Pinc (GeV/c)
Pinc (GeV/c)

Figure 13 contd.

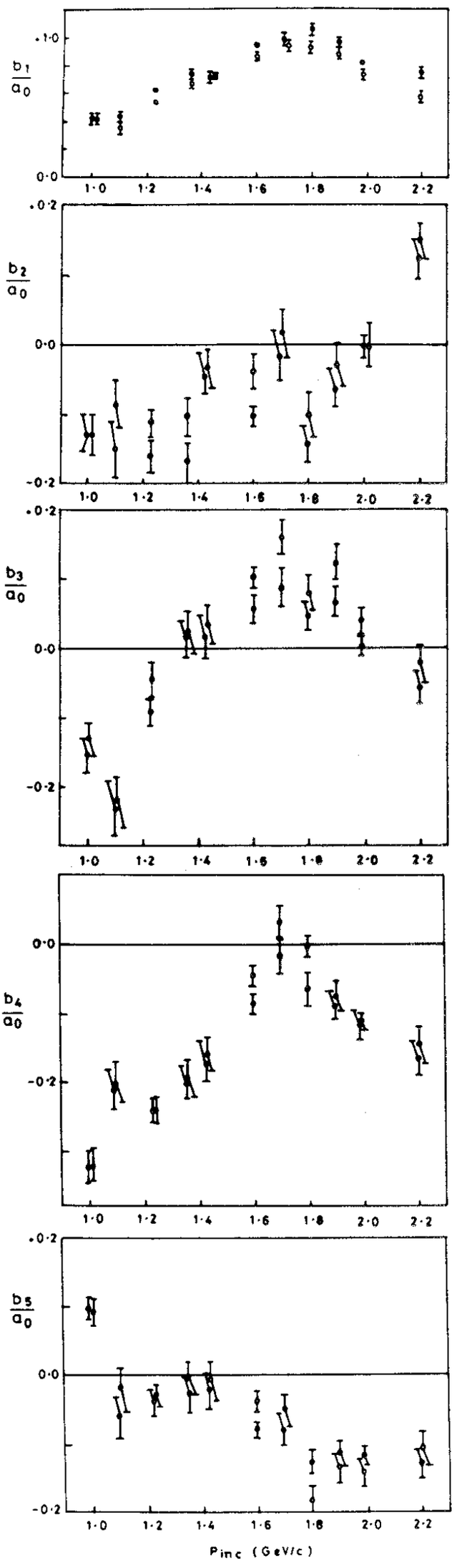


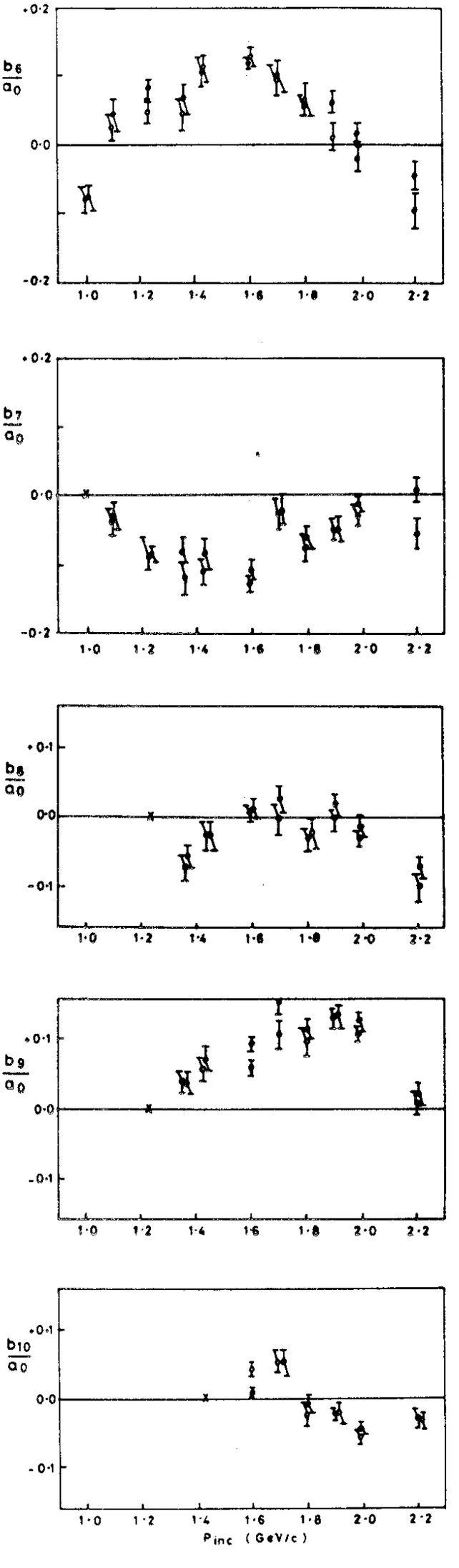

Figure 14

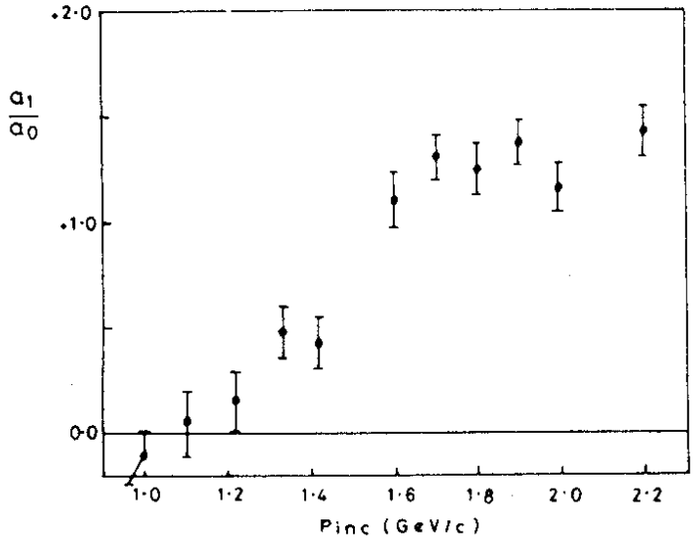
+2·0
+1·0
0·0
a1/a0
1·0 1·2 1·4 1·6 1·8 2·0 2·2
Pinc (GeV/c)

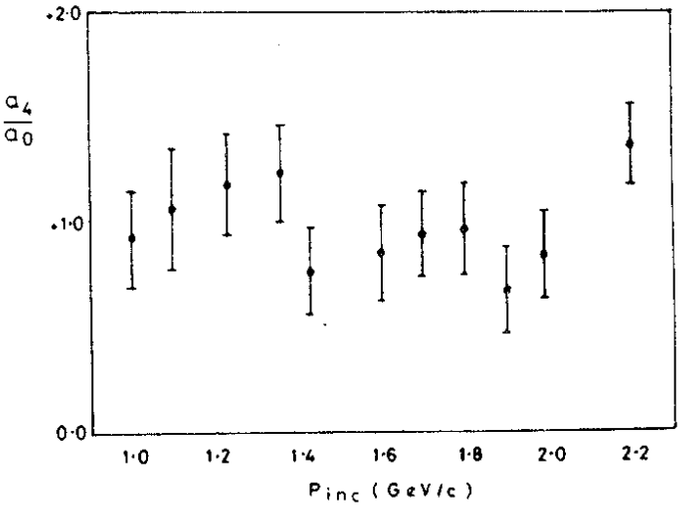
+2·0
+1·0
0·0
a4/a0
1·0 1·2 1·4 1·6 1·8 2·0 2·2
Pinc (GeV/c)

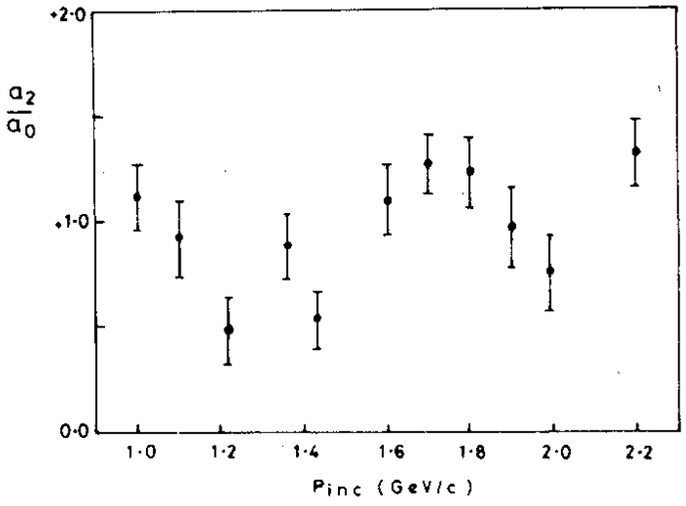
+2·0
+1·0
0·0
a2/a0
1·0 1·2 1·4 1·6 1·8 2·0 2·2
Pinc (GeV/c)

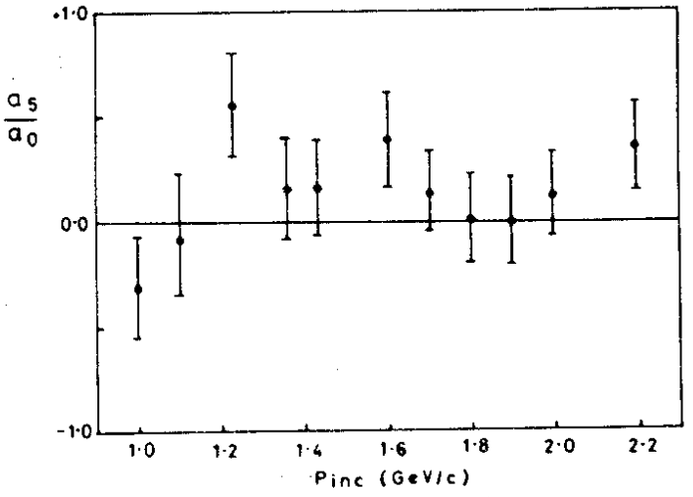
+1·0
0·0
-1·0
a5/a0
1·0 1·2 1·4 1·6 1·8 2·0 2·2
Pinc (GeV/c)

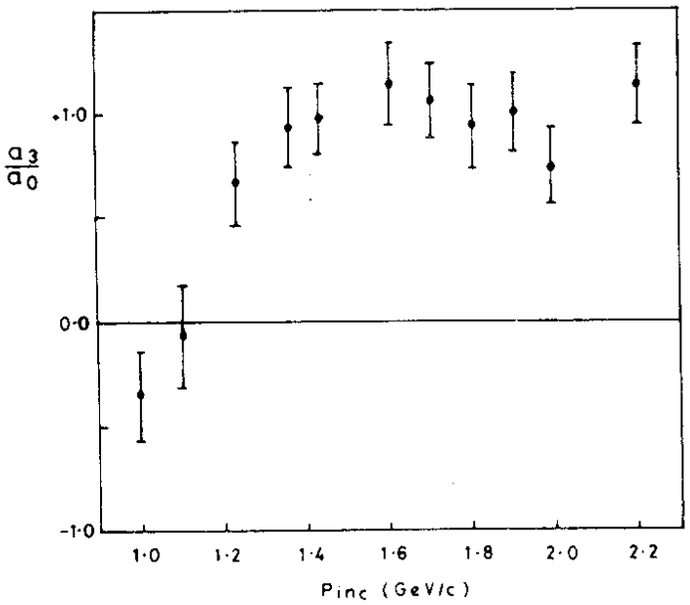
+1·0
0·0
-1·0
a3/a0
1·0 1·2 1·4 1·6 1·8 2·0 2·2
Pinc (GeV/c)

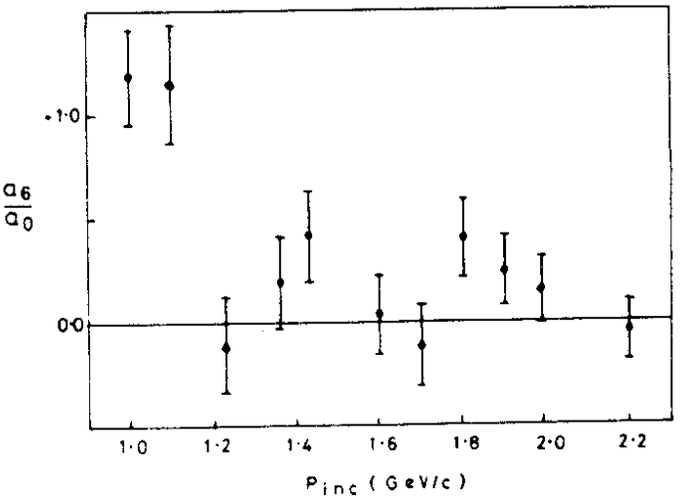
+1·0
0·0
a6/a0
1·0 1·2 1·4 1·6 1·8 2·0 2·2
Pinc (GeV/c)

Figure 14 contd.